



**UNIVERSIDAD EUROPEA DE
MADRID**

**ESCUELA DE ARQUITECTURA, INGENIERÍA Y DISEÑO
BACHELOR'S DEGREE IN AEROSPACE ENGINEERING
FINAL PROJECT REPORT**

**HORIZONTAL DOUBLE BUBBLE AIRCRAFT DESIGN FOR THE MIDDLE
OF THE MARKET**

ÁLVARO TRIVIÑO RAMIREZ

YEAR 2023-2024

TITLE: HORIZONTAL DOUBLE BUBBLE AIRCRAFT DESIGN FOR THE
MIDDLE OF THE MARKET

AUTHOR: ÁLVARO TRIVIÑO RAMÍREZ

SUPERVISOR: RAUL CARLOS LLAMAS SANDIN

DEGREE OR COURSE: AEROSPACE ENGINEERING

DATE: 28/01/2024

Abstract

The design of a horizontal double bubble aircraft for the middle of the market appears as a possible solution for the middle of the market segment, allowing to increase the number of passengers per row of seats and opening the way for new concept designs. The possibility of entering this market niche means a big opportunity for airlines.

The design proposed offers new structural possibility as well as an improvement in the use of cabin space giving passengers more comfortable seats and a quicker and more efficient trip.

After the design phase, the weight estimation will be carried out in depth, covering the entire structure of the aircraft, and the different systems that make it up. This step together with the computational fluid dynamic analysis of the aircraft wing, obtaining the values of the main aerodynamic forces will be of vital importance to evaluate the feasibility, the aerodynamic efficiency, and the range of the aircraft.

At the end of the project, the conclusions of the project and possible future works and improvements will be stated.

Acknowledgments

I would like to express my sincere gratitude to my final degree project supervisor Raúl Llamas, for his expert guidance and advice during the entire process. His suggestions and continuous feedback have been decisive during the realization of this project.

I want to express my thanks to my classmates, who have given me important suggestions and ideas during the university journey. I also cannot forget my family and friends, to whom I am deeply grateful for their unquestioning support during this stage of my life. Their words of encouragement and motivation were crucial to push me forward all these years.

Contents

Abstract.....	4
Acknowledgments	5
Chapter 1. Introduction	13
1.1 Problem approach	14
1.2 Project objectives	14
1.3 Report structure.....	14
Chapter 2. Market Positioning	15
2.1 Middle of the market segment	15
2.1.1 Boeing position.....	16
2.1.2 Airbus position	18
2.2 Circular fuselage structure	19
2.3 Double Bubble fuselage structure.....	21
2.4 Aurora’s proposal	23
2.5 Airbus’ proposal	26
2.6 Russian proposal	27
2.7 Boundary layer ingestion	29
2.8 Service possibilities	30
Chapter 3. Aircraft design	32
3.1 Introduction.....	32
3.2 Preliminary designs.....	32
3.2.1 First sketches	32
3.2.2 Fuselage shape	34
3.2.3 Cross-Section.....	34
3.2.4 Engine location.....	35
3.3 Final design.....	37
3.4 Fuselage	39
3.4.1 Cross-section	39
3.4.2 Seats configuration	42
3.4.3 Cargo distribution.....	44
3.4.1 Cargo doors	45
3.4.2 Passenger’s doors	47

3.5	Wings	49
3.5.1	Airfoil	49
3.5.2	Wing dimensions	49
3.5.3	Final wing design in Open VSP	54
3.5.4	Control surfaces	55
3.5.5	Wings fuel tanks	57
3.5.6	Internal structure.....	59
3.6	Landing gear	60
3.6.1	Front landing gear.....	60
3.6.2	Main landing gear	63
3.7	Empennage.....	66
3.7.1	Airfoil	67
3.7.2	Horizontal tail plane dimensions	68
3.7.3	Horizontal tail plane final design.....	71
3.7.4	Vertical tail plane dimensions	72
3.7.5	Vertical tailplane final design.....	73
3.7.6	Final Empennage	74
3.8	Propulsion systems	75
3.8.1	Engines selection	75
3.8.2	Engine location for boundary layer ingestion.....	78
Chapter 4.	Aircraft performance and wing analysis.....	80
4.1	Fuel estimations	80
4.2	Aircraft weight estimation	82
4.2.1	Fuselage weight estimation	82
4.2.2	Wings weight estimation	83
4.2.3	Empennage weight estimation.....	83
4.2.4	Landing gear weight estimation	84
4.2.5	Engine weight estimation	85
4.2.6	Aircraft systems weight estimation	85
4.2.7	Final estimated weight.....	89
4.3	Wing analysis.....	91
4.3.1	Velocity	92
4.3.2	Pressure.....	94

4.3.3	Mach number	95
4.3.4	Skin friction coefficient	96
4.3.5	Aerodynamic efficiency	98
4.4	Range calculation.....	101
Chapter 5.	Conclusions and future works	103
5.1	Conclusions.....	103
5.2	Future works	105
APPENDICES	106
APPENDIX A	106
REFERENCES	108

Figures

Figure 1 Middle of the market segment diagram	16
Figure 2. Boeing 797 Preliminary design.....	17
Figure 3. Airbus A321XLR.....	18
Figure 4. Airbus A321XLR market positioning.....	19
Figure 5. Circular fuselage cross-section	20
Figure 6. A380 Double bubble cross-section	21
Figure 7. Horizontal double bubble cross-section.....	22
Figure 8. Aurora D8 main characteristics.....	23
Figure 9. Aurora D8 Drag and lift distribution.....	24
Figure 10. Aurora D8 conceptual design.....	25
Figure 11. Airbus P500 sketches	26
Figure 12. Frigate Ecojet concept design	27
Figure 13. Frigate Ecojet Fuselage cross-section view	27
Figure 14. Frigate Ecojet cabin arrangement.....	28
Figure 15. Boundary layer ingestion description of Aurora D8	29
Figure 16. ICAO prediction for future air traffic.....	30
Figure 17. Sketch top view	33
Figure 18. Sketch isometric view	33
Figure 19. Sketch side view.....	33
Figure 20. Fuselage left side view	34
Figure 21. Fuselage isometric view	34
Figure 22. Double bubble cross-section layout	35
Figure 23. Front view of the engine location	36
Figure 24. Isometric view of engines	36
Figure 25. Final design isometric view	37
Figure 26. Final design left view	37
Figure 27. Final design front view.....	38
Figure 28. Final design with translucent fuselage.....	38
Figure 29. Cross-section final design	39
Figure 30. Passengers located in the cross-section.....	40
Figure 31. Isometric view of the passengers and seats.....	41

Figure 32. Seat configuration	42
Figure 33. isometric view of cabin layout	43
Figure 34. Side view of the cabin layout with passengers.....	43
Figure 35. LD3-45 container dimensions	44
Figure 36. Cargo compartment location	45
Figure 37. Right side cargo doors.....	46
Figure 38. Left side cargo door	46
Figure 39. Exit doors left view	47
Figure 40. Exit doors distances	48
Figure 41. NASA SC (2)-0412 Airfoil	49
Figure 42. Isometric view of the final wing 3D design.....	54
Figure 43. Top view of the final wing 3D design.....	54
Figure 44. Wings final 3D design.....	55
Figure 45. Fowler flap mechanism	55
Figure 46. Flaps location in 3D wing	56
Figure 47. Aileron, spoilers and slats location in 3D wing	56
Figure 48. Isometric view of the wing with high lift devices.....	57
Figure 49. Wing box fuel tanks	57
Figure 50. Wing fuel tanks distribution in the wing.....	58
Figure 51. Four wing fuel tanks distribution along the wing	58
Figure 52. Wing internal structure.....	59
Figure 53. Nose landing gear side view design.....	60
Figure 54. Nose landing gear front view design.....	61
Figure 55. Nose landing gear side view in 3D	61
Figure 56. Nose landing gear front view in 3D	62
Figure 57. Main landing gear side view design.....	63
Figure 58. Main landing gear front view design	64
Figure 59. Main landing gear front view in 3D	64
Figure 60. Main landing gear isometric view in 3D.....	65
Figure 61. T- tail with double vertical tail plane	66
Figure 62. NACA 0012	67
Figure 63. Airfoil NACA 0012 in HTP.....	67
Figure 64. Isometric view of the HTP final 3D design	71

Figure 65. Top view of the HTP final 3D design with dimensions.....	71
Figure 66. Vertical tail plane side view	73
Figure 67. Isometric view of the VTP final 3D design	73
Figure 68. Isometric view of the final empennage design.....	74
Figure 69. Front view of the final empennage design	74
Figure 70. Pratt & Whitney PW2043 interior	77
Figure 71. Pratt & Whitney PW2043 engine.....	77
Figure 72. Side view of engines location	78
Figure 73. Isometric view of engines location	79
Figure 74. Side view of the enclosure mesh.....	91
Figure 75. Isometric view of the enclosure mesh.....	91
Figure 76. Flow field contours of velocity magnitude	92
Figure 77. Wing contours of velocity magnitude	93
Figure 78. Static pressure contours along the wing.....	94
Figure 79. Static pressure contours along the wing.....	94
Figure 80. Static pressure contours in the flow field.....	94
Figure 81. Mach number values along the wing	95
Figure 82. Mach number in the flow field.....	95
Figure 83. Skin friction coefficient along the wing.....	96
Figure 84. Skin friction coefficient contour of the flow field	97
Figure 85. First possible seats configuration	106
Figure 86. Second possible seats configuration.....	107

Tables

Table 1. 767 Family maximum range.....	16
Table 2. Boeing 767 family seats capacity per variant.....	17
Table 3. Evolution of aircraft designs in the history and future opportunities.....	31
Table 4. 3D Human physical dimensions.....	41
Table 5. LD3-45 Container technical specifications.....	44
Table 6. Boeing Aircraft weights.....	49
Table 7. Airbus aircraft weigh.....	50
Table 8. MTOW vs Wpayload lineal regression.....	50
Table 9. A320 family wing parameters.....	51
Table 10. Boeing aircraft wing parameters.....	51
Table 11. Aspect ratio vs Taper ratio linear regression.....	52
Table 12. Airbus aircraft HTP dimensions.....	68
Table 13. Boeing aircraft HTP dimensions.....	68
Table 14. HTP Area vs Wing Area linear regression.....	69
Table 15. HTP Area vs HTP Span linear regression.....	69
Table 16. Airbus aircraft range and thrust.....	75
Table 17. Airbus aircraft engines.....	75
Table 18. Boeing aircraft range and thrust.....	76
Table 19. Boeing aircraft engines.....	76
Table 20. Thrust vs Range linear regression.....	76
Table 21. Pratt & Whitney PW2043 specifications.....	80
Table 22. Total estimated weight of the structure.....	89
Table 23. Total estimated weight of the systems.....	89
Table 24. Total estimated weight of the payload.....	90
Table 25. Total estimated weight of the aircraft.....	90
Table 26. Cl vs angle of attack.....	98
Table 27. Cd vs angle of attack.....	99
Table 28. Aerodynamic efficiency vs angle of attack.....	100

Chapter 1. Introduction

The design of the double bubble fuselages in aircraft were first introduced in the decade of 1960 and is characterized by the two transversal sections united in a bigger section that forms the fuselage structure of the aircraft. This double fuselage structures surged as a response to the necessity of increasing the passenger capacity of the aircraft and the efficiency in the use of the cabin space. Due to the growing demand for aviation during the decades of 1960 and 1970, manufacturing companies looked for solutions capable of satisfying the necessities previously mentioned.

The traditional fuselage with a circular cross-section was becoming less practical for bigger aircraft and taking advantage of the limited inside space was becoming a challenging task. The idea of the horizontal double bubble orientation offered many possibilities for integrating into the aircraft larger fuel tanks, bigger cargo compartments, and an increase in seating capacity. Having a wider cabin enables the manufacturers to provide more efficient aircraft and to meet the demands of aviation in segments that are uncovered as it is the middle of the market segment.

Nowadays, the double bubble fuselage is widely used in different aspects of aviation such as regional commercial flights or military transport aircraft. These kinds of aircraft offer a bigger capacity combined with an efficient performance, which is why important manufacturing companies have chosen this design for their commercial transport aircraft like Airbus A380 and Boeing 747. Double bubble fuselage offers the possibility of taking advantage of the aircraft's cabin space in order to introduce larger fuel tanks, and bigger cargo compartments and improve the circulation of air inside the cabin.

Double bubble fuselages appeared in the industry as a possible solution to seat capacity and improvement of space use and have become a main concept in the aerospace industry currently.

1.1 Problem approach

During the last 50 years, aircraft design concepts have barely changed and a new concept proposal could open new possibilities for commercial air transport. In addition to designing a different concept, there is the possibility to enter market segments that are uncovered nowadays and, to increase the number of passengers in a single aircraft only by modifying the fuselage structure. Having more passengers will be a huge opportunity for the future as air transport is growing with leaps and bounds and according to the air transport tendency, the number of users of this kind of transport could duplicate the actual one in the next 10 years.

1.2 Project objectives

The objective of this project is to carry out a preliminary design of an aircraft with a double bubble fuselage structure that could operate in the middle of the market segment. Making a wider fuselage, the objective is to cover a segment of the market increasing the number of passengers per row. The aircraft is going to be designed and modeled in 3D and the wing will be analyzed with Ansys Fluent in order to prove the aerodynamic efficiency and aimed range.

1.3 Report structure

A study of the market will be done to see the necessities that a middle of the market aircraft should cover and obtain the necessary data to carry out the fuselage design and the cabin arrangement. The design of the aircraft will be done in 3D using Open VSP, then, another objective of the project is to obtain a CFD calculus of the wing and obtain the main aerodynamic parameters using Fluent.

Chapter 2. Market Positioning

Aircraft market positioning is the process of defining the target market and the competitive position for a specific aircraft model or family. This means identifying the needs and preferences of the target customer, as well as analyzing the market landscape and identifying the unique selling points that the aircraft has.

The middle of the market positioning aims to offer aircraft models designed to meet the needs of passengers and airlines between the narrow body aircraft segment and the wide body aircraft segment. This concept emerged in the aviation industry in the late 2000s when the airlines started looking for a new aircraft, more efficient and cheaper than the wide body aircraft and with greater range and passenger capacity than the narrow body aircraft.

If the middle of the market segment had to be defined, it would be a segment in which aircraft have a seating capacity between 175 and 300 passengers and a range between 4.000 and 5.000 nautical miles. The segment's importance comes from the need to renew the aircraft that fit in this segment because they are getting old and inefficient nowadays.

2.1 Middle of the market segment

The middle of the market (MOM) segment refers to a market niche in the aviation industry that is situated between the narrow-body and wide-body aircraft segments. It typically includes aircraft with passenger capacity from 200 to 300 passengers, with ranges up to 5.000 nautical miles.

The MOM segment has emerged due to the increasing demand for cheap and efficient aircraft that could cover medium haul routes that are too long for narrow body aircraft and too short for a wide body one. Another important aspect to take into account, is the advance in technology in terms of aerodynamic design and fuel efficiency of the engines with respect to the old ones, which means that some new aircraft can meet perfectly the requirements of the segment and the demand of the clients.

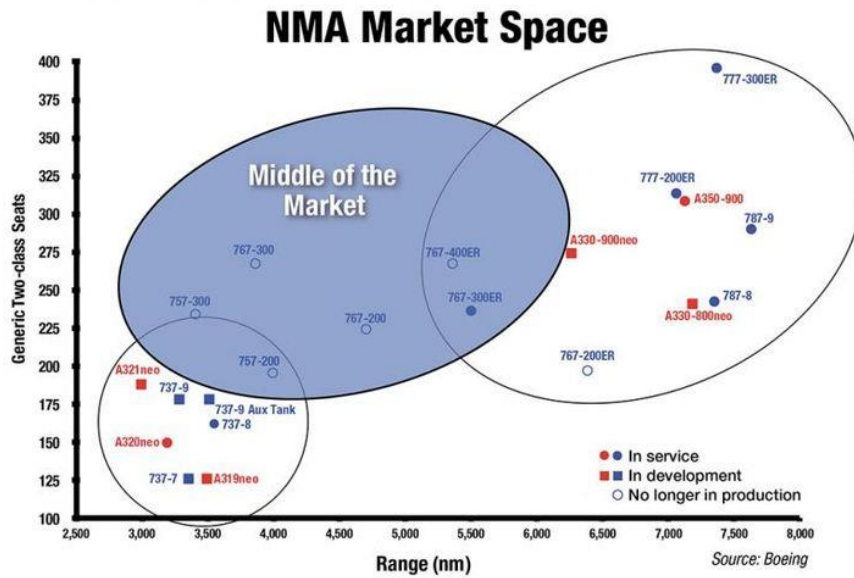


Figure 1 Middle of the market segment diagram

For airlines, having a long fleet of similar aircraft will be better as the maintenance cost would be reduced and in the case of a middle of the market aircraft, the same aircraft could cover routes of different ranges at a reduced maintenance cost.

Nowadays, there are some aircraft that fit in this market segment but in service, the only one is the 767-300ER, which has the needed range and the aimed seat capacity of the segment as can be seen in the upper graph

2.1.1 Boeing position

In September of 1982, Boeing delivered the Boeing 767, their first wide body twin-engine aircraft that they fabricated. This aircraft had a seating capacity between 181 and 375 depending on the cabin arrangement and the model and had an autonomy between 3850 and 6385 nautical miles depending on the model. There are three variables of this aircraft, 767-200, 767-300, 767-300ER and 767-400ER being ER the extra range version.

Variant	767-200	767-200ER	767-300	767-300ER/F	767-400ER
Range	7.200 km	12.200 km	7.200 km	11.070 km	10.415 km

Table 1. 767 Family maximum range

It can be seen in the table that the ER versions (Extra Range) offer more range capacity at the same seat configurations which makes it able to cover a great part of the market niche

Variant	767-200	767-200ER	767-300	767-300ER/F	767-400ER
3-class	174		210		243
2-class	214		261		296
1-class	245		290		409

Table 2. Boeing 767 family seats capacity per variant

In the previous graphs can be seen that, according to the definition of middle of the market, Boeing 767 fits perfectly with the demands of the segment in terms of passenger capacity and range. The problem is that many of the variants of the aircraft are no longer in production and the middle of the market segment remains uncovered.

Boeing faced this situation thinking that the middle of the market segment was big enough to launch a new aircraft model, Boeing 797, the new midsize aircraft (NMA) proposed to cover the segment. This aircraft would have a twin-aisle, twin-engine, and elliptical cross-section and would be available in two versions of 225 passengers and 9.300 km and a bigger one of 275 seats and 8.300 km.



Figure 2. Boeing 797 Preliminary design

With this aircraft, Boeing is expecting to generate 30% more revenue than with a narrow body aircraft and reduce the cost of flight by 40% compared with the wide body aircraft. Boeing 797 would be powered by a 220 KN turbofan manufactured by Pratt & Whitney or GE Aviation/CFM International with an expected by-pass ratio of 10:1 and an overall pressure ratio of more than 50:1

This reduction in flight costs could result in a very demanded aircraft.

2.1.2 Airbus position

In the case of Airbus, the middle of the market segment is placed between the narrow body aircraft of the A320 family and the wide body A350 and A330 aircraft. Airbus has been looking for a solution to this segment demand for several years, in 2017 airbus launched the A321XLR that is an extra-long-range version of the A321 neo that is a narrow body aircraft with a range of up to 4.700 nautical miles and a seating capacity of 240 passengers. Considering the previous data of the aircraft and the parameters that define the middle of the market, the A321XLR could cover perfectly the demand of the segment.



Figure 3. Airbus A321XLR

Airbus' position in the middle of the market segment has been strengthened by many factors, such as the grounding of the Boeing 737 MAX due to its accidents, which has left an important gap in the market of narrow-body aircraft with medium-haul range operability. In addition, the A321neo has made a big impact in the market and the main airlines in the world have demanded a large number of aircraft for their fleet.

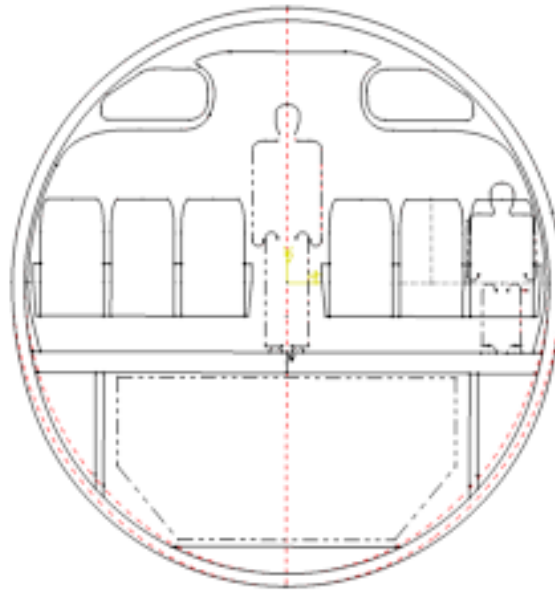


Figure 5. Circular fuselage cross-section

Circular cross-sections provide a uniform distribution of the pressure along the section of the fuselage which reduces the stress concentrations and helps to maintain the structural integrity of the aircraft. Besides, it is very simple to manufacture and requires less time and costs than other types of cross-sections. This kind of fuselage maximizes the efficiency of the cargo and passenger compartments, being this very important in small aircraft where each inch of space is remarkable.

Overall, the circular cross-section fuselage provides a versatile and efficient solution for a wide range of aircraft applications, particularly in smaller aircraft where weight, efficiency, and cost are critical factors.

2.3 Double Bubble fuselage structure

The double bubble cross-section is a variation of the oval cross-section that is widely used in the design of modern commercial aircraft, such as Airbus A350 and the Boeing 787 Dreamliner.

The double bubble cross-section owns its name because it is formed by two rounded bubbles in the fuselage design, one on top of the other, creating an ellipsoid shape that looks like two ovals stacked on top of each other. This design provides additional space in the cabin for greater passenger comfort while reducing the overall weight of the aircraft.

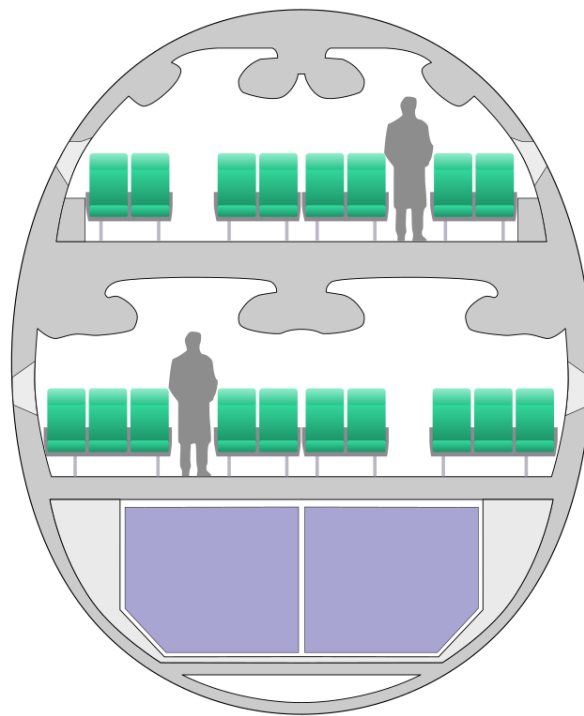


Figure 6. A380 Double bubble cross-section

The double bubble section is achieved through the use of composite hull materials that are lighter and stronger than traditional aluminum. Two air bubbles provide more overhead storage space, and larger windows can make the cabin feel more open and spacious.

The double bubble cross-section also improves aerodynamics, reducing drag on the plane and allowing it to fly more efficiently. The hull shape helps reduce turbulence and reduces cabin noise, providing a more comfortable ride for passengers. The horizontal double bubble cross-section is a type of aircraft fuselage design that features two

circular cross-sections connected by a flattened center section, resulting in a shape that resembles two bubbles side-by-side.

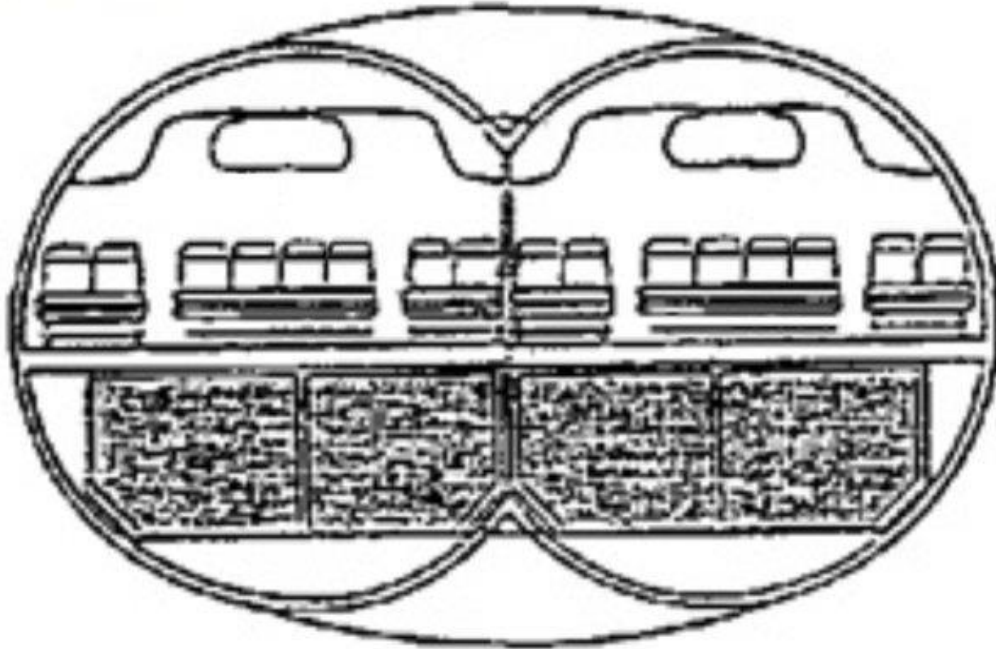


Figure 7. Horizontal double bubble cross-section

The double bubble design increases the cabin volume compared to traditional circular cross-sections, allowing for more passenger or cargo space. Also, the flattened section of the fuselage reduces drag and turbulences, which can improve the aircraft's performance and fuel efficiency. The double bubble shape also reduces the wing-body interference, which further enhances the aerodynamic performance.

To sum up, the horizontal double bubble fuselage is a new and efficient design that offers many benefits to aircraft manufacturers, airlines, and passengers. This design is becoming popular in the regional and narrow-body aircraft market, as it allows for having more comfortable aircraft, with greater capacity and with a higher fuel efficiency.

2.4 Aurora's proposal

There is an existing project with this idea that is Aurora D8. This project was started by Aurora Flight, the Massachusetts Institute of Technology (MIT) and Pratt & Whitney with the financing of NASA. Aurora D8 is aimed to be a low consume aircraft with a capacity of 180 seats and a range of 3000 nautical miles, which fits perfectly in the market of A320 and Boeing 737

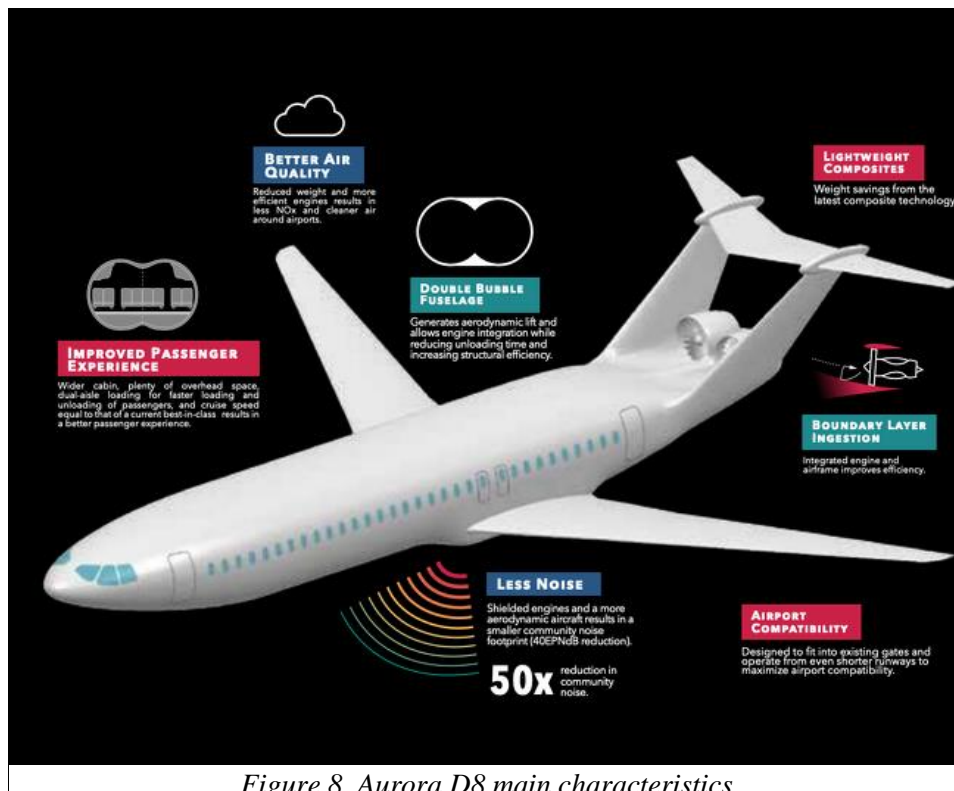


Figure 8. Aurora D8 main characteristics

Aurora D8 aircraft design eliminates the traditional tail section and places the engines at the rear of the aircraft, which is expected to provide greater fuel efficiency and reduced noise levels compared to traditional aircraft designs. This new location gives the aircraft a great reduction of the wake drag due to the fact that the motor's wake drag is into the fuselage wake drag.

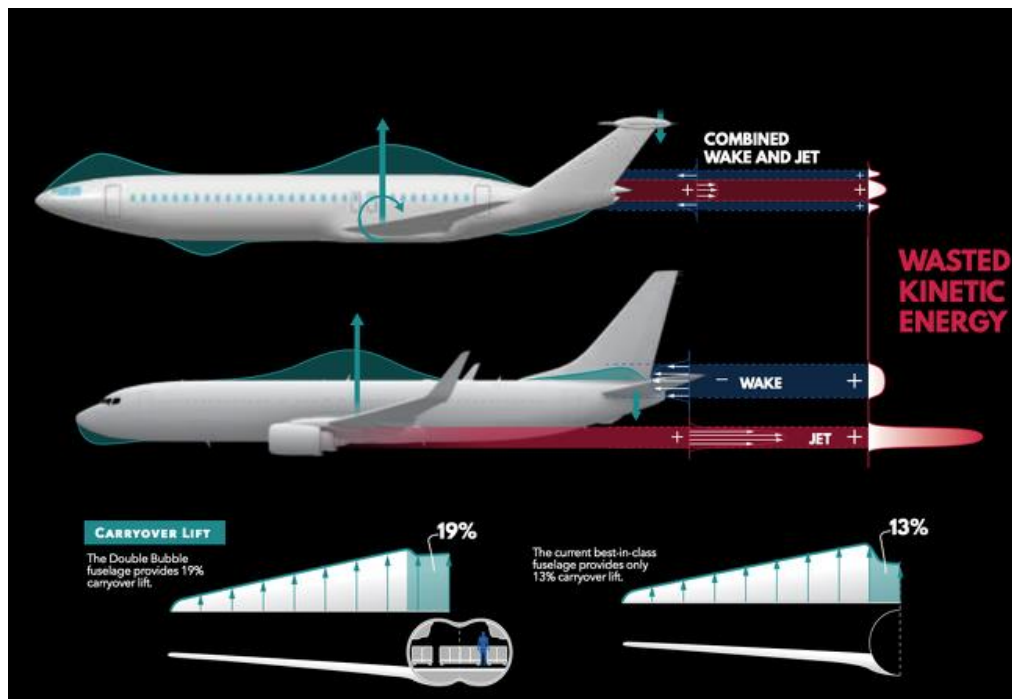


Figure 9. Aurora D8 Drag and lift distribution

According to Boeing, the Aurora D8 is 70 percent more fuel efficient than current aircraft. The aircraft design allows for a more aerodynamic shape, which reduces drag and improves fuel efficiency.

Placing the engine at the rear of the aircraft is expected to reduce noise levels for passengers and ground crew. The Aurora D8's increased fuel efficiency can significantly reduce the aircraft's environmental impact and could be an attractive feature for airlines looking to reduce their carbon footprint.

The Aurora D8 has the potential to offer a larger passenger capacity than traditional aircraft designs. The wide and flattened body of the aircraft provides more usable space for passengers, and the absence of a tail section allows for more flexibility in seating arrangements.



Figure 10. Aurora D8 conceptual design

The future of the Aurora D8 remains uncertain currently. While the aircraft design represents an innovative approach to commercial aviation, it is still in the concept phase, and there are no immediate plans to build a prototype or bring the aircraft to market.

Developing a new aircraft design is a complex and expensive process that requires significant investment, research, and testing. Before the Aurora D8 can become a reality, it will need to undergo extensive testing and certification processes to ensure that it meets safety and performance standards.

2.5 Airbus' proposal

Before Airbus launched the A380, they considered multiple designs for their new project. Boeing 747 has been dominating the high-capacity market since 70's and Airbus was aiming to enter that market with a new design.

Airbus studied the possibility of placing two bubbles side by side instead of having the bubbles on top of each other as we see in A380.

The project that Airbus developed of the double bubble aircraft was called Airbus P500. This project was aiming to encase two fuselages in a single outer fuselage having it the shape of an oval. This aircraft adopted the name P500 because of its capacity which could have been of 500 passengers.

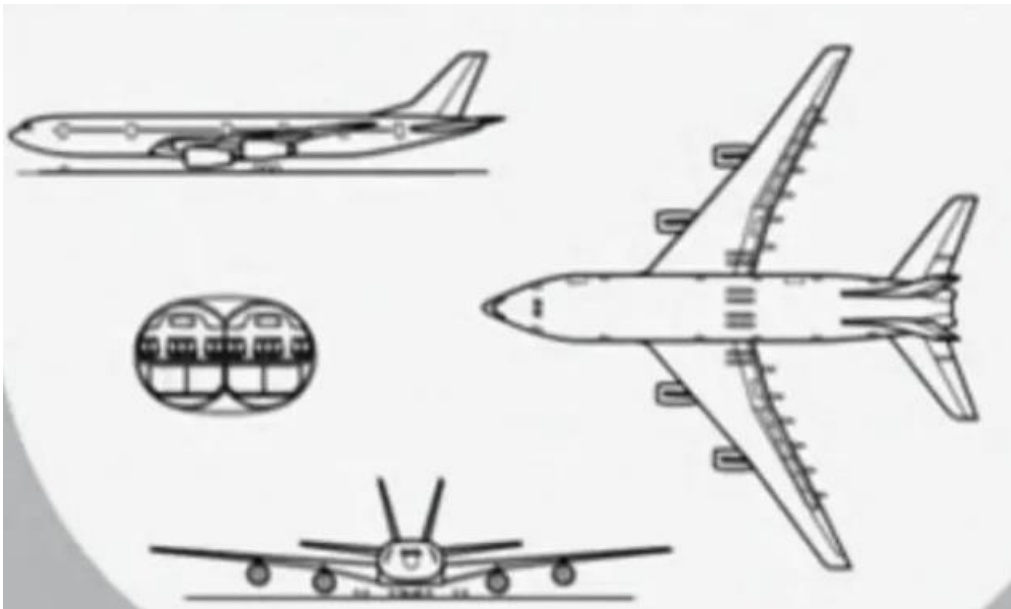


Figure 11. Airbus P500 sketches

The highest challenge that Airbus faced in this project was the distribution of seats. The aircraft was planned to have 16 seats per row divided into four aisles, but this could be a problem when evacuating the aircraft quickly and effectively in a possible emergency. Finally, Airbus decided not to take the risk of the difficult evacuation and opted for designing the double bubble vertically giving rise to A380

2.6 Russian proposal

Russia also thought about developing a design of a wide body aircraft using new fuselage structures and design configurations. This project started in 1991 was called Frigate Ecojet and was initially aiming to transport up to 500 passengers. The main objective of this aircraft was to create a wide body aircraft with medium haul operability that was intended to enter into service in 2018.



Figure 12. Frigate Ecojet concept design

The fuselage cross-section of the aircraft has an ovoid shape, giving the aircraft a capacity up to 400 passengers in one economy class layout. In three class layout, the aircraft could transport between 300 and 350 passengers with three aisles of 500 mm minimum wide and 810 mm of minimum space between seats.

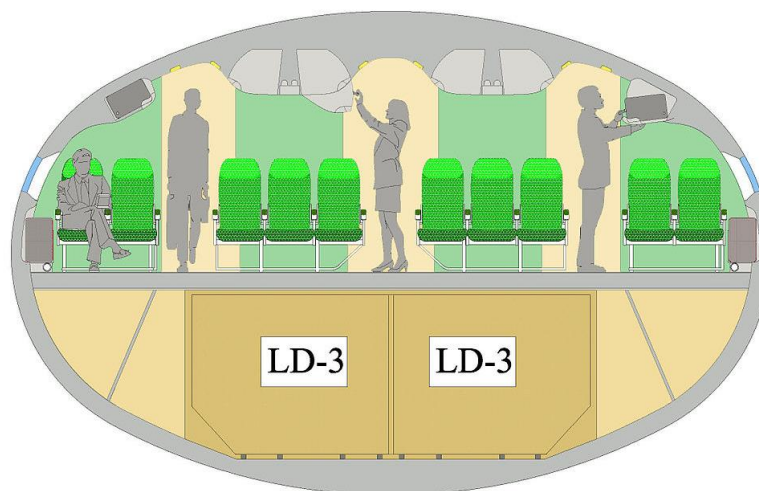


Figure 13. Frigate Ecojet Fuselage cross-section view

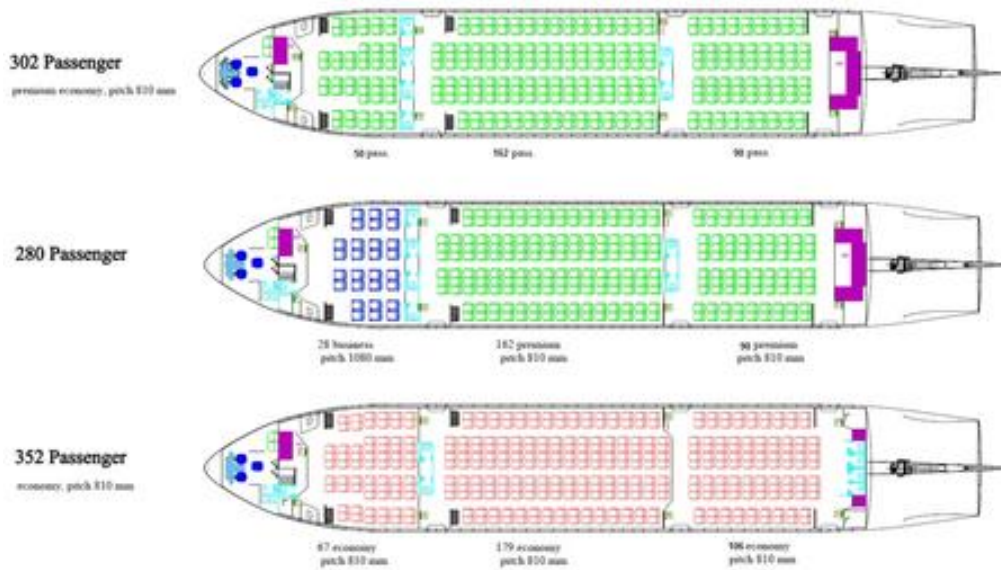


Figure 14. Frigate Ecojet cabin arrangement

In 2015, the company decided to relocate from Moscow to an undisclosed non-EU European country, applying for flight certification to EASA rather than Russia, as the host country determined that the certification would be cheaper. If the company was based in a country that has EASA certification, the aircraft would receive both EASA and FAA certification by doing only one program test. Moving the company to Europe, they also looked to cooperate with other companies in the cockpit design and so reduce the pilot training costs

In 2017, the Ecojet twin engine design was initially propelled by two PD-18 R or PS-90 A20 of a force of 177 – 226 KN (40.000 - 51.000 lbs) and evolved to a four engines design adopting the name of Freejet and being propelled by Pratt & Whitney PW1100G or CFM International LEAP that are the engines used in A320neo and B737 MAX. This change in the engine design increases the weight and reduces the aerodynamics but increases the maximum take-off weight in 10 t for a range of 3.500 km with 300 passengers in full economy configuration.

2.7 Boundary layer ingestion

There are a lot of different concepts that have been proposed as a possibility for future aircraft with the intention of reducing fuel consumption and reaching more efficient aircraft designs.

The boundary layer ingestion is a concept in aircraft design where the engines are located in a way that they can ingest the slow-moving boundary layer air that flows along the surface of the fuselage and wings of an aircraft. This boundary layer air is typically slower-moving and higher in pressure than the air outside of it, which can lead to increased fuel efficiency and reduced noise levels.



Figure 15. Boundary layer ingestion description of Aurora D8

This technology could potentially offer several benefits such as improved fuel efficiency by ingesting slower moving air leading to a better operation. The location of the engines also leads to the possibility of adding space in the wings or fuselage so as to increase payloads. This proposal will enable the aircraft to fly longer distances or remain in the air for longer periods of time without needing to refuel due to the boundary layer ingestion benefits.

However, there are also some challenges associated with boundary layer ingestion. For example, the engines must be designed to tolerate the turbulent airflow created by the boundary layer air, and the inlet design must be carefully optimized to avoid airflow separation and subsequent loss of efficiency. Despite these challenges, boundary layer ingestion technology is being actively studied by aerospace engineers and several

research programs are currently underway to explore its potential for future aircraft design

2.8 Service possibilities

Air traffic has been increasing linearly during the last 50 years and is expected to continue growing in the following years by at least 5%. This has resulted in an emphasis on emissions reduction and low fuel consumption, trying to manufacture more efficient and environmental-friendly aircraft

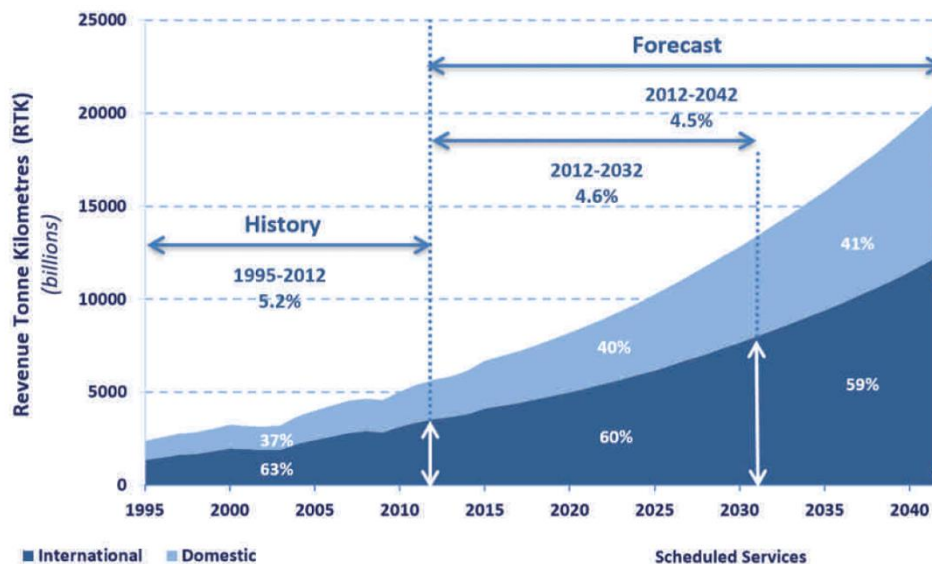


Figure 16. ICAO prediction for future air traffic

In addition to this, designing a different concept from the one that we have nowadays, and we have been using during the last 50 years with hardly any variation and also the possibility to increase the number of passengers in a single aircraft only by modifying the fuselage structure. Having more passengers will be a huge opportunity for the future as air transport is growing with leaps and bounds due to the fact that, as previously mentioned, the number of users of this kind of transport could duplicate the actual one in the next years.

The horizontal double bubble aircraft could be proposed as a potential solution for the middle of the market segment. The unique wide-body and flattened cross-section design of a horizontal double bubble could offer several advantages over traditional narrow-body planes, including improved fuel efficiency, increased passenger comfort and reduced noise levels.

In addition, the horizontal double bubble cross-section could potentially offer a lower cost per seat than traditional mid-sized planes, due to its improved aerodynamics and reduced fuel consumption, which will lead to a reduction of the prices by the airlines.

Considering all the characteristics of this design, the fuel consumption could be highly reduced thanks to the boundary layer ingestion of the motors. The new concept could revolutionize the idea that we have currently and evolve it into a more sustainable, efficient, and silent aviation in the future.

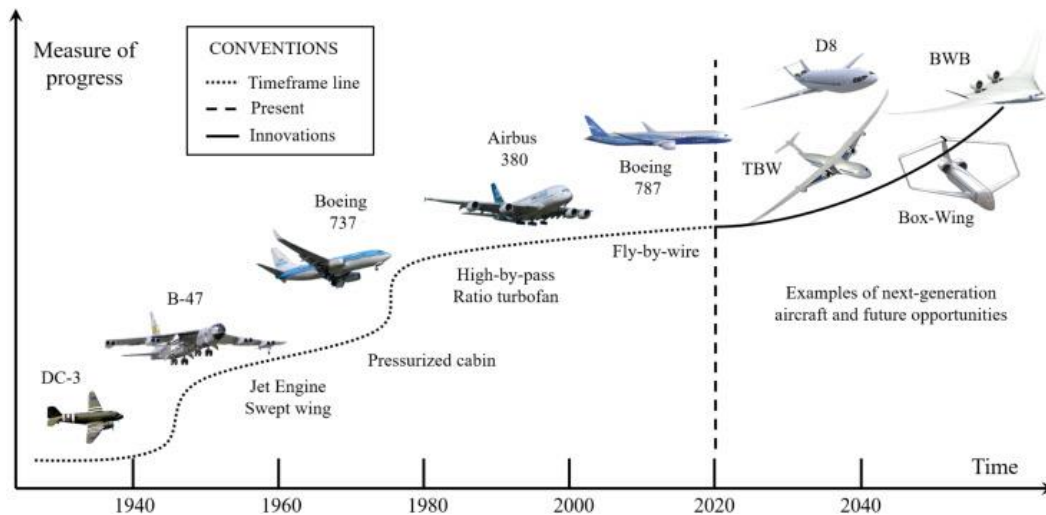


Table 3. Evolution of aircraft designs in the history and future opportunities

However, if the horizontal double bubble reaches an efficient and viable design for the middle of the market segment, it could offer a great range of benefits to airlines and passengers alike, and help shape the future of air travel.

Chapter 3. Aircraft design

3.1 Introduction

This chapter is going to go through the design of the horizontal double bubble aircraft that is going to be called ATR-1. This chapter starts with the initial sketches and drawings of the double bubble idea and then it will cover more specific aspects such as the kind of tail selected, the cross-section and wing dimensions, etc.

At the time of designing the aircraft, the size and dimensions are chosen taking into account other ideas and designs such as the ones mentioned in the previous chapter

3.2 Preliminary designs

The preliminary design of a double bubble fuselage involves several key elements. These elements are going to be studied in detail in this section.

The double bubble fuselage design is a unique aircraft design that has several distinct design elements that differentiate it from traditional aircraft designs. These design elements contribute to improving aerodynamic efficiency, increase passenger comfort, and reduce operating costs. In this section, some of the key design elements of the double bubble fuselage are going to be discussed.

3.2.1 First sketches

First of all, some preliminary sketches of ATR-1 double bubble aircraft are in order to have an idea follow during the final design. The aircraft will use a different type of tail which will be composed of two vertical tail planes and a horizontal tail plane placed on the top of both vertical ones, as can be seen in the design of Aurora D8 and in the figure below.

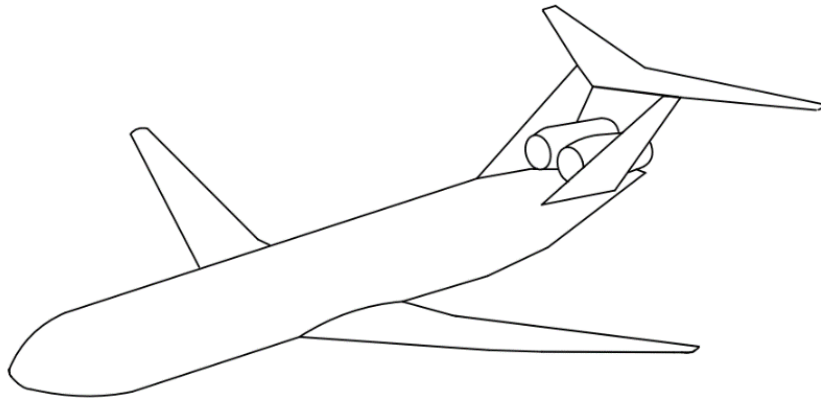


Figure 18. Sketch isometric view

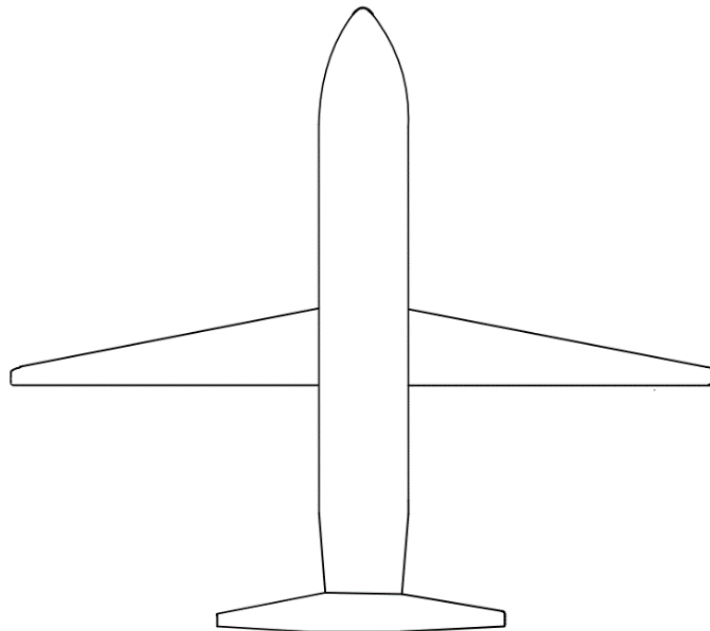


Figure 17. Sketch top view

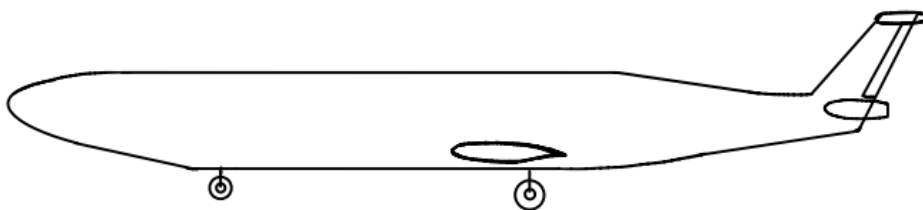


Figure 19. Sketch side view

3.2.2 Fuselage shape

The shape of the double bubble fuselage is going to be an ovoid. This ovoid shape of the fuselage is going to be the most distinctive element of the design. The shape of the fuselage is wider and bigger than in a traditional commercial aircraft which reduces the turbulences and drag created by the structure and offers less fuel consumption and better comfort to the passengers due to the noise reduction.

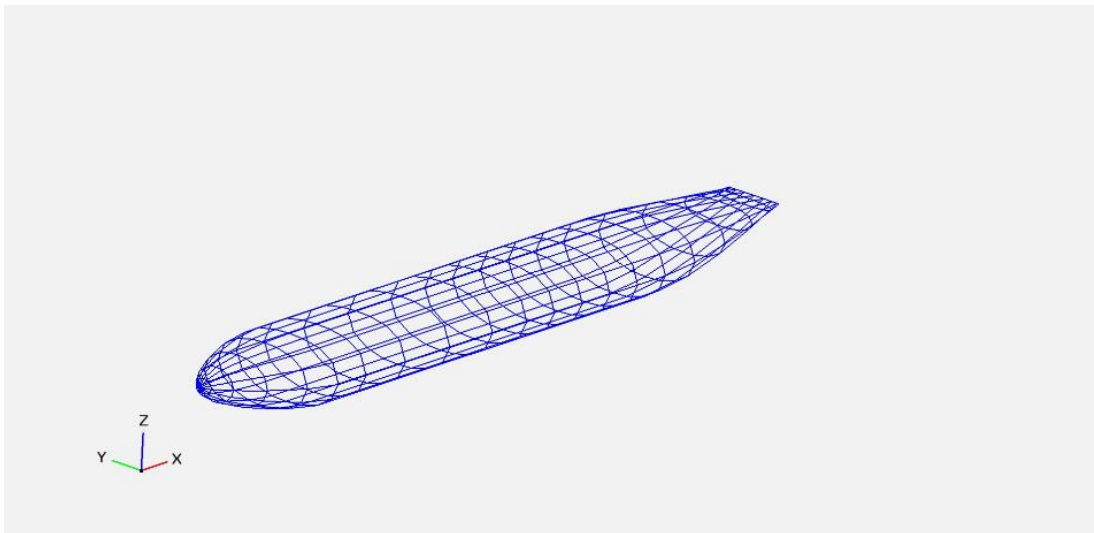


Figure 21. Fuselage isometric view

3.2.3 Cross-Section

The double bubble cross-section of the fuselage makes this kind of design unique. The double bubble fuselage comes from the union of two circular fuselages and allows for improving the cabin space and getting higher aspect ratio wings which means weakening the wing tip vortices, creating less drag and increasing fuel efficiency.

As aircraft are designed from the inside out, in order to fit eight passengers per row comfortably, two circular sections of 1,36 meters of radius are going to conform the double bubble cross-section of the aircraft as can be seen in the figure below.

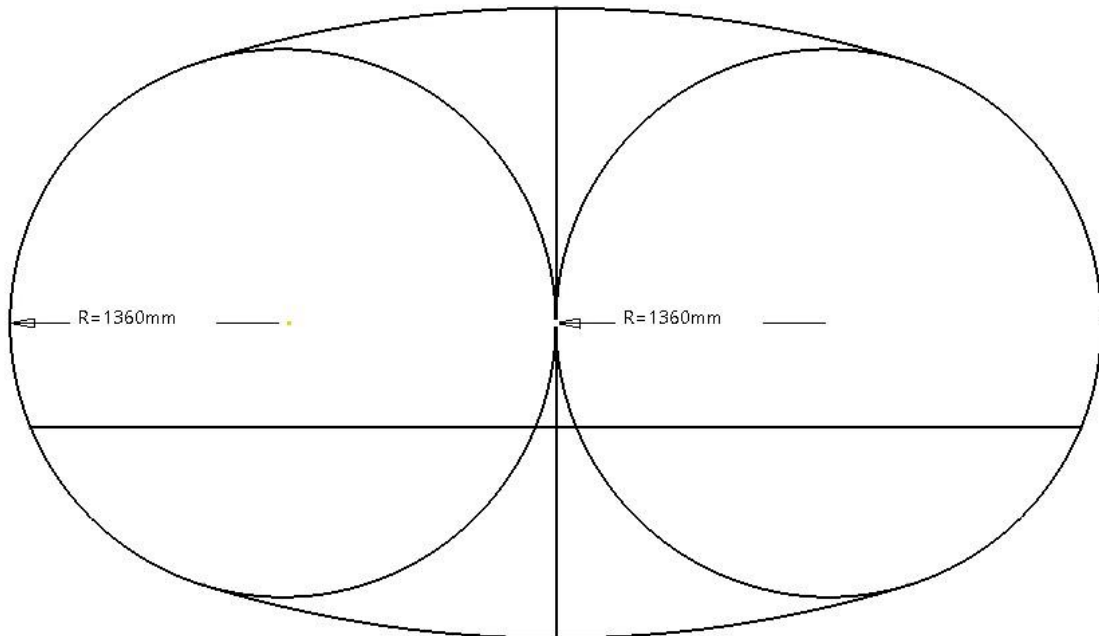


Figure 22. Double bubble cross-section layout

3.2.4 Engine location

Another important aspect in the design of horizontal double bubble aircraft is the location of the engines. Traditionally, aircraft engines are located at the wings, but in this horizontal double bubble design, the engines are going to be placed on top of the fuselage between the vertical tail planes. This location allows for boundary layer ingestion which means less fuel consumption taking advantage of the slower airflow and also reduces the noise levels inside and outside the aircraft, resulting in a more comfortable experience for passengers.

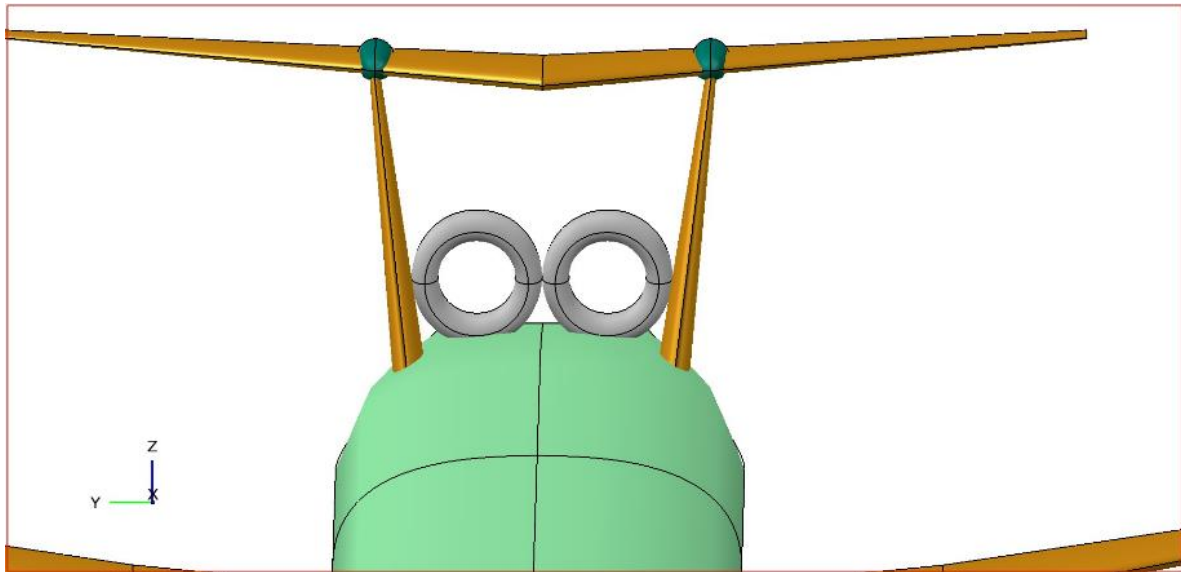


Figure 23. Front view of the engine location

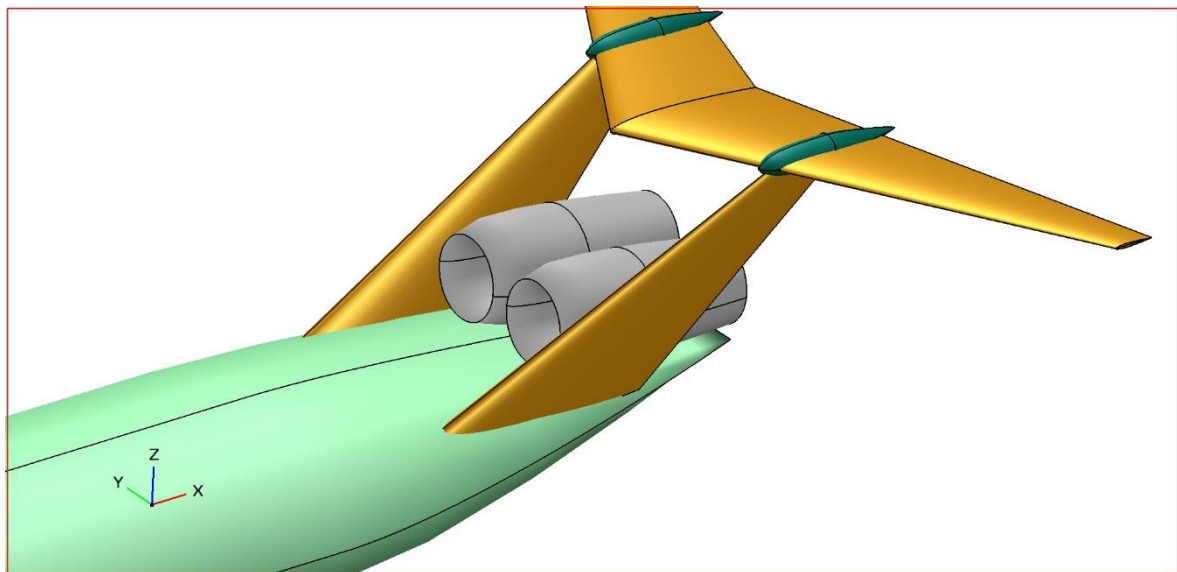


Figure 24. Isometric view of engines

In summary, the horizontal double bubble design incorporates important design elements that enhance aerodynamic efficiency, passenger comfort, and reduce operational costs. The ovoid cross-sectional, the fuselage shape and the engine location are three key features that make this innovative design stand out. This design is an innovative idea in aircraft manufacturing which means several improvements in costs and efficiency.

3.3 Final design

After the preliminary designs is done, the final design is reached in this part and each part of the aircraft will be shown with its corresponding dimensions.

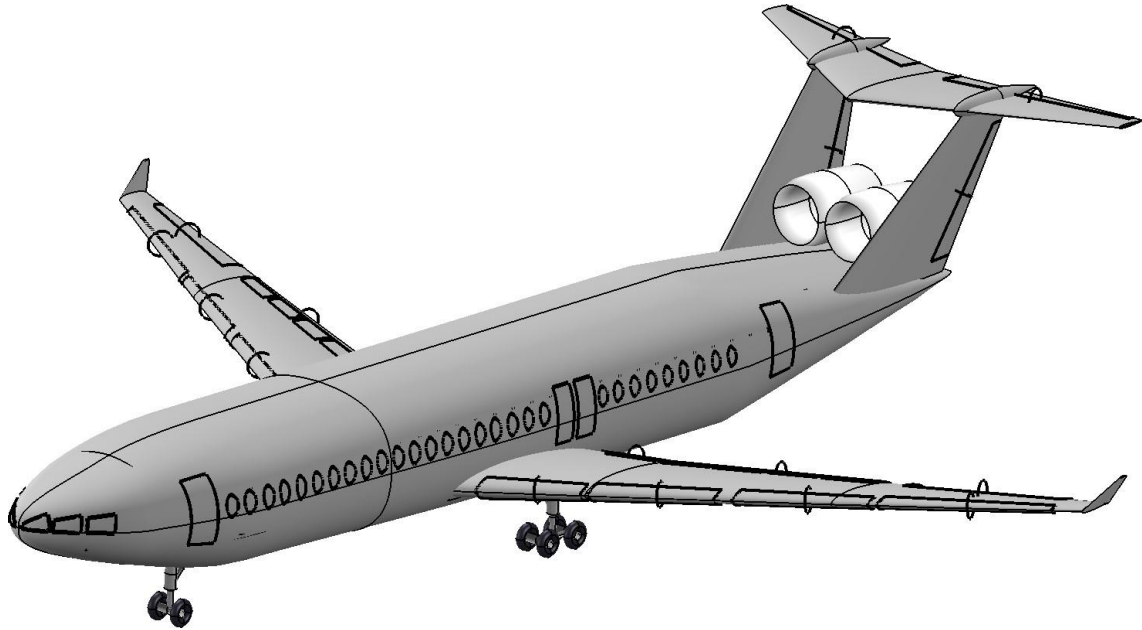


Figure 25. Final design isometric view

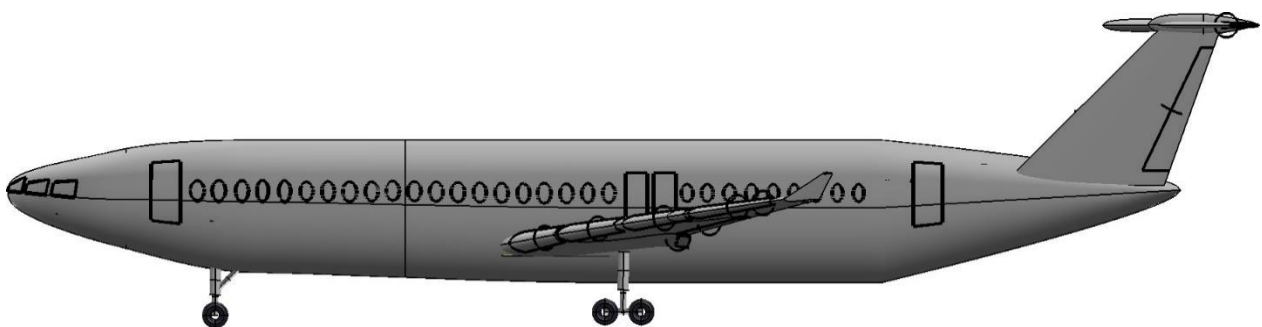


Figure 26. Final design left view

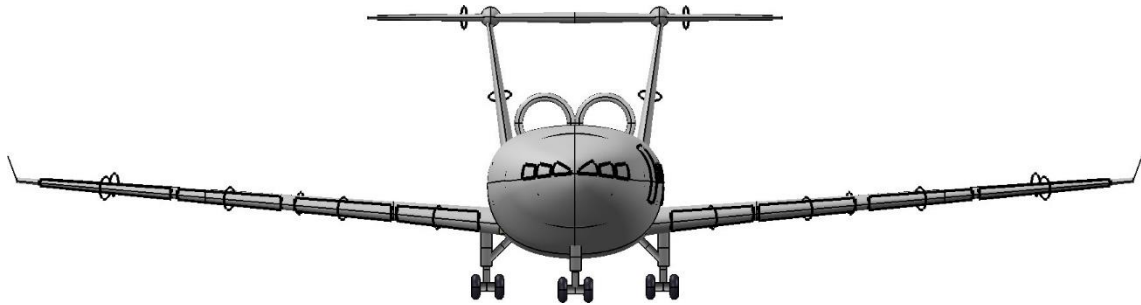


Figure 27. Final design front view

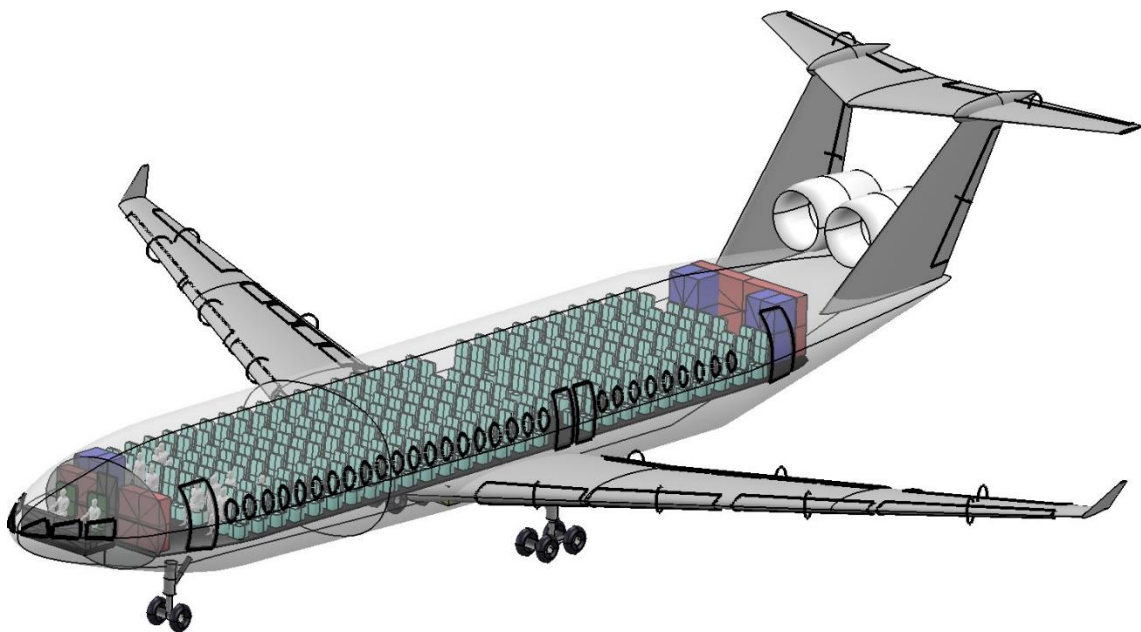


Figure 28. Final design with translucent fuselage

3.4 Fuselage

3.4.1 Cross-section

The design of the cross-section is one of the most important aspects in the design of an aircraft because it has an important impact on the performance and efficiency of the aircraft. In terms of cabin space, the double bubble gives us the advantage of increasing the passenger capacity per row of seats as well as a bigger cargo capacity than conventional cross-sections can offer.

The final design for the double bubble cross-section has been carried out taking into account the seat layout, looking for taking advantage of the space given by this kind of cross-section. Having a wider cross-section involves also higher weight because it will need reinforcements to support the loads of expansion and compression that will be generated due to pressure. The thickness of the fuselage, which is going to be higher in this kind of section must taken into account in the final design.

The final design of the cross-section shape including the seat location and the cargo compartment is shown in the picture below.

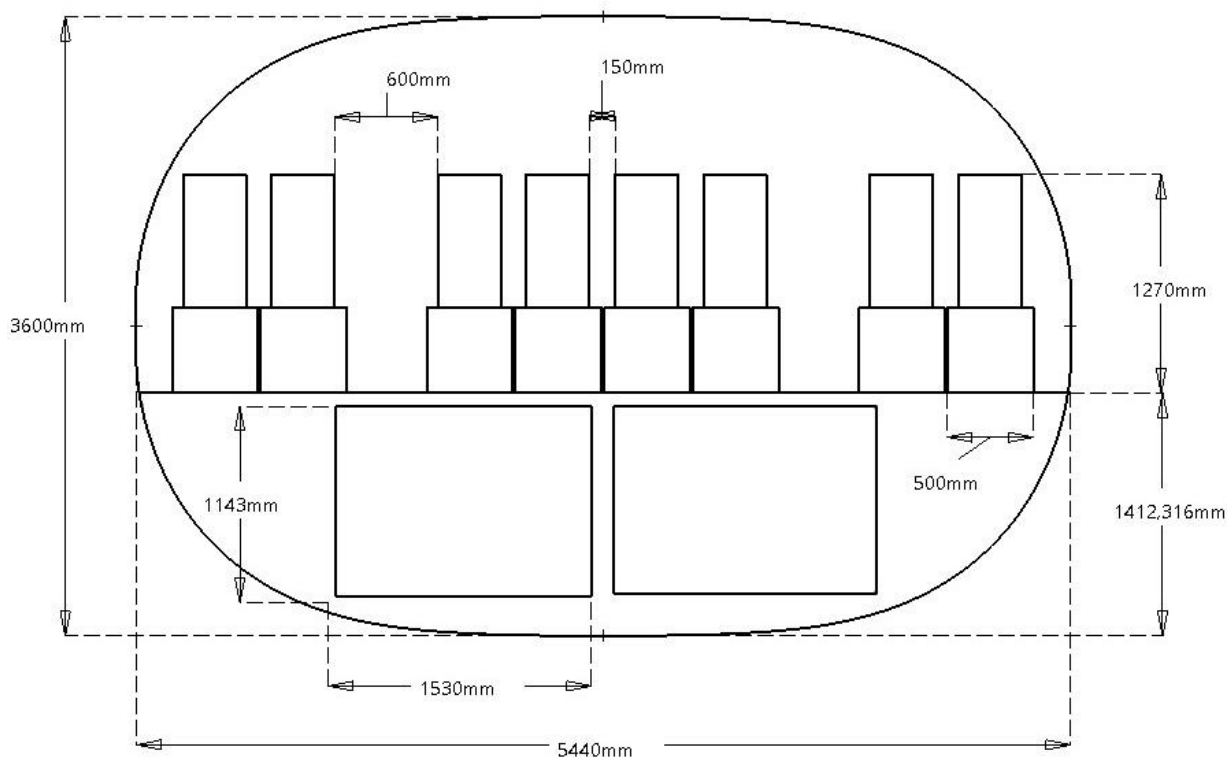


Figure 29. Cross-section final design

The location of the floor is a key aspect so as to take advantage of the space generated by the double bubble. In the picture shown upwards, the wider part of the cross-section is used for placing the door and the seats in order to have eight seats per row and therefore have the maximum passenger per row number possible. Besides, it reminds a wide cargo compartment where a LD3-45 cargo container fits perfectly but will remain a lot of free space. In order to solve this problem, two LD3-45 containers will be placed transversally in the cargo compartment filling more space. The rest of the cargo compartment could be used for bulk cargo, passenger suitcases and integrating the aircraft systems.

The double bubble design also has the objective of giving the passengers a more comfortable experience on board, this is reached by offering wider seats, aisles and higher pitch distance than a low-cost carrier aircraft. In the picture below, can be seen how seats and humans will be after modeling it in 3D using Open Vsp.

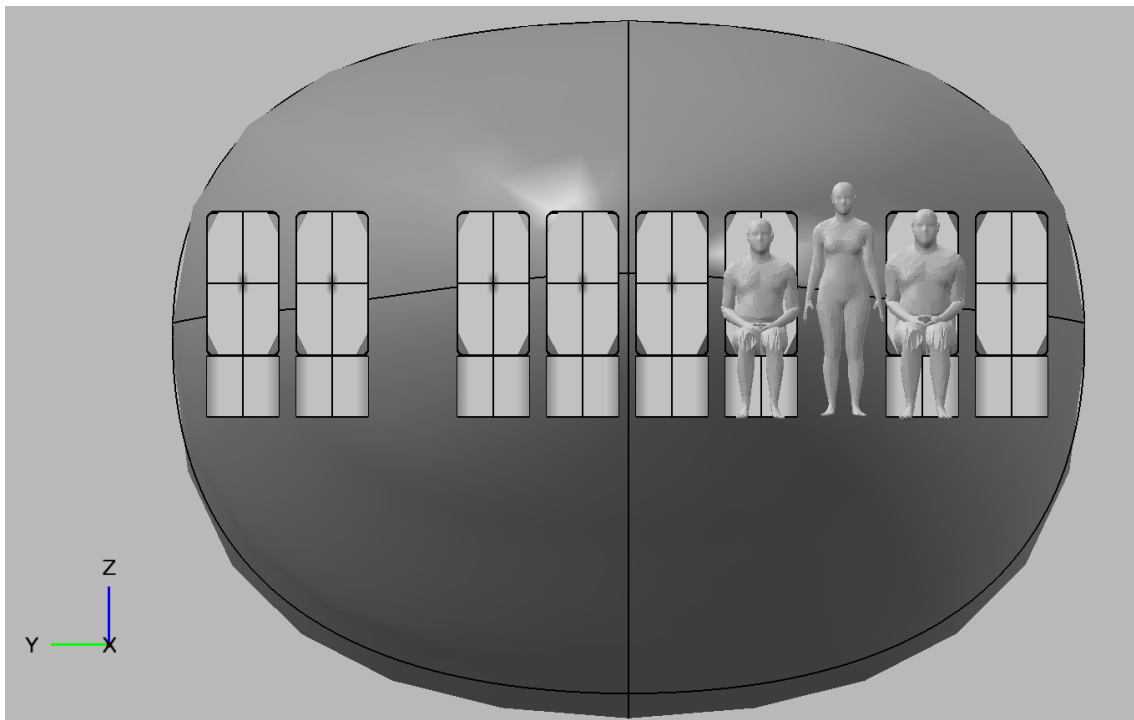


Figure 30. Passengers located in the cross-section

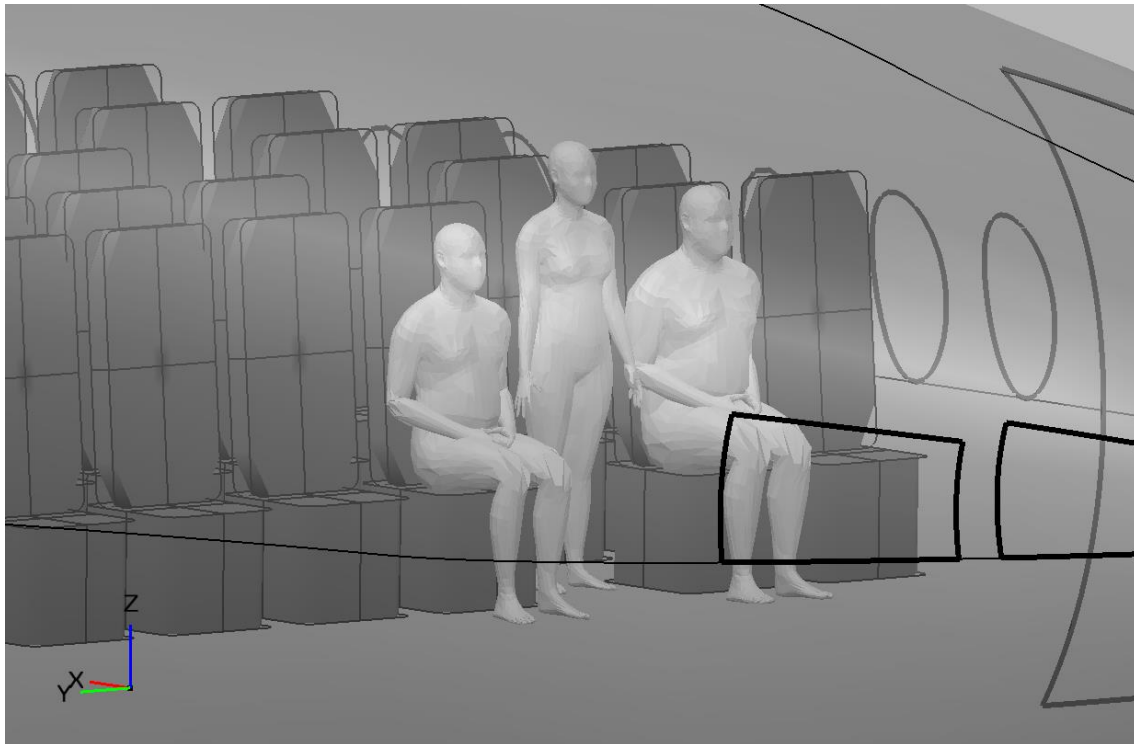


Figure 31. Isometric view of the passengers and seats

The humans shown in the picture have the average dimensions of stature, weight and BMI that can be seen in the graph below:

3D Human	6 th Seat	Aisle	7 th seat
Gender	Male	Female	Male
Age	38	30	49
Stature	1.8 m	1.634 m	1.88 m
Mass	89.04 kg	65.680 kg	140.66 kg
BMI	0.484	0.314	0.950

Table 4. 3D Human physical dimensions

The aircraft is designed for a single configuration of seats, in which the gap between seats is 150 mm, the aisle gap is 500 mm and the seat width is of 500 mm. These dimensions fit perfectly with the normal business-class seats in commercial aircraft

giving all the passengers an extra comfort compared with most aircraft that operate in this market segment.

3.4.2 Seats configuration

The seat configuration must be designed taking into account the aimed number of passengers for the middle of the market segment. Passengers' comfort, safety, emergency exits and accessibility are considered in this segment as well as the lavatories and galleys, in order to optimize the passenger experience.

The aircraft cabin has been designed in a single business class configuration which gives the passengers an extra of comfort and a better experience apart from taking them from one place to another.

The increment of passengers per row with respect to other competitors of the segment as A321 and Boeing 737 has been achieved

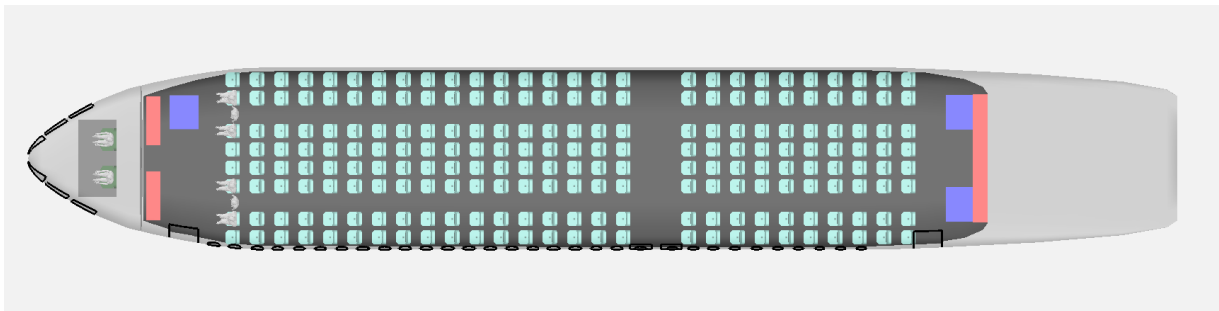


Figure 32. Seat configuration

This layout of the seats has a capacity for 216 passengers with a 2-4-2 configuration and counts with two aisles of 500 mm wide, a gap between seats of 140 mm and a seat pitch of 850 mm. There are 17 rows until the emergency exits and 10 rows after the exits.

The blue squares that are located front and back of the cabin are the toilets while the red ones are the galleys.

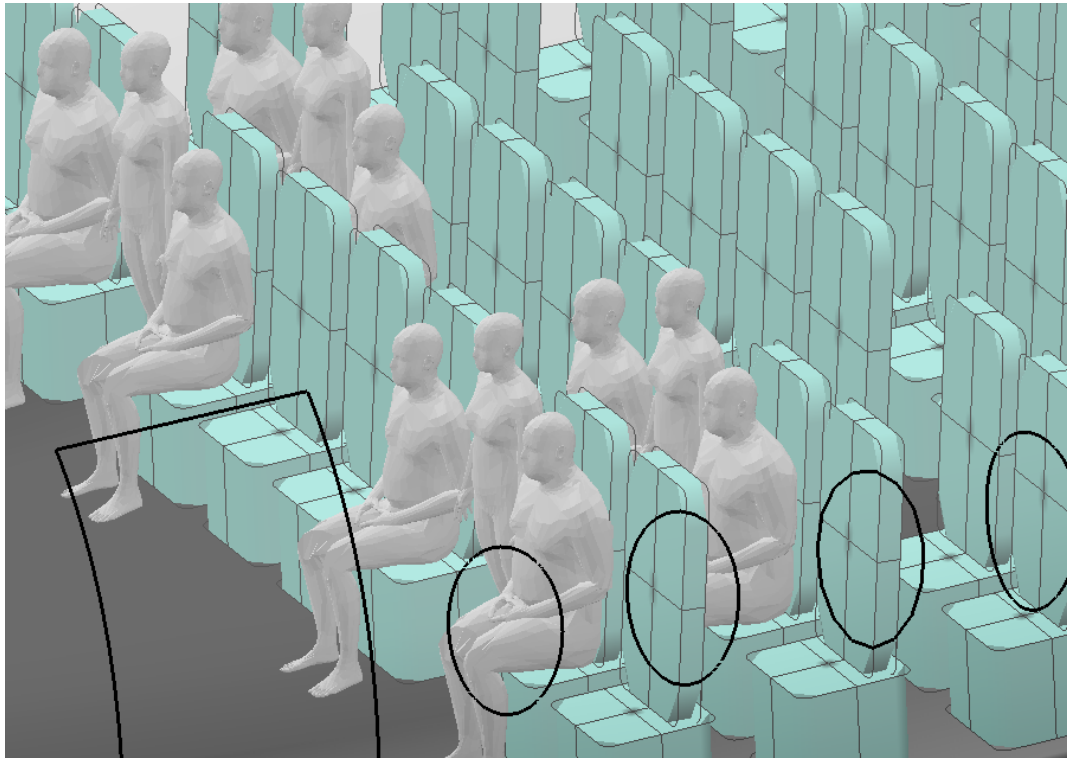


Figure 33. isometric view of cabin layout

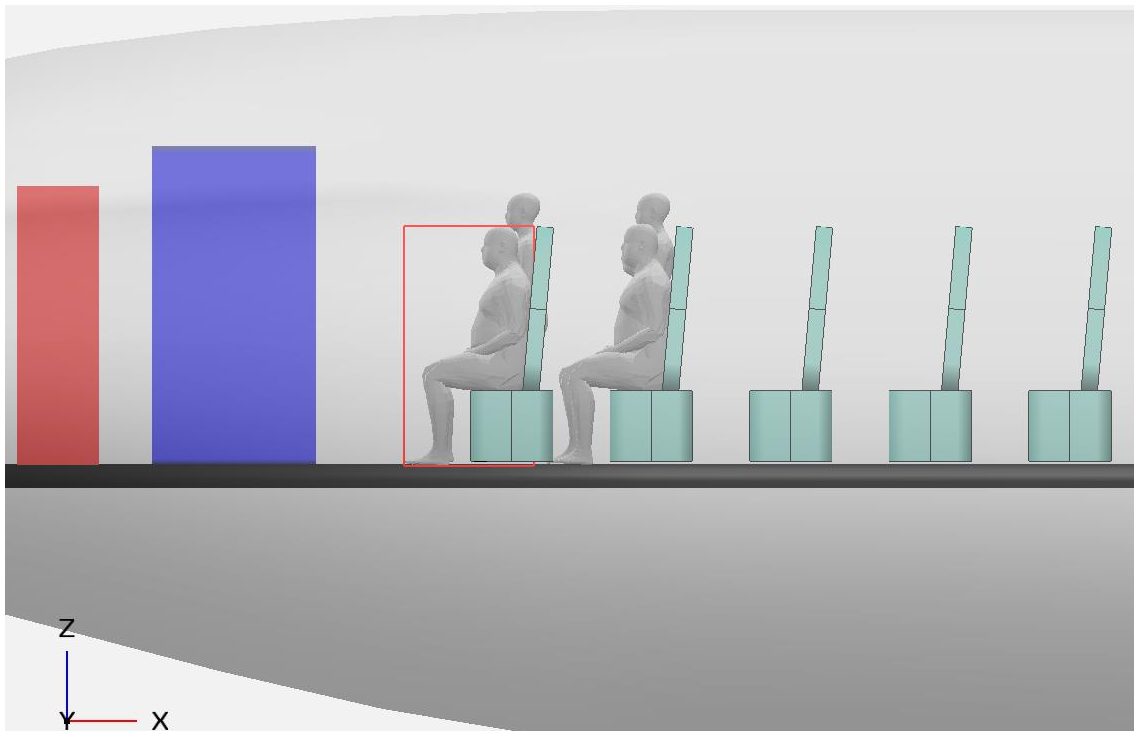


Figure 34. Side view of the cabin layout with passengers

3.4.3 Cargo distribution

As shown in Figure 25, behind the floor of the cabin there is large space for a cargo compartment although the double bubble cross-section is wider than higher. The container that fits better to the compartment is LD3-45 which is the same that other competitors in the middle of the market use for their circular cross-sections, like A320 A319 and A321, and in terms of operability is better than choosing a different one.

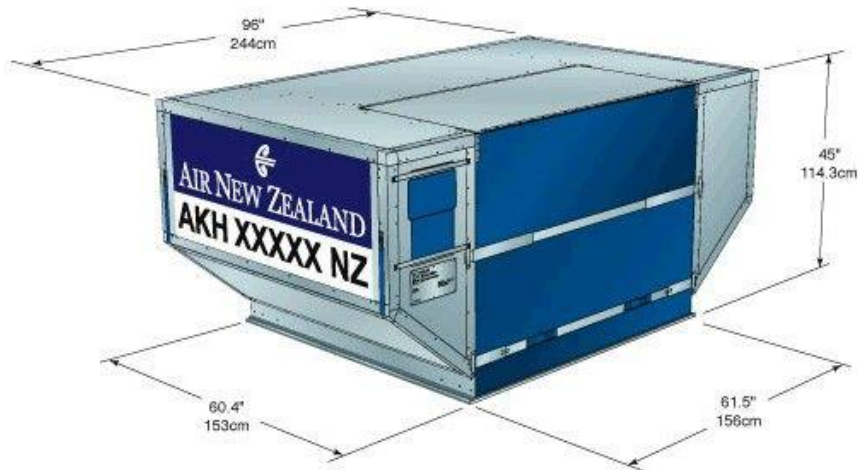


Figure 35. LD3-45 container dimensions

Technical Specifications		
IATA		AKH
NAS3610 class		2K2C
Nordisk P/N		126540-1()
Base size	1534 x 1562 mm	60.4 x 61.5 in
Height	1143 mm	45 in
Roof length	2438 mm	96 in
Max. gross weight	1588 kg	3500 lb
Internal volume	3.7 cu m	131 cu ft
External volume	3.9 cu m	138 cu ft
Door opening	1422 x 1090 mm	56 x 42.9 in
Tare weight from	80 kg	176 lb

Table 5. LD3-45 Container technical specifications

As mentioned before, the containers will be placed transversally, which allows us to take better advantage of the space and increment the number of containers that the aircraft can get inside.

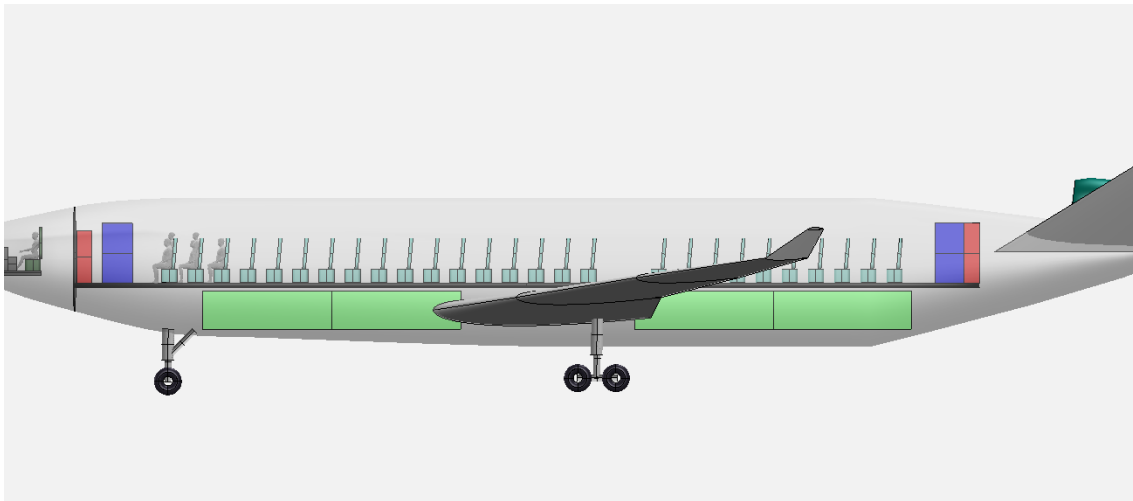


Figure 36. Cargo compartment location

The cargo compartment is represented in green color, the first one has a length of 8.4 meters and the rear one has a length of 9 meters. Both are limited in space, the one that is forward is limited by the front landing gear and the wing box while the afterward compartment is limited by the fuselage end and the wing box.

Taking into account the position of the containers, which are going to be placed transversally, and their dimensions, we can place a total number of 14 LD3-45 containers between both cargo compartments.

3.4.1 Cargo doors

The aircraft has three cargo doors on the right side and another one on the left side. Assuming that the containers must enter transversally in the cargo compartment to avoid rotating them inside, and only have to slide then through the balls floor making the process faster.

The dimensions of the cargo doors must be wider than in the rest of commercial aircraft that use LD3-45 containers.



Figure 37. Right side cargo doors

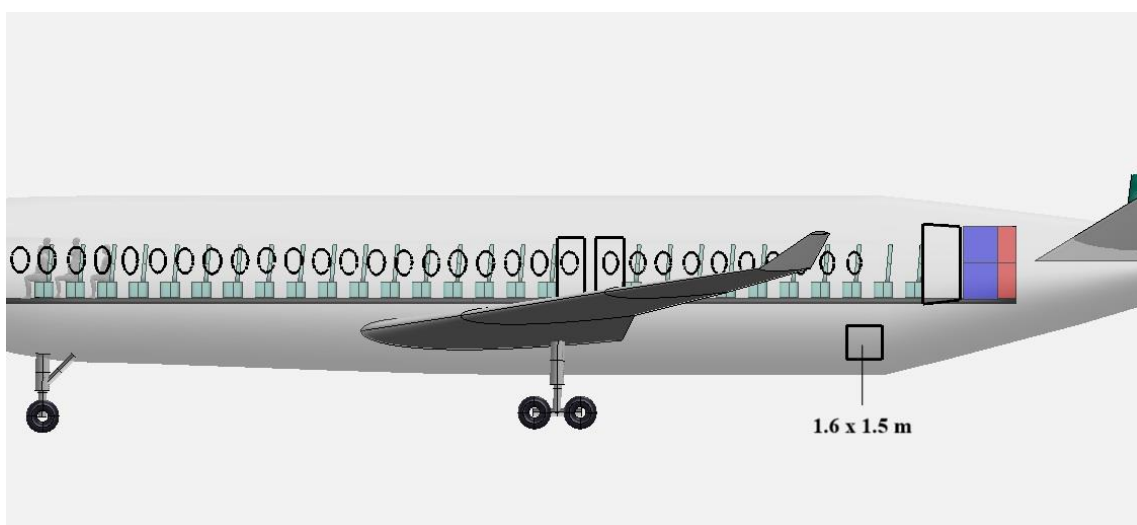


Figure 38. Left side cargo door

As can be seen in the figures, the bigger cargo doors on the right side are bigger and are dedicated to the containers, with dimensions of 2,7 meters wide and 1,5 meters high, while the rear one, which is smaller will be used for bulk cargo, 1,6 meters wide and 1,5 meters high. On the left side, there is only one small cargo door of the same dimensions as the one on the right side.

3.4.2 Passenger's doors

The passenger exits layout is limited by the FAR-25 regulations of the airworthiness standards. These standards must be complied with at the time of designing an aircraft to allow a safe evacuation of the aircraft in case of emergency. The regulation establishes among many other safety measures that an aircraft of more than 44 passengers, including crew members, must be evacuated from the aircraft to the ground within 90 seconds.

The distance between the emergency exit doors of the aircraft shall be less than 60 ft (18,28 meters). The types of doors that are used in the aircraft are two type I and two type A, which allow a maximum number of passengers of 45 and 110 per door respectively.

- Type I: the aircraft has two type I exit doors, both at the mid-section of the fuselage, which are a floor level exit with a rectangular form of not less than 48 inches high (1,22 meters) and 24 inches wide (0,61 meters) according to the FAR-25 regulation.
- Type A: the aircraft has two type A exit doors, one at the front and one at the rear part of the cabin, which are a floor level exits with a rectangular form of no less than 72 inches high (1,83 meters) and 42 inches wide (1,06 meters) with corner radii not greater than 7 inches, according to the FAR-25 regulation

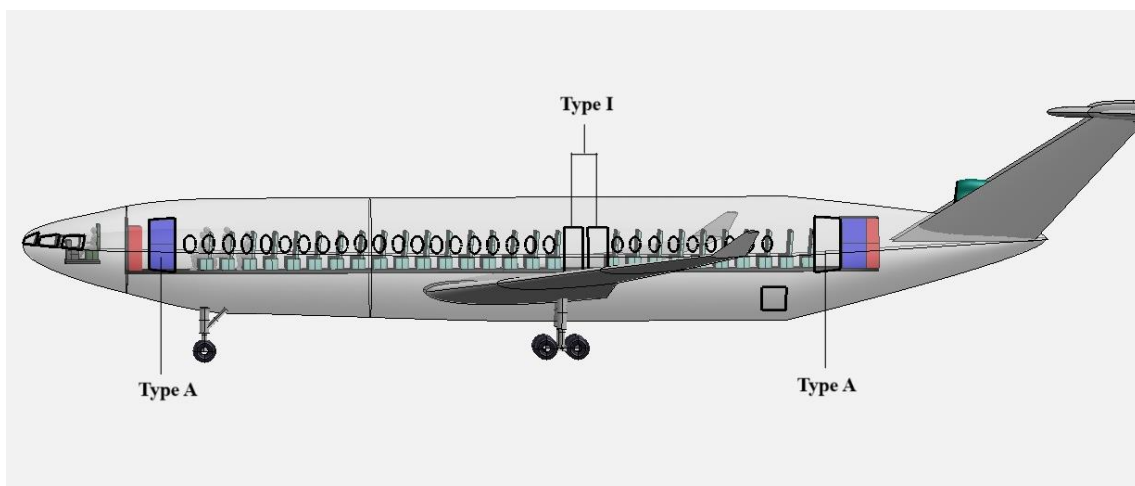


Figure 39. Exit doors left view

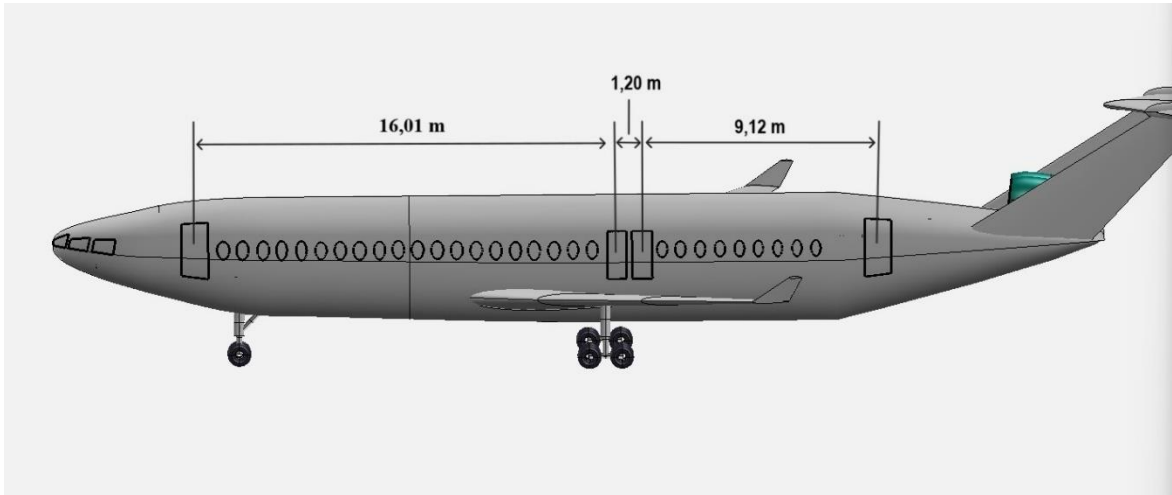


Figure 40. Exit doors distances

3.5 Wings

3.5.1 Airfoil

The airfoil is an essential part of the aerodynamics of aircraft because many properties of aircraft depend on it, such as aerodynamic efficiency, stability, lift generated and flight control.

The kind of airfoil selected for this design is a supercritical airfoil, it is going to give the aircraft a reduced drag at high cruise velocities and so better efficiency, the range of efficient velocities is higher and the maneuverability is going to be improved. In terms of noise, the supercritical airfoil has been demonstrated to produce less noise, been this better for the environment.

The airfoil selected for the aircraft is the NASA SC (2)-0412 which is optimal for Mach 0,7-0,8 that the aircraft is going to reach at cruise and will help to delay the onset of the wave drag at transonic speed

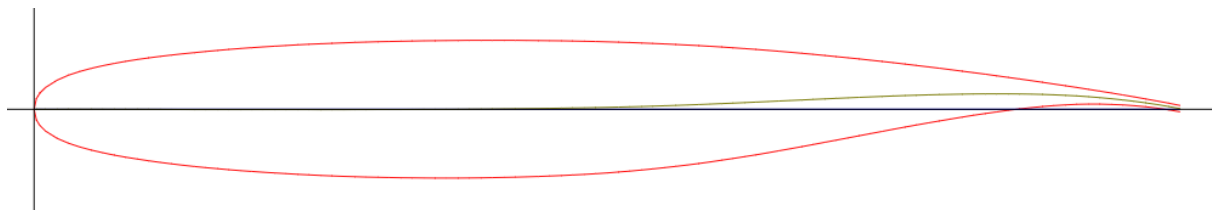


Figure 41. NASA SC (2)-0412 Airfoil

3.5.2 Wing dimensions

In order to choose the dimensions of the wing a weight estimation is going to be done, taking into account the number of passengers of the configuration proposed for payload weight and the maximum take of weight is going to be obtained from comparing different aircraft from the same segment of the market with similar number of passengers and the same number of engines. In the following table can be seen the MTOW and the payload weight Boeing middle of the market aircraft:

	Boeing 737 MAX 8	Boeing 737 MAX 9
MTOW	82.191 kg	88.314 kg
Payload	20.882 kg	23.883 kg

Table 6. Boeing Aircraft weights

In the next table are shown the Airbus aircraft weights:

	A321 Neo	A321
MTOW	97.000 kg	93.500 kg
Payload	21.200 kg	25.300 kg

Table 7. Airbus aircraft weights

To obtain the payload weight that the aircraft is going to have we assume the following data:

- I. Weight of passengers: 90 kg
- II. Passenger luggage: 15 kg
- III. Number of passengers: 216
- IV. Crew members: 2 pilots + 5 flight stewards

$$W_{\text{payload}} = 216 \cdot 15 \text{ kg} + 90 \cdot (216 + 5 + 2) = 23310 \text{ kg}$$

With this data assumption, the payload can be calculated and we obtain a total of 23310 kg of payload weight.

Now, with the calculated payload and with the data from Table 6 and Table 7 we can obtain a linear regression for obtaining the MTOW.

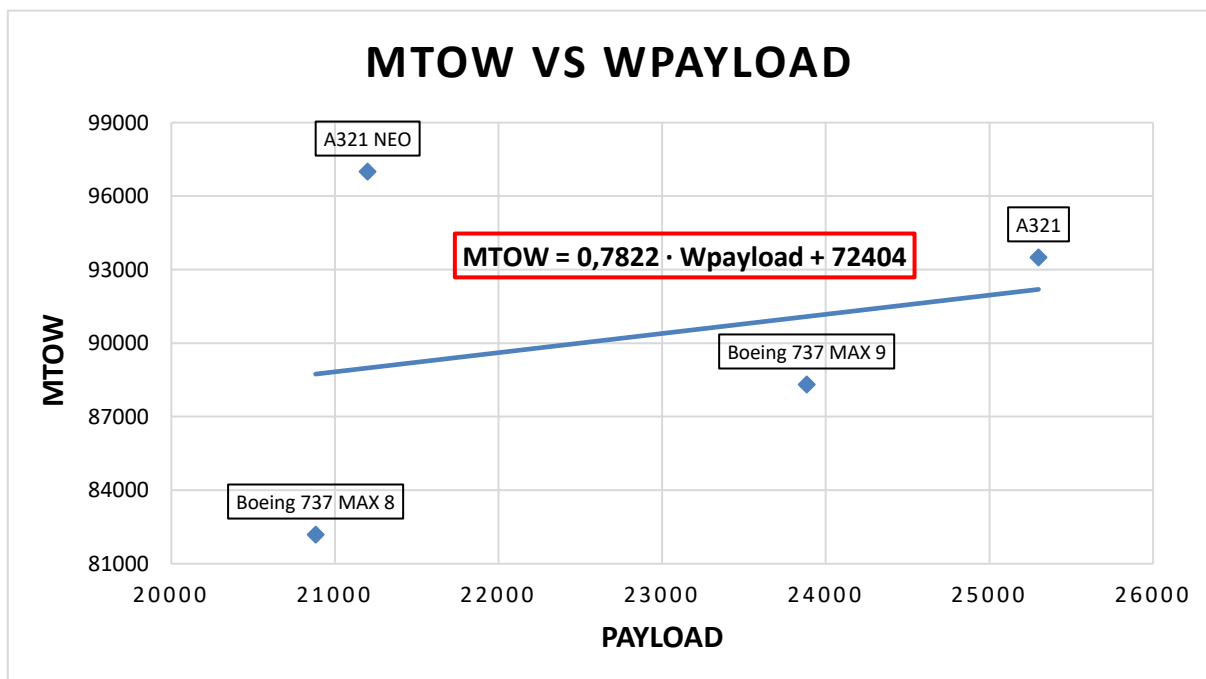


Table 8. MTOW vs Wpayload lineal regression

As it is shown in the table, we can obtain the MTOW using the following formula:

$$\mathbf{MTOW} = 0,7822 \cdot W_{\text{payload}} + 72404 = \mathbf{90637 \text{ kg}}$$

The wing area is calculated by dividing the MTOW by the wing loading. The wing loading can not be calculated with the program but is going to be obtained by searching in the market and comparing results. The A320 family (A318, A319, A320, A321) generally has a wing loading in the range of 105 to 145 pounds per square foot which is 514 to 708 kg/m². For the next calculus is going to be assume a mid-value of 611 kg/m² (5993,91 N/m²).

$$\mathbf{Wing \ Area} = \frac{\mathbf{MTOW}}{\mathbf{Wing \ Loading}} = \frac{90637 \text{ kg} \cdot 9,81}{5999,91 \text{ N/m}^2} = \mathbf{148,19 \text{ m}^2}$$

The rest of the parameters of the aircraft wing like taper ratio, aspect ratio, dihedral and sweep angle are going to be calculated by the same way as the maximum take-off weight, making a correlation between data obtained from other aircraft.

	A310	A319	A320	A320 neo	A321	A321 neo
Taper ratio	0,283	0,24	0,24	0,24	0,24	0,24
Aspect ratio	8,8	9,4	9,4	9,4	9,4	10
1/4 chord sweep angle	28	25	25	25	25	25
dihedral angle	6	6	6	6	6	6

Table 9. A320 family wing parameters

	B 757	B 737- 600	B 737-700	B 737-900
Taper ratio	0,351	0,31	0,31	0,31
Aspect ratio	7,82	9,45	9,45	9,45
1/4 chord sweep angle	25	25,02	25,02	25,02
dihedral angle	5	6	6	6

Table 10. Boeing aircraft wing parameters

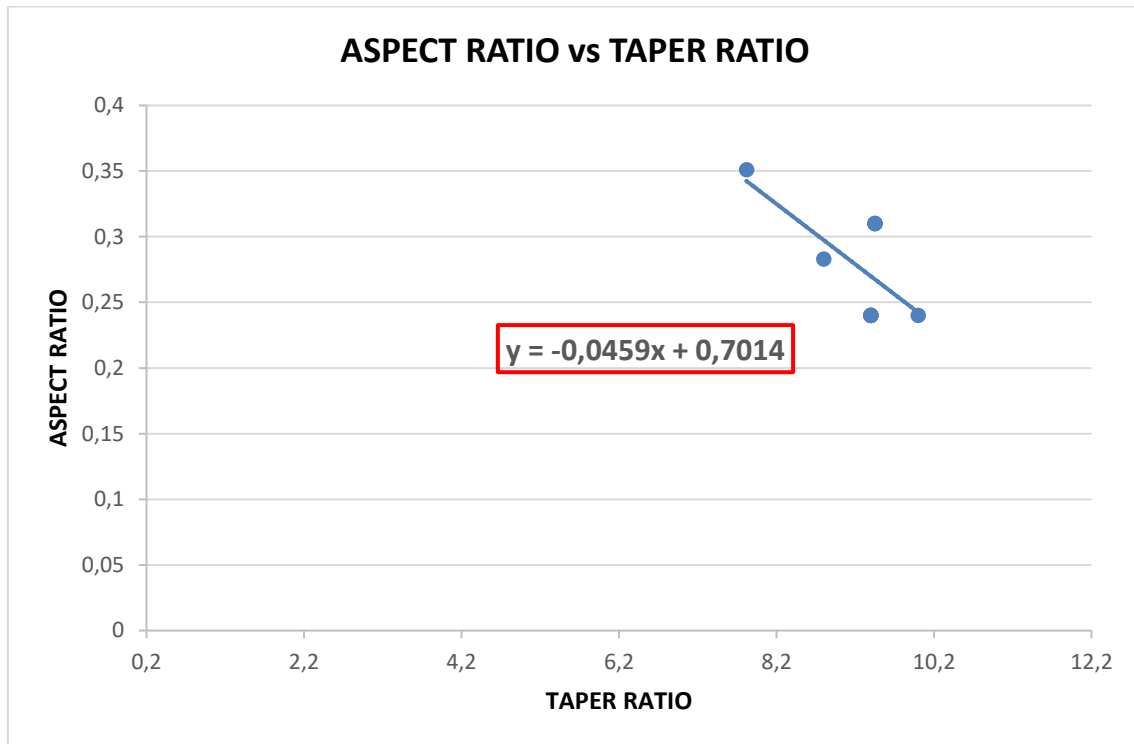


Table 11. Aspect ratio vs Taper ratio linear regression

As commented before in this chapter, one of the objectives is to increase the aspect ratio compared with the aircraft of the tables before. The aircraft is going to have a **10,37 meters aspect ratio**, with this value the taper ratio can be calculated with the formula of Table 11.

$$\mathbf{Taper\ Ratio} = -0,0459 \cdot 10,31 + 0,7014 = \mathbf{0,228}$$

Also, the wingspan can be calculated with the wing area and the aspect ratio:

$$\mathbf{Wing\ Span} = \sqrt{Wing\ Area \cdot Aspect\ Ratio} = \mathbf{39,08\ m}$$

Now, once we have the wing span, wing area and taper ratio, the tip and root chords can be obtained:

$$\mathbf{Root\ Chord} = \frac{2 \cdot Wing\ Area}{Wing\ Span \cdot (1 + Taper\ Ratio)} = \frac{2 \cdot 148,19}{39,08 \cdot (1 + 0,228)} = \mathbf{6,17\ m}$$

$$\mathbf{Tip\ Chord = Root\ chord \cdot Taper\ Ratio = 1,408\ m}$$

The last parameters that we need for the wing are the wing dihedral angle and the sweep angle, which are going to be obtained by taking the arithmetic mean of the values from the previous tables. The results obtained are a Sweep angle at the quarter chord of 25,30 ° and a Dihedral Angle = 5,61 °

$$\mathbf{Mean\ Geometric\ chord = \frac{4}{3} \sqrt{\frac{Wing\ Area}{Aspect\ Ratio} \cdot \left(\frac{1 + Taper\ Ratio + Taper\ Ratio^2}{1 + 2 \cdot Taper\ Ratio + Taper\ Ratio^2} \right)}}$$

$$\mathbf{Mean\ Geometric\ Chord = 4,657\ m}$$

Once all the parameters of the wing are calculated, the wing can be modeled in 3D

- Wing Area = 148,19 m²
- Aspect Ratio = 10,31
- Wing span = 39,08 m
- Taper ratio = 0,228
- Root chord = 6,17 m
- Tip chord = 1,408 m
- Dihedral angle = 5,61°
- Sweep angle = 25,3°
- Mean geometric chord = 4,657 m

3.5.3 Final wing design in Open VSP

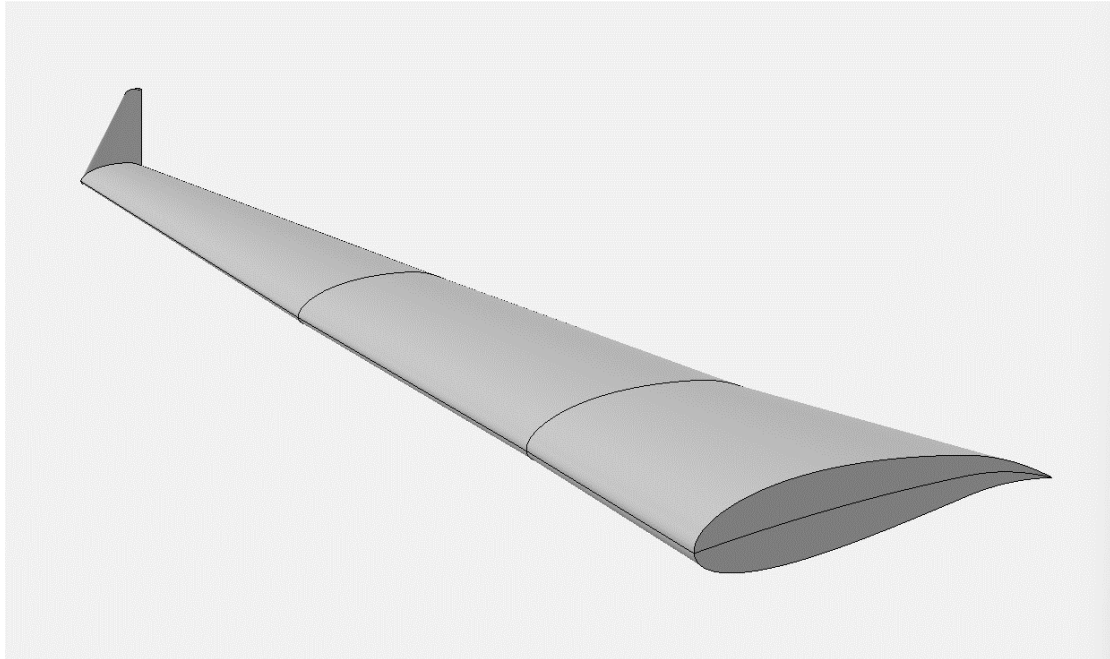


Figure 42. Isometric view of the final wing 3D design

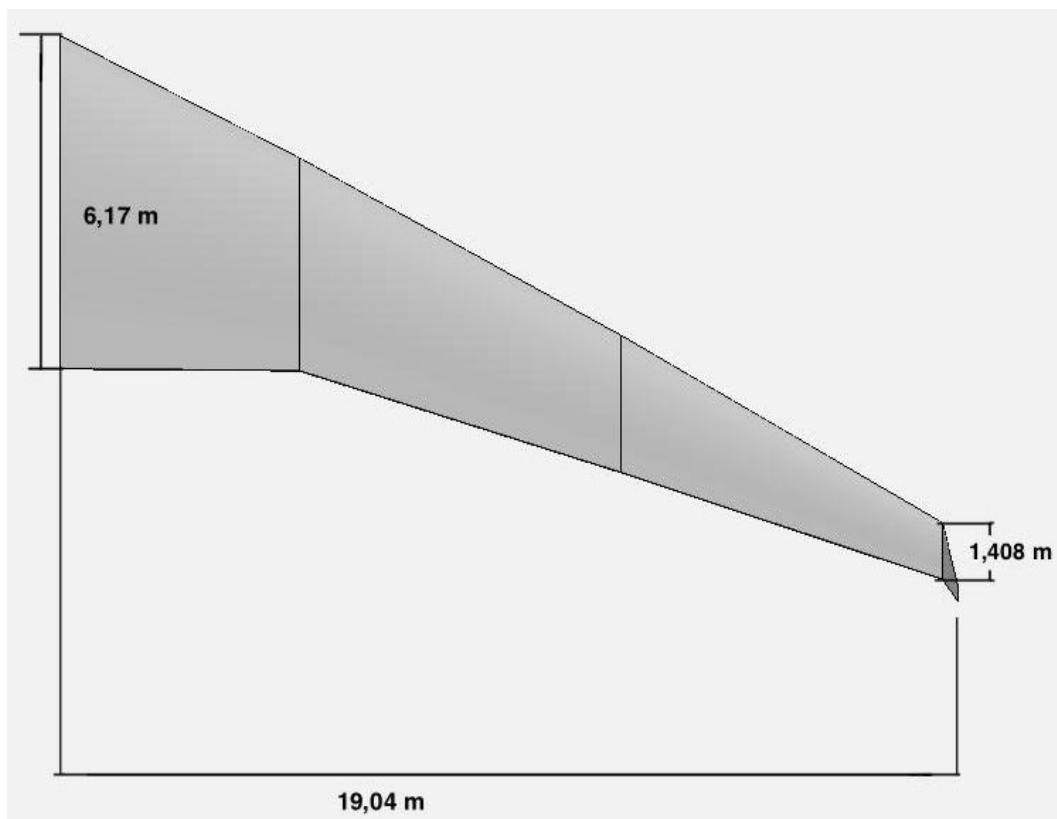


Figure 43. Top view of the final wing 3D design

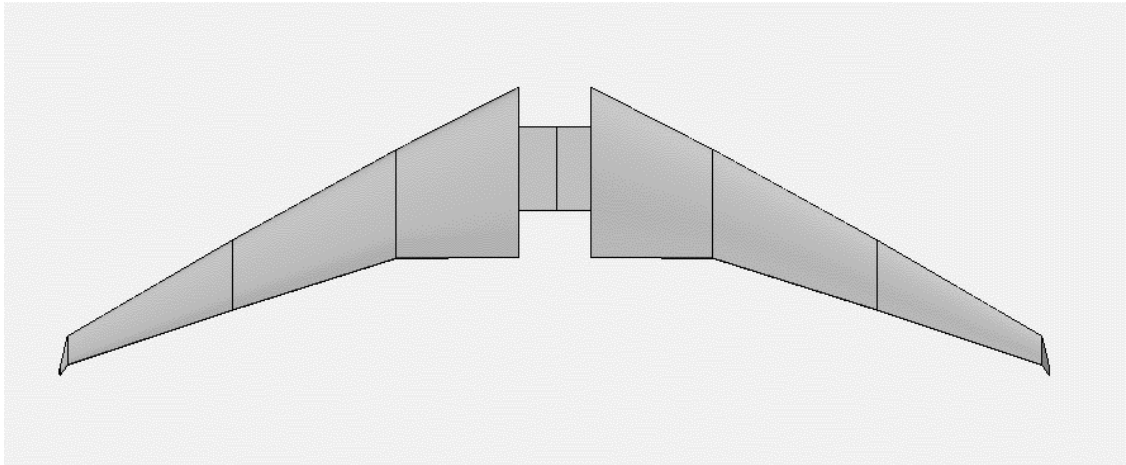


Figure 44. Wings final 3D design

3.5.4 Control surfaces

The control surfaces are movable devices that allow the pilots to control the direction and orientation of the aircraft by increasing the wing surface and improving the maneuverability and stability at take-off and landings and during flight.

The flaps selected for the wing are the same used in A320 aircraft, fowler flaps, which can be extended or deployed to change the wing surface or its shape. This kind of flap provides an additional lift at low speeds and is very useful during landing and take-off maneuvers. Since it is a part of the aircraft wing that acts retracting, allows the air to pass between the trailing edge of the wing and the flap energizing the boundary layer and improving the lift at slow speeds as commented before.

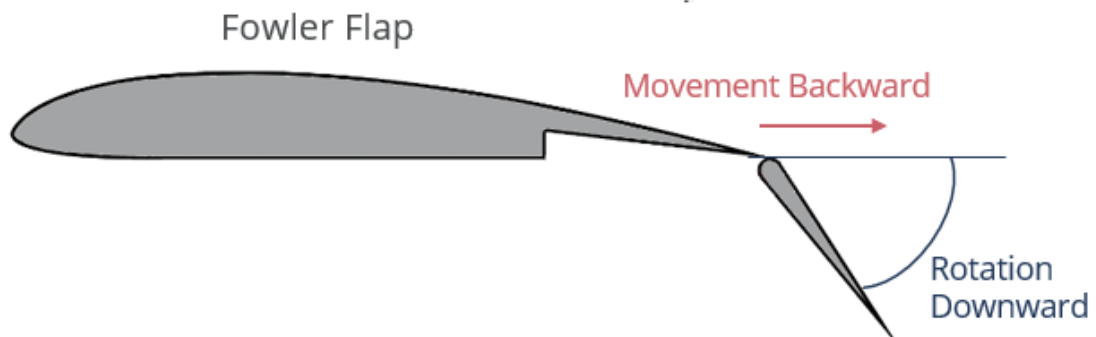


Figure 45. Fowler flap mechanism

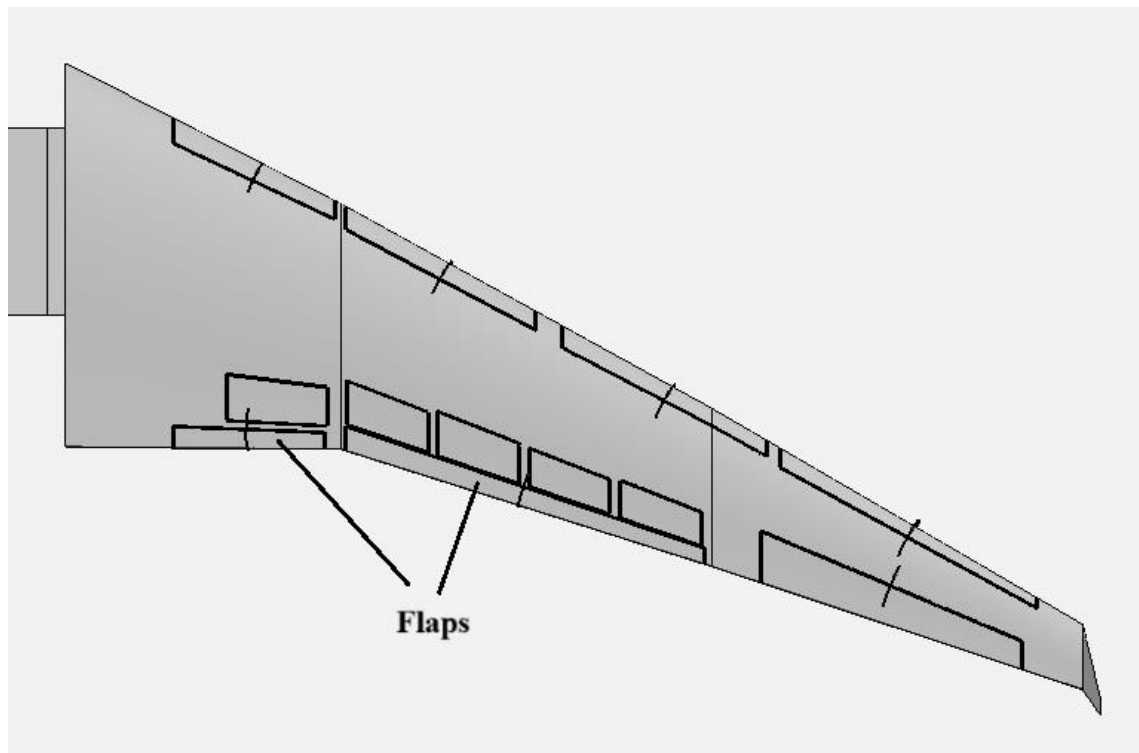


Figure 46. Flaps location in 3D wing

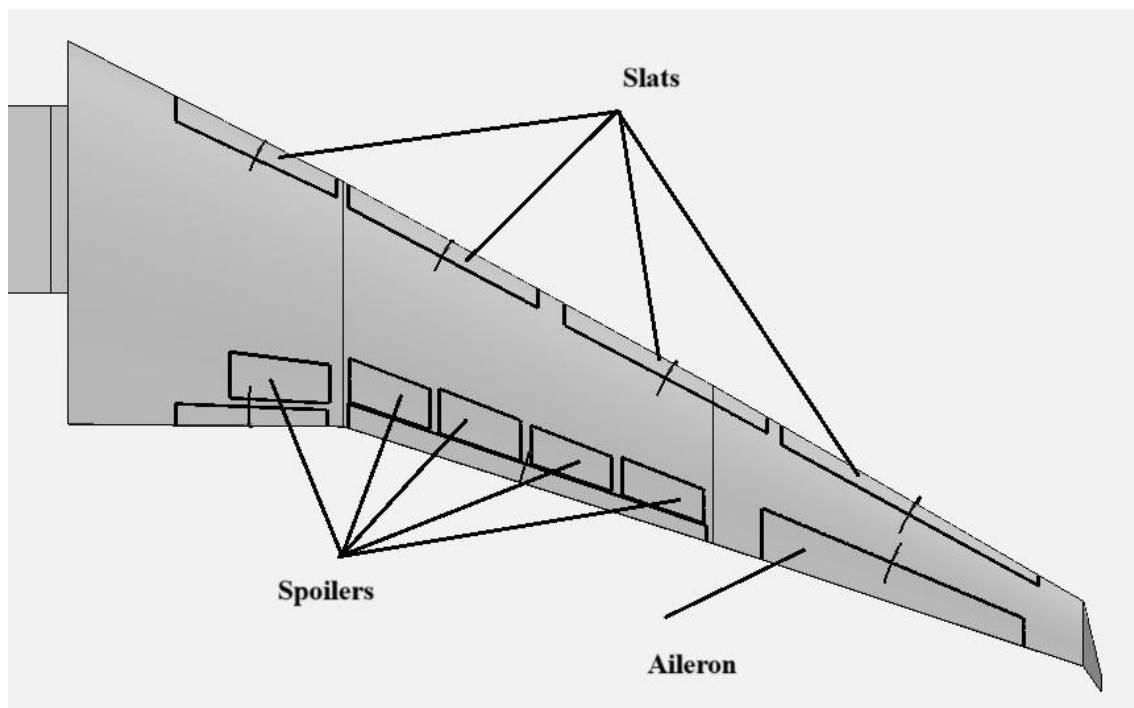


Figure 47. Aileron, spoilers and slats location in 3D wing

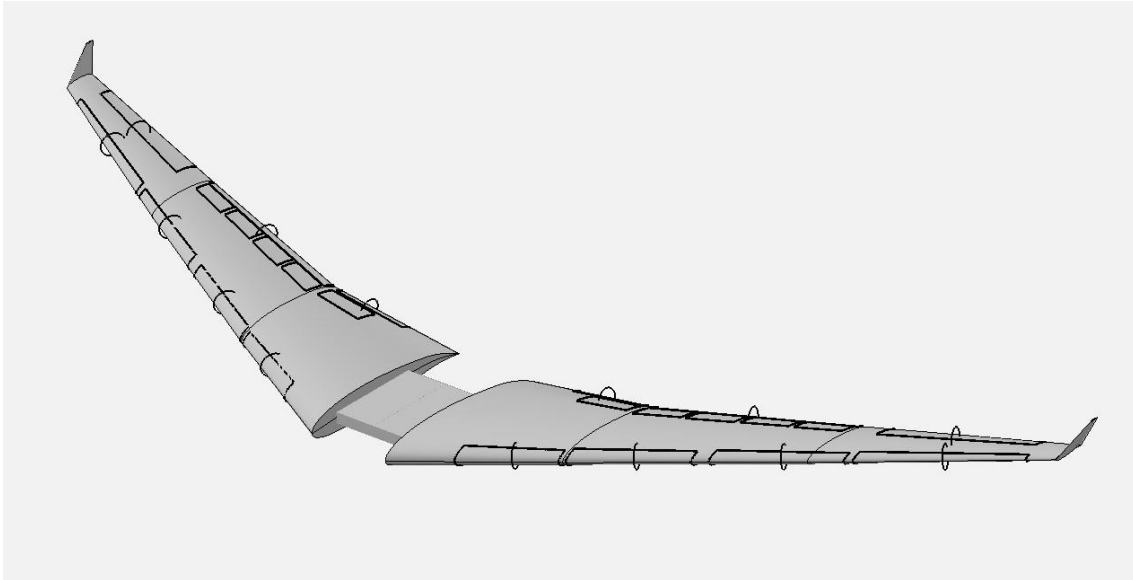


Figure 48. Isometric view of the wing with high lift devices

3.5.5 Wings fuel tanks

The center wing box and the wings are designed so as to have the capacity to carry a fuel tank inside. The wing box fuel tanks are 2,5 meters wide, 3,63 meters long and 0,9 meters high which gives us a total volume of $8,167 m^3$

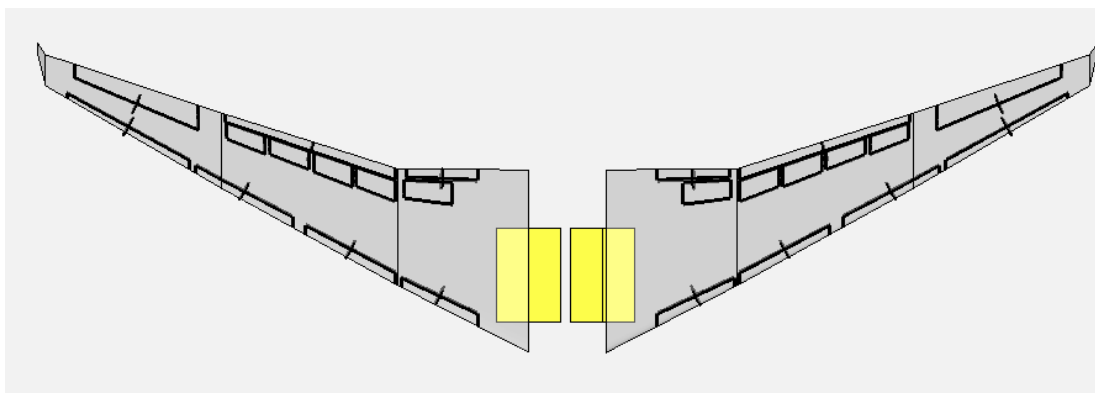


Figure 49. Wing box fuel tanks

The rest of the fuel is going to be stored in the wing fuel tanks. Each wing is going to incorporate inside 2 fuel tanks, one in the first section and another along the rest of the wing

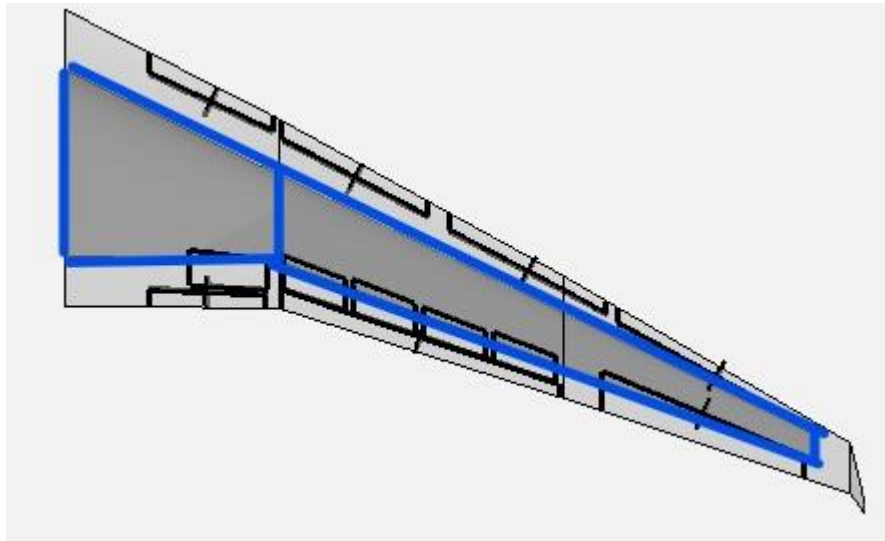


Figure 50. Wing fuel tanks distribution in the wing

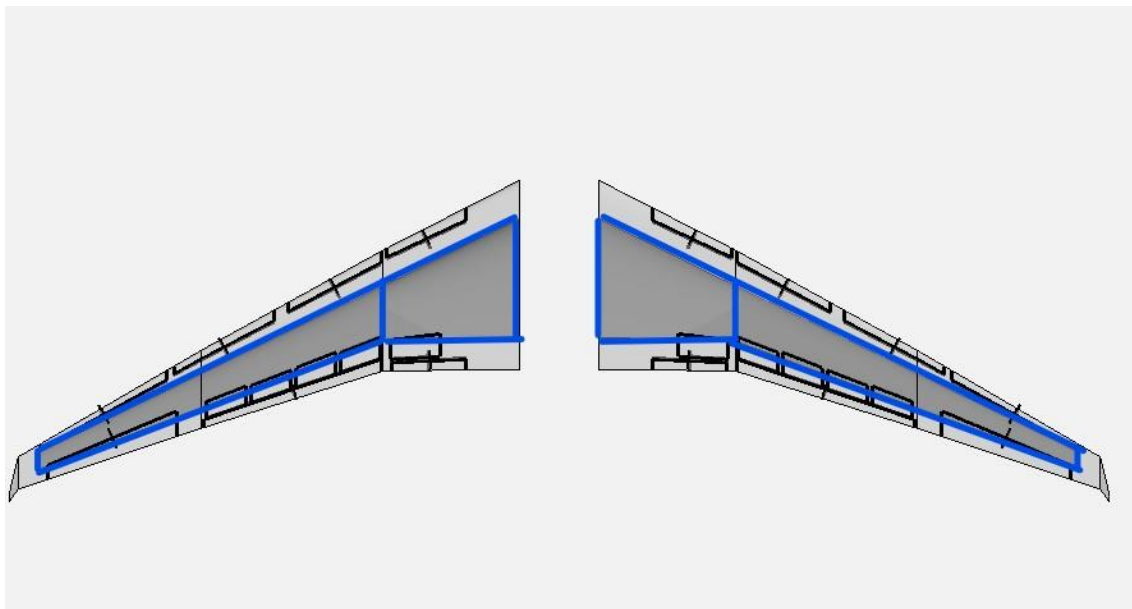


Figure 51. Four wing fuel tanks distribution along the wing

3.5.6 Internal structure

The internal structure of the wing is composed of spars, ribs and the stringers. The stringers are internal and longitudinally inside the wing and the spars are longitudinally also but external, having in between the stringers, while the ribs are transversally located along the wing.

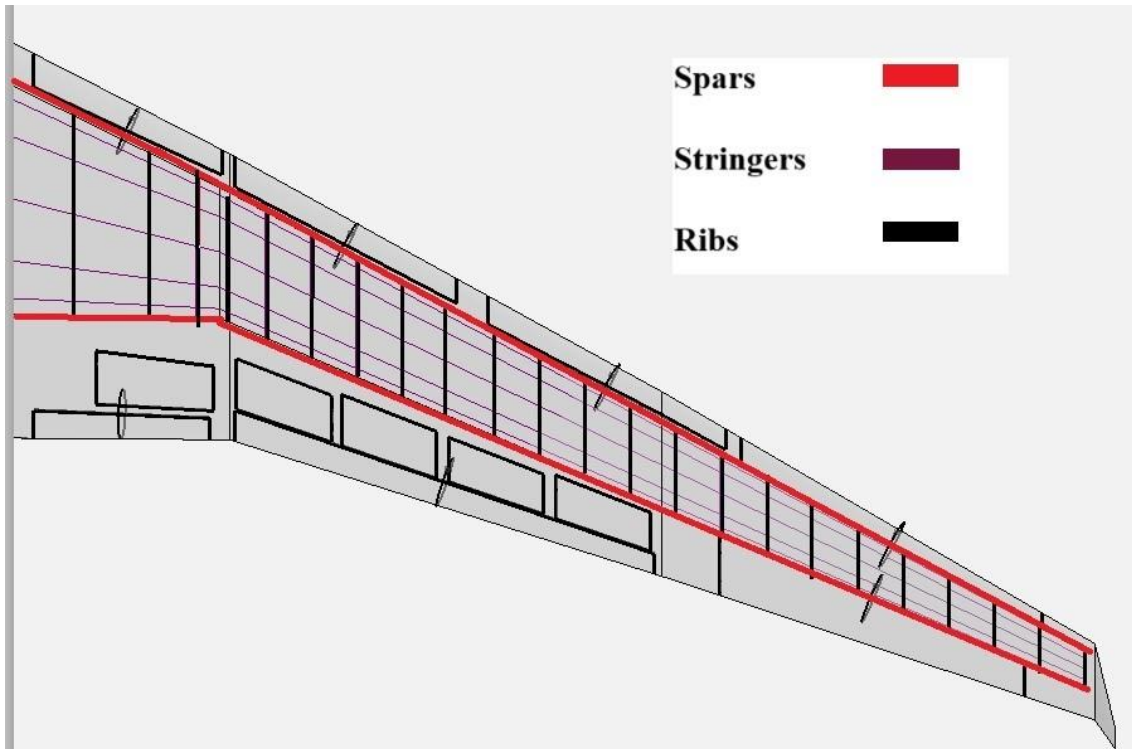


Figure 52. Wing internal structure

3.6 Landing gear

The landing gear is the part of the aircraft that must absorb the kinetic energy that is produced when the aircraft contacts the landing track. This kinetic energy is very high and the landing gear has a cushioning system to reduce the impact.

The landing gear is a retractable conventional one, which has one placed at the nose of the aircraft and two more placed in the fuselage near the wings. The dimensions of the landing gear are selected considering the weight of this aircraft and aircraft with similar characteristics.

3.6.1 Front landing gear

In the front landing gear, the configuration selected is a single-bogie or dual with two wheels of 1,01 meters of diameter and a width of 0.5 meters. The nose landing gear is located under the first row of seats of the aircraft and retracts backward into the fuselage.

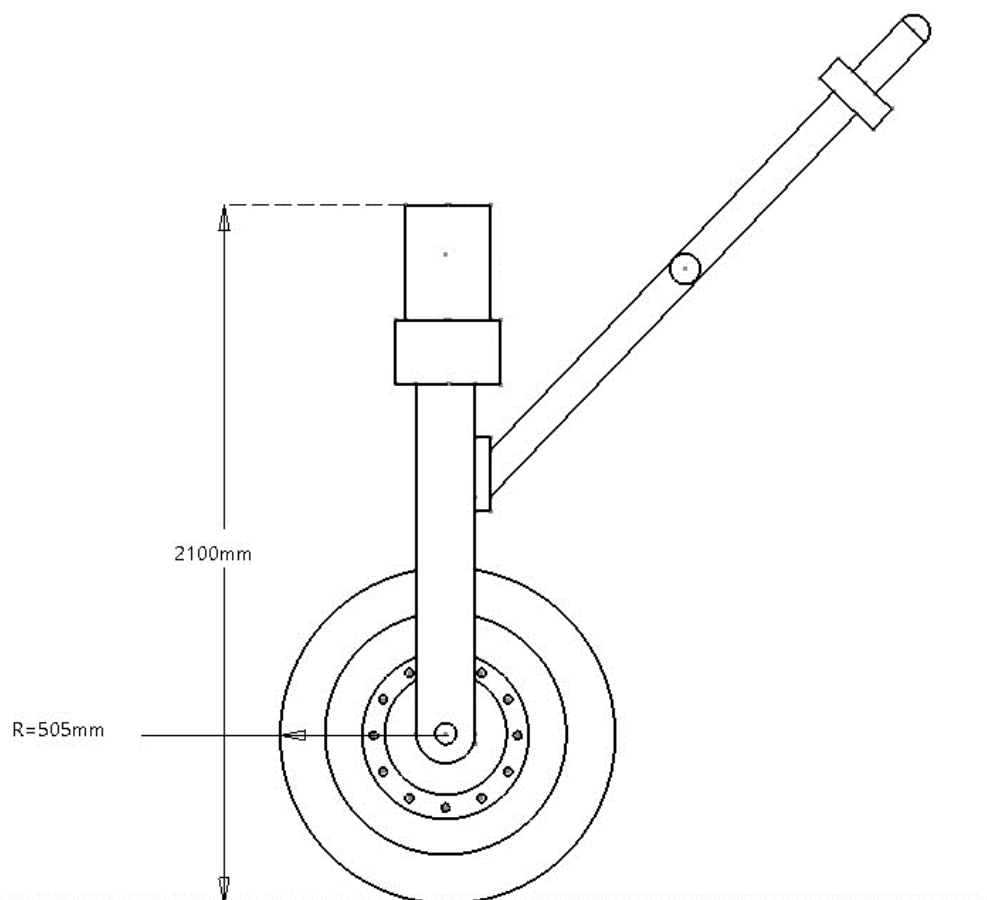


Figure 53. Nose landing gear side view design

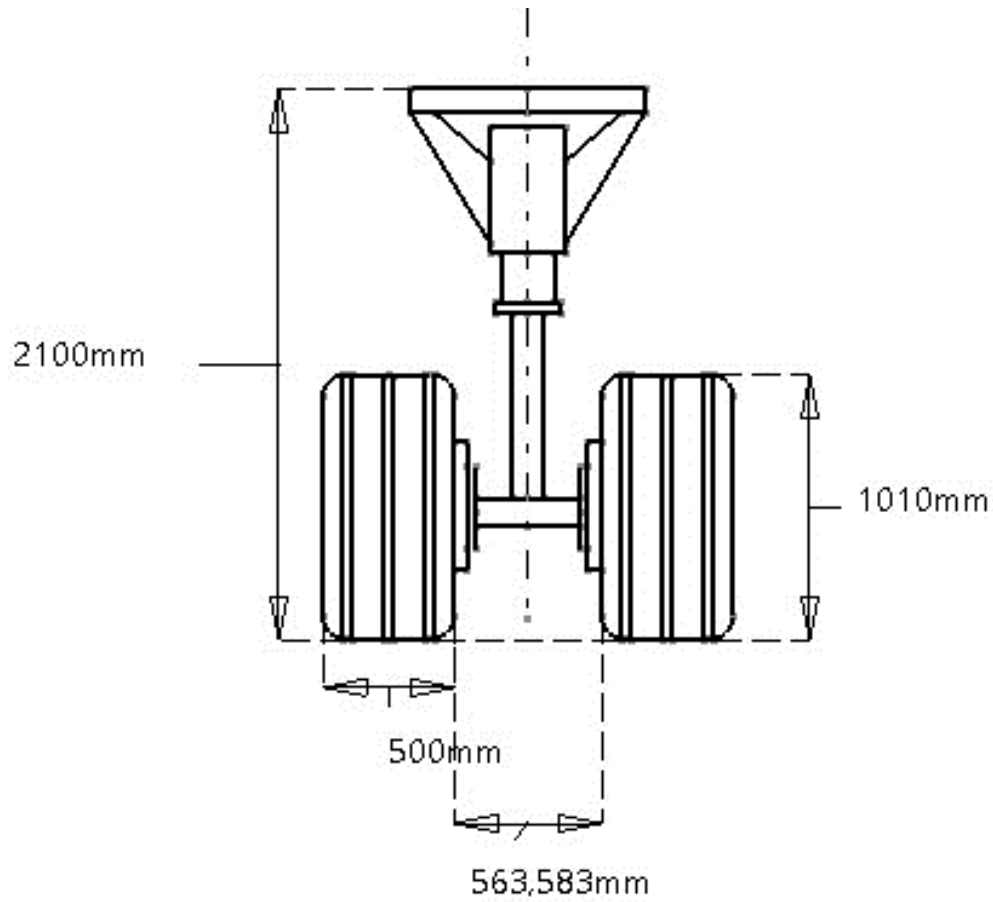


Figure 54. Nose landing gear front view design



Figure 55. Nose landing gear side view in 3D

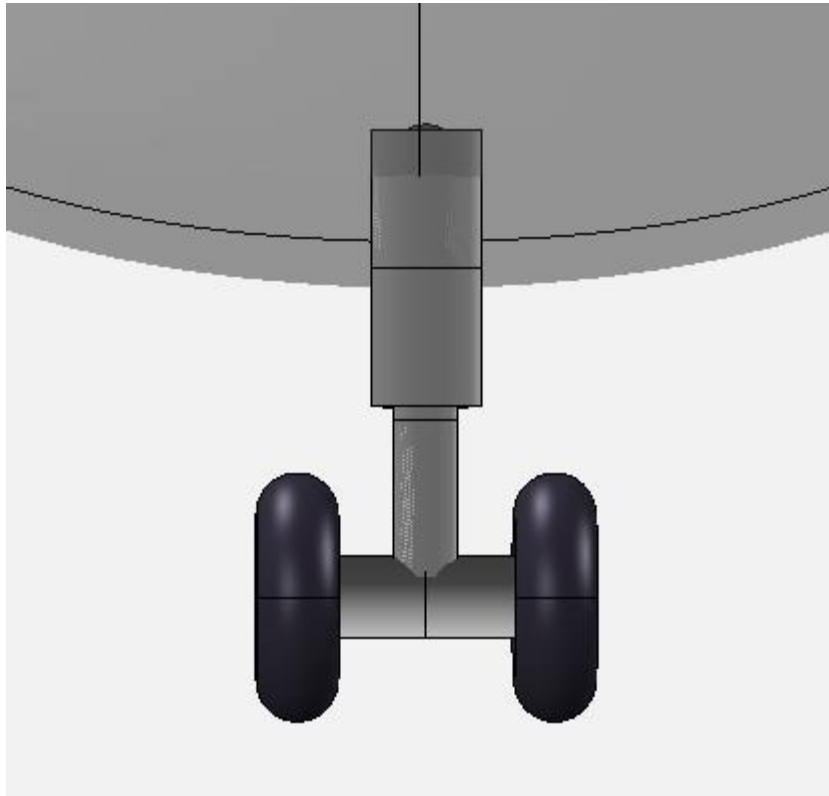


Figure 56. Nose landing gear front view in 3D

3.6.2 Main landing gear

The main landing gear of the aircraft has a double-bogie configuration, in which wheels have similar dimensions to the nose landing gear, 1,01 meters of diameter and a width of 0.5 meter

The main landing gear is located at the first section of the wings and retracts into the fuselage

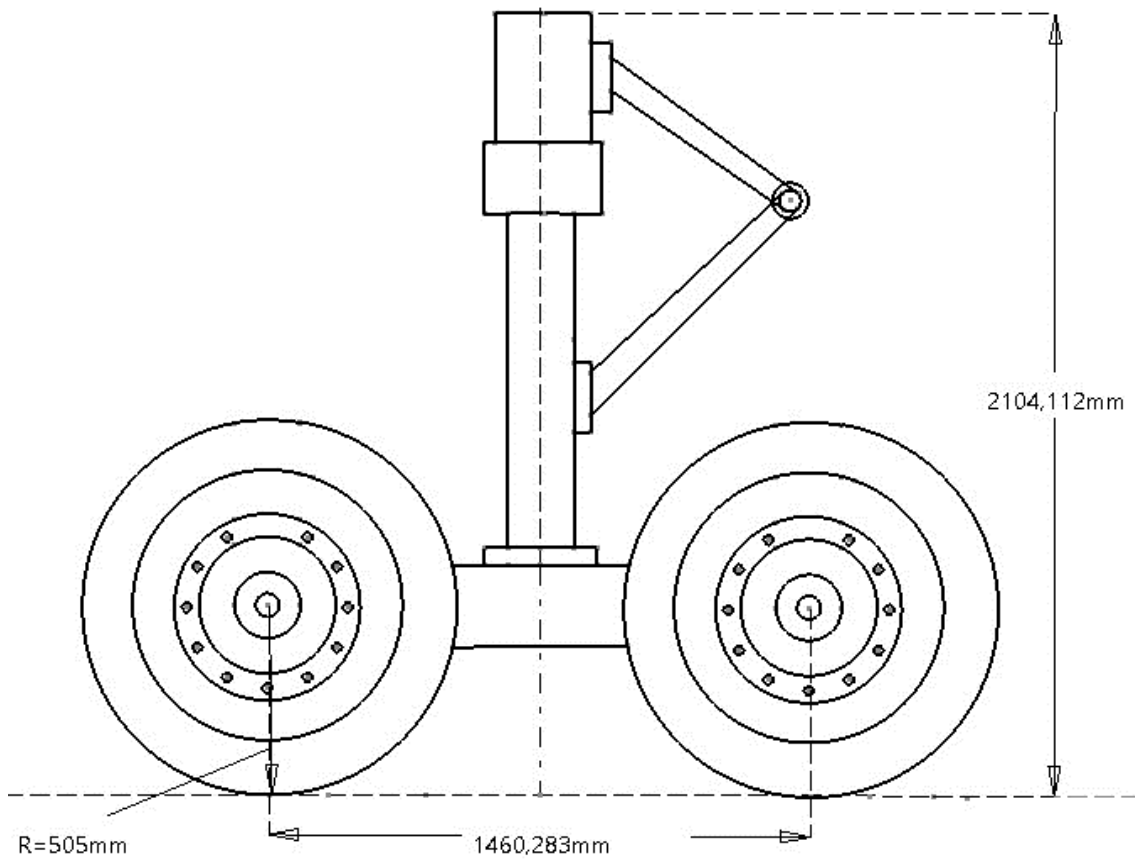


Figure 57. Main landing gear side view design

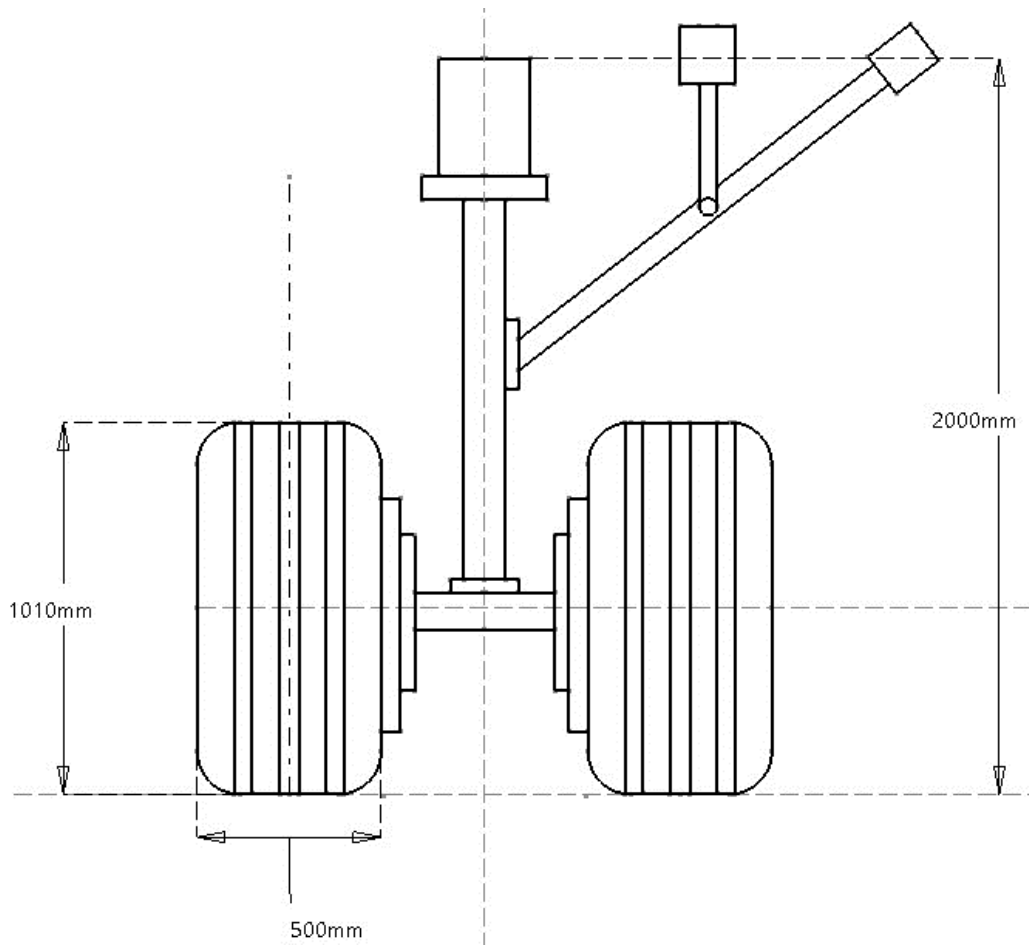


Figure 58. Main landing gear front view design



Figure 59. Main landing gear front view in 3D

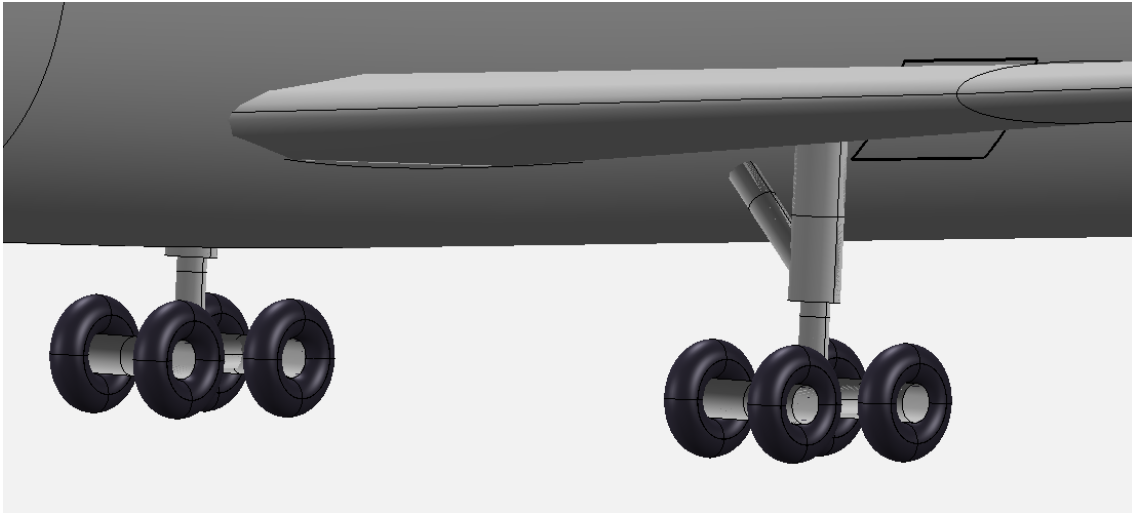


Figure 60. Main landing gear isometric view in 3D

3.7 Empennage

The tail configuration selected for the aircraft is a T-tail with a double vertical tail plane, which is a configuration where the horizontal tail plane is located at the top of the vertical tail plane and gives the empennage a T aspect. This tail configuration offers a high aerodynamic and also, a better rate of displacement due to the vertical separation of the tail with respect to the wing which means that the horizontal surfaces are not going to be affected by the wing wake.

The bigger advantage of having this kind of tail configuration is that it gives the possibility of placing the engines between the vertical tail planes, getting the ingestion of the fuselage boundary layer.

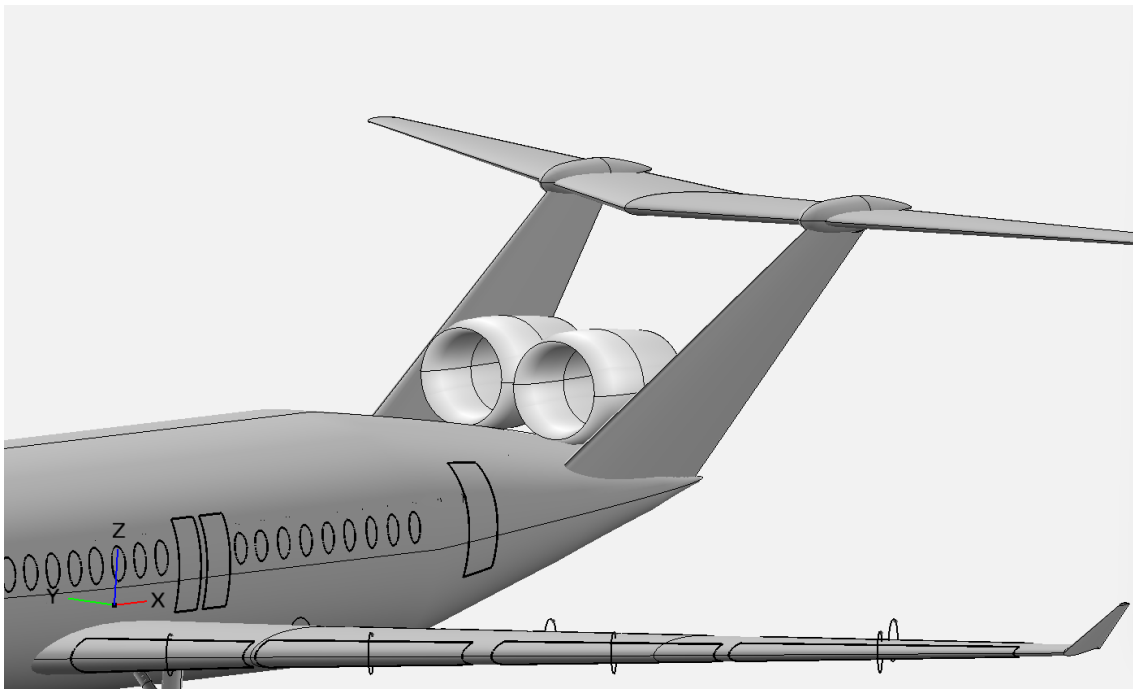


Figure 61. T- tail with double vertical tail plane

3.7.1 Airfoil

The airfoil selected for the vertical and horizontal tail plane is NACA 0012 which is a symmetric airfoil and will give more stability to the aircraft than an asymmetrical one, being the pressure difference smaller in the upper and lower part of the airfoil giving control and stability.

It is very important to choose a symmetrical airfoil for the vertical stabilizer so as to prevent it from provoking a force and a moment, which could be dangerous.

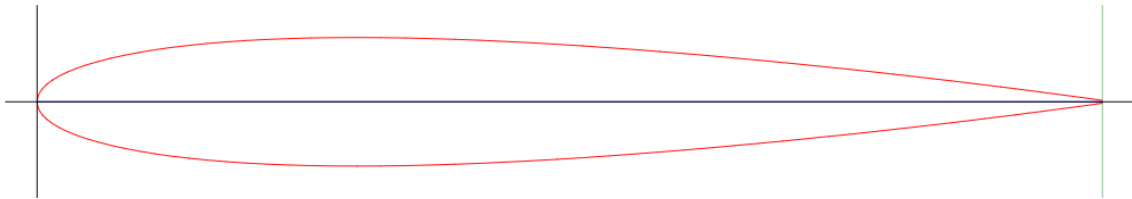


Figure 62. NACA 0012

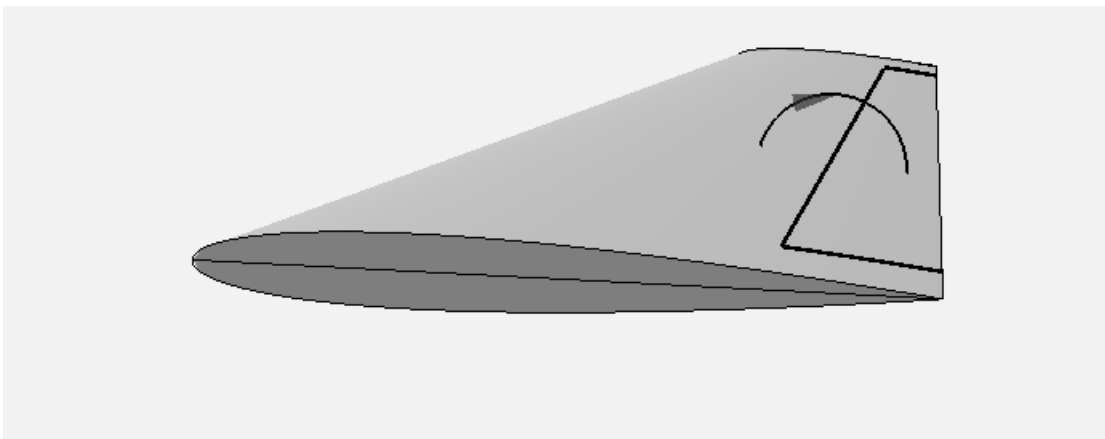


Figure 63. Airfoil NACA 0012 in HTP

3.7.2 Horizontal tail plane dimensions

The horizontal tail plane for this configuration is going to be located at the upper part of the vertical tail planes. In order to obtain the dimensions, a linear regression is going to be done with data of similar planes as it has been done before with the wings.

HTP	A310	A319	A320	A320 neo	A321	A321 neo
Area	64 m ²	31 m ²				
Span	16,26 m	12,45 m				
Aspect Ratio	4,13	5	5	5	5	5
Sweep angle	34 °	29 °	29 °	29 °	29 °	29 °
Taper ratio	0,417	0,256	0,256	0,256	0,256	0,256

Table 12. Airbus aircraft HTP dimensions

HTP	B 757	B 737- 600	B 737-700	B 737-900
Area	50,35 m ²	32,78 m ²	32,78 m ²	32,78 m ²
Span	15,21 m	14,35 m	14,35 m	14,35 m
Aspect Ratio	4,6	6,16	6,16	6,16
Sweep angle	27,5 °	30 °	30 °	30 °
Taper ratio	0,33	0,203	0,203	0,203

Table 13. Boeing aircraft HTP dimensions

By doing linear regressions, following the same process done for the wing we can obtain the mean values for the HTP dimensions. Comparing the values of the wing area of the aircraft from the tables with the HTP area, our HTP area is obtained

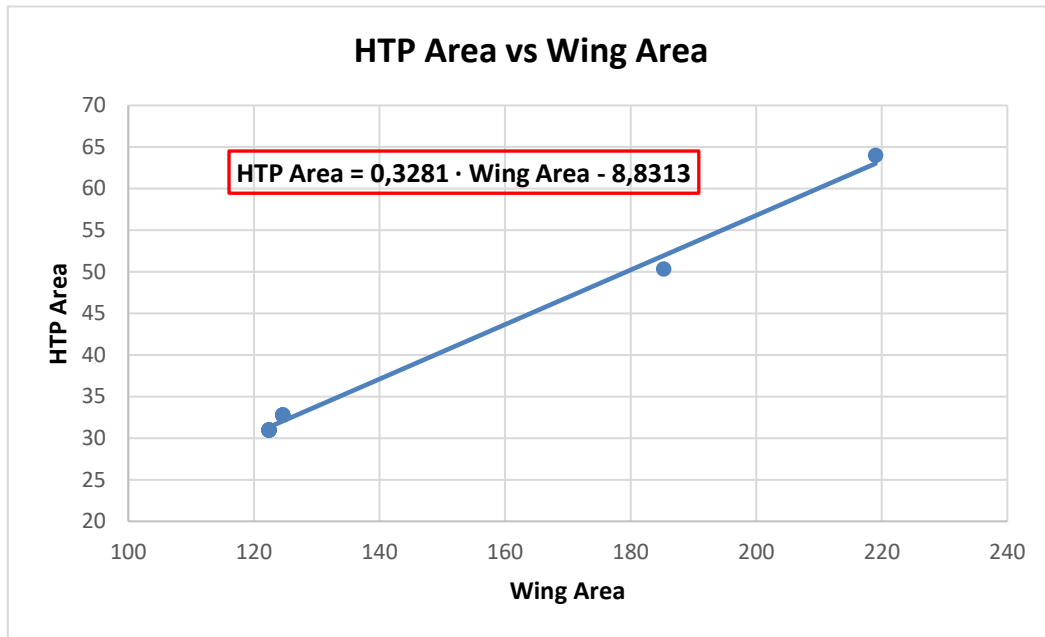


Table 14. HTP Area vs Wing Area linear regression

$$\text{HTP Area} = 0,3281 \cdot 148,19 \text{ m}^2 - 8,8313$$

$$\text{HTP Area} = 39,78 \text{ m}^2$$

As the wing area is 148,19 m², the HTP area for the aircraft is going to be 39,78 m². The same process is done for the HTP span and the HTP area that we have calculated.

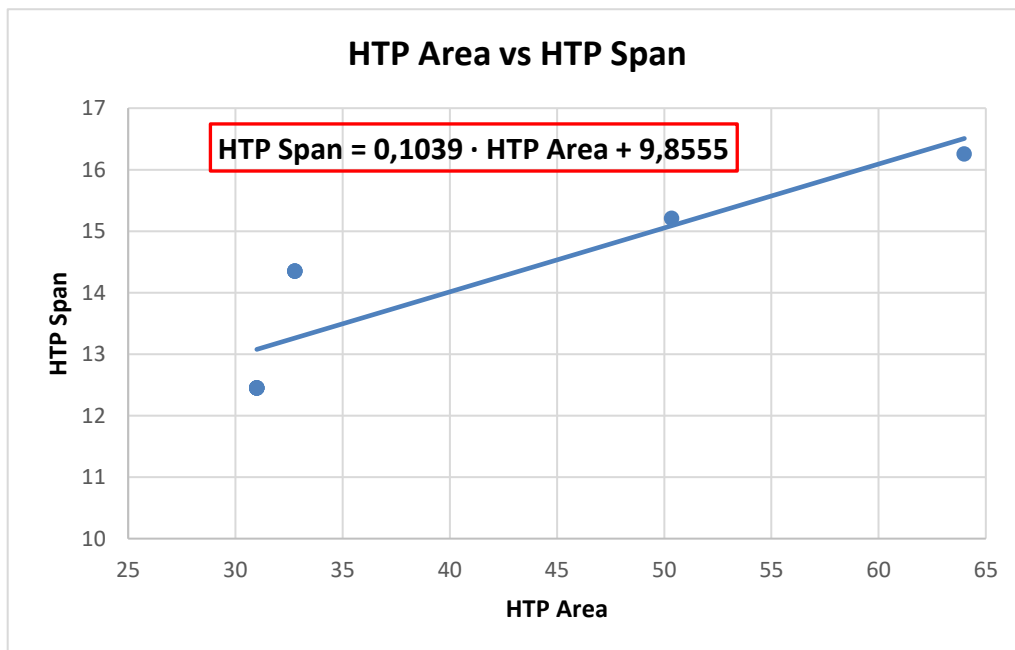


Table 15. HTP Area vs HTP Span linear regression

$$\text{HTP Span} = 0,1039 \cdot \text{HTP Area} + 9,8555$$

$$\text{HTP Span} = 13,88 \text{ m}$$

The rest of the parameters of the aircraft HTP are obtained by doing the geometric mean of the taper ratio, sweep angle and aspect ratio of the aircraft from the tables.

$$\text{Mean Geometric chord} = \frac{4}{3} \sqrt{\frac{\text{HTP Area}}{\text{Aspect Ratio}} \cdot \left(\frac{1 + \text{Taper Ratio} + \text{Taper Ratio}^2}{1 + 2 \cdot \text{Taper Ratio} + \text{Taper Ratio}^2} \right)}$$

$$\text{Mean Geometric Chord} = 3,36 \text{ m}$$

The final dimensions for the HTP are the following:

- HTP Area = 39,78 m²
- Aspect Ratio = 5,221
- HTP span = 13,88 m
- Taper ratio = 0,263
- Sweep angle = 29,65°
- Mean geometric chord = 3,36 m

3.7.3 Horizontal tail plane final design

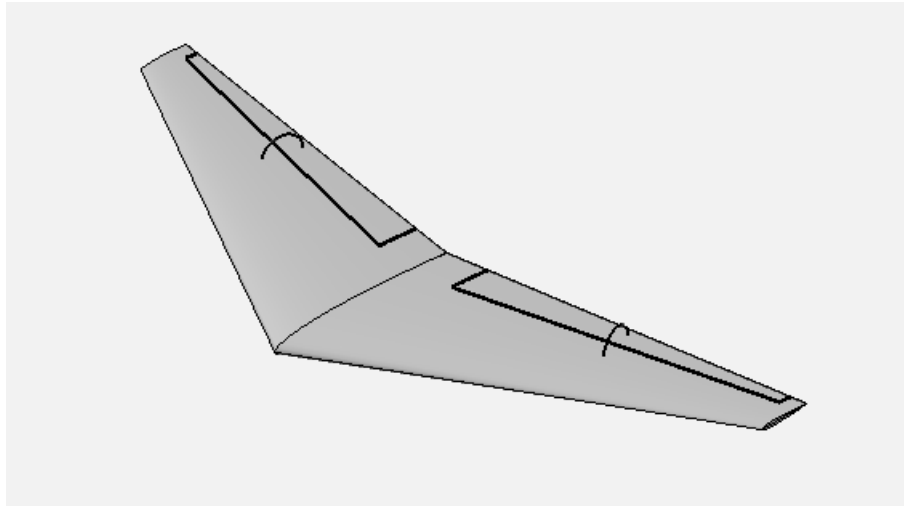


Figure 64. Isometric view of the HTP final 3D design

The elevators, as can be seen in Figure 59 and Figure 60, are placed one at each horizontal tail plane at the rear part. This kind of control surface is an up and down system that creates a downward force which helps the pilot to balance the nose-down moment created by the lift generated by the wings.

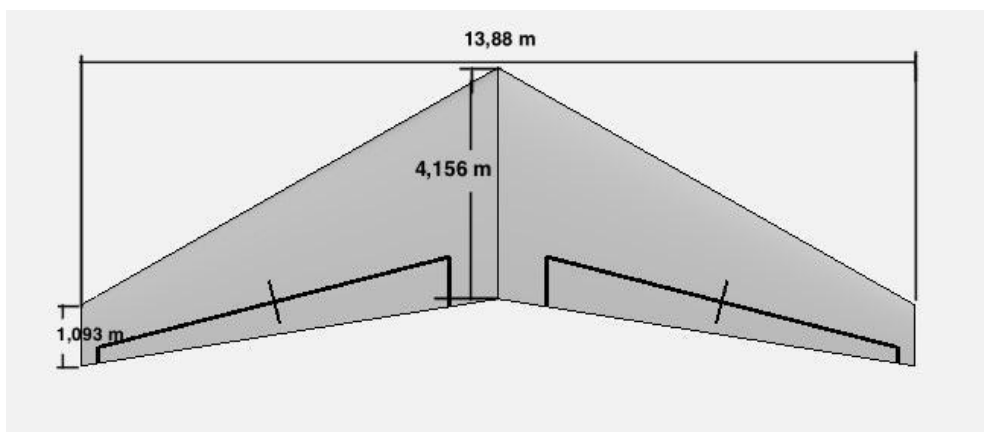


Figure 65. Top view of the HTP final 3D design with dimensions

3.7.4 Vertical tail plane dimensions

In the case of the VTP, there are no aircraft with a double T-tail in the market and the measures are obtained by comparing the plane layout from the prototype Aurora D8.

After comparing both aircraft at the same scale, and modeling it in Open VSP with the same dimensions, the values obtained for each VTP are the following:

- VTP Area = 20,78 m²
- Aspect Ratio = 1,455
- HTP span = 5,50 m
- Taper ratio = 0,361
- Tip chord = 2 m
- Root chord = 5,54 m
- Sweep angle = 45°
- Dihedral angle = -8.45 °

With the data obtained from Open VSP, the mean geometric chord of the VTP can be calculated:

$$\mathbf{Mean\ Geometric\ chord} = \frac{4}{3} \sqrt{\frac{VTP\ Area}{Aspect\ Ratio} \cdot \left(\frac{1 + Taper\ Ratio + Taper\ Ratio^2}{1 + 2 \cdot Taper\ Ratio + Taper\ Ratio^2} \right)}$$

$$\mathbf{Mean\ Geometric\ chord} = \mathbf{4,52\ m}$$

3.7.5 Vertical tailplane final design

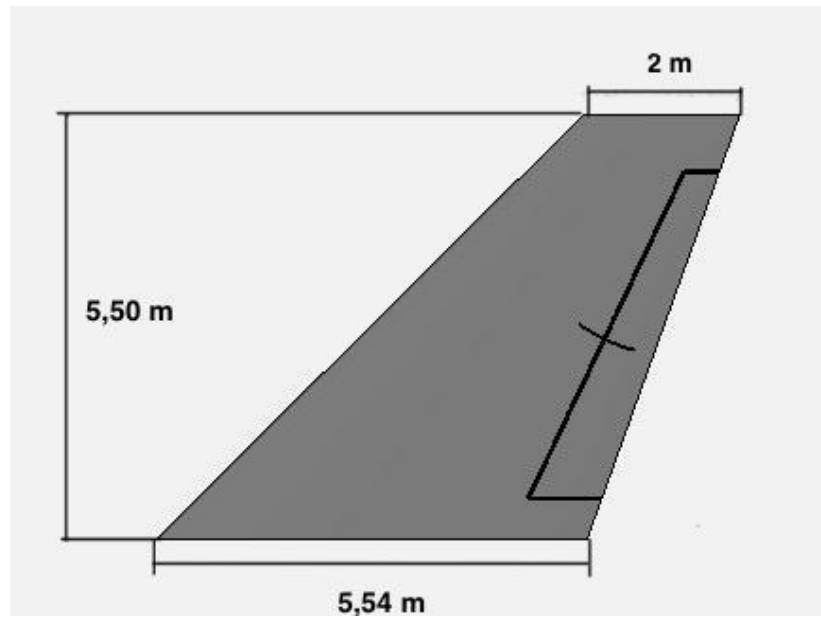


Figure 66. Vertical tail plane side view

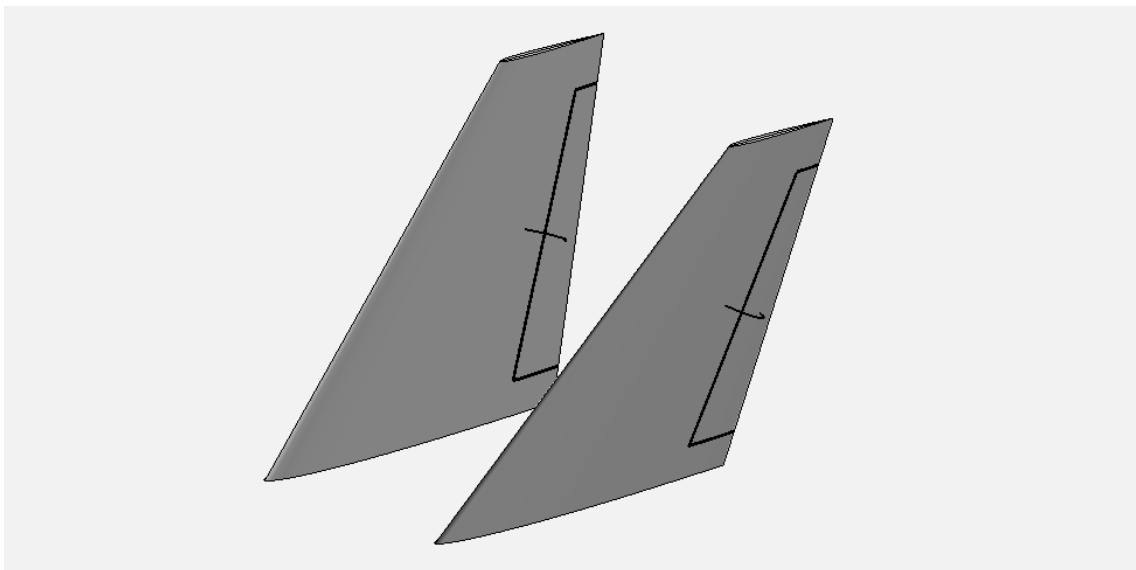


Figure 67. Isometric view of the VTP final 3D design

3.7.6 Final Empennage

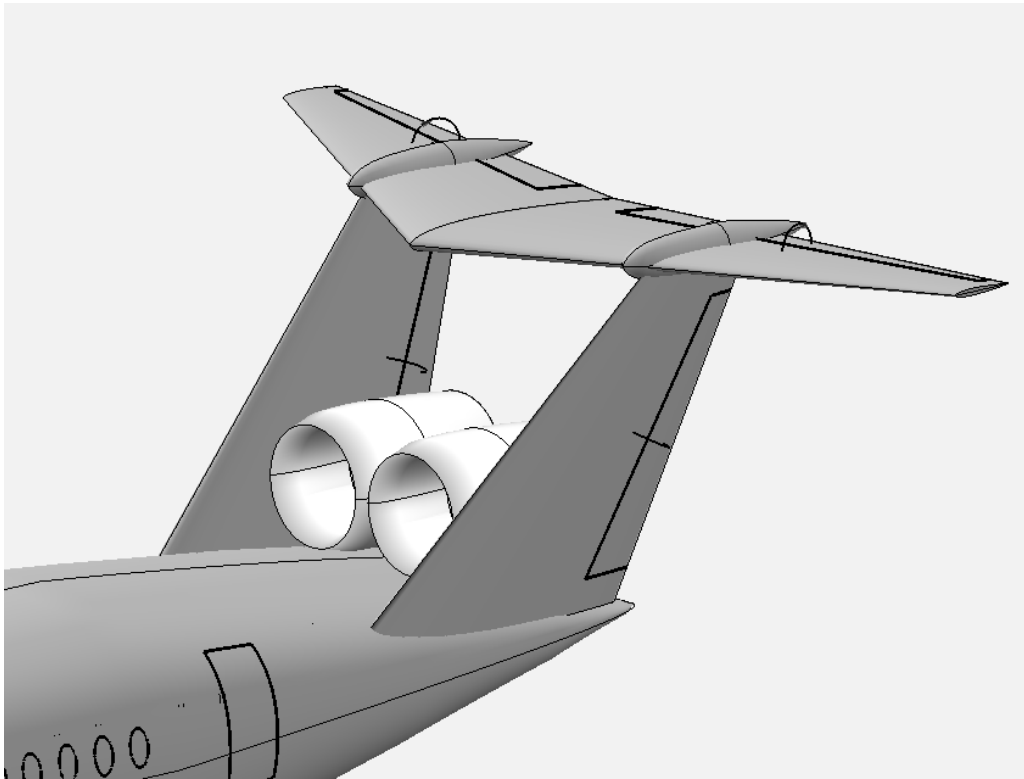


Figure 68. Isometric view of the final empennage design

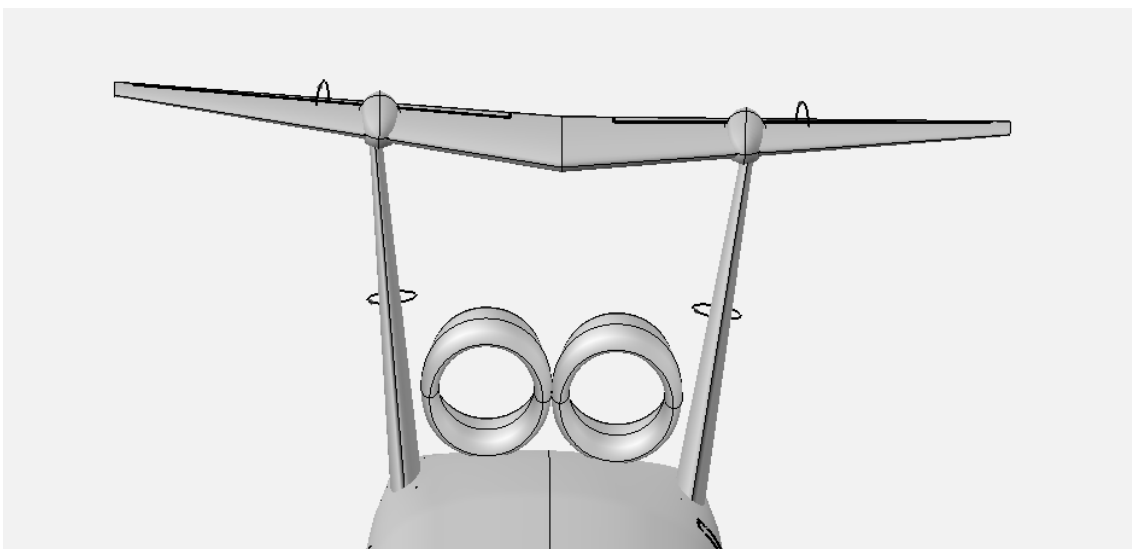


Figure 69. Front view of the final empennage design

3.8 Propulsion systems

The final design of the propulsion system in the double bubble aircraft involves several considerations to ensure efficient and reliable engine performance, integration with the aircraft structure, fuel efficiency, and compliance with safety regulations.

3.8.1 Engines selection

In terms of operability and costs, the cheaper option is to select an existing engine used nowadays in aircraft with similar passenger capacity and weight. Also, as the aircraft is thought to cover the middle of the market segment, the range must be considered (between 4000 nmi and 5000 nmi)

For getting an estimated value of the thrust needed, similar aircraft are going to be compared and a linear regression is going to be done as in the wings and the horizontal tail plane.

	A320	A320 neo	A321	A321 neo	A330-200
Range	3790 nmi	4320 nmi	4000 nmi	4600 nmi	7240 nmi
Thrust	133-147 kN	110–160 kN	133-147 kN	110–160 kN	287–311 kN

Table 16. Airbus aircraft range and thrust

	A320	A320 neo	A321	A321 neo	A330
Engine	CFM International CFM56	Pratt & Whitney PW1900G / CFM International LEAP-1A	CFM International CFM56	Pratt & Whitney PW1900G / CFM International LEAP-1A	Pratt & Whitney PW4000

Table 17. Airbus aircraft engines

	B 757-200	B 737 MAX 7	B 737 MAX 8	B 767-200
Range	4000 nmi	3850 nmi	3610 nmi	3900 nmi
Thrust	163–189 kN	130 kN	130 kN	214–234 kN

Table 18. Boeing aircraft range and thrust

	B 757-200	B 737 MAX 8	B 737 MAX 9	B 767-200
Engine	Pratt & Whitney PW2000	CFM LEAP-1B	CFM LEAP-1B	Pratt & Whitney PW4000

Table 19. Boeing aircraft engines

With the data in the tables and with the desired range of 4500 nmi, we can obtain the required thrust and decide which engine is going to fit better with the aircraft

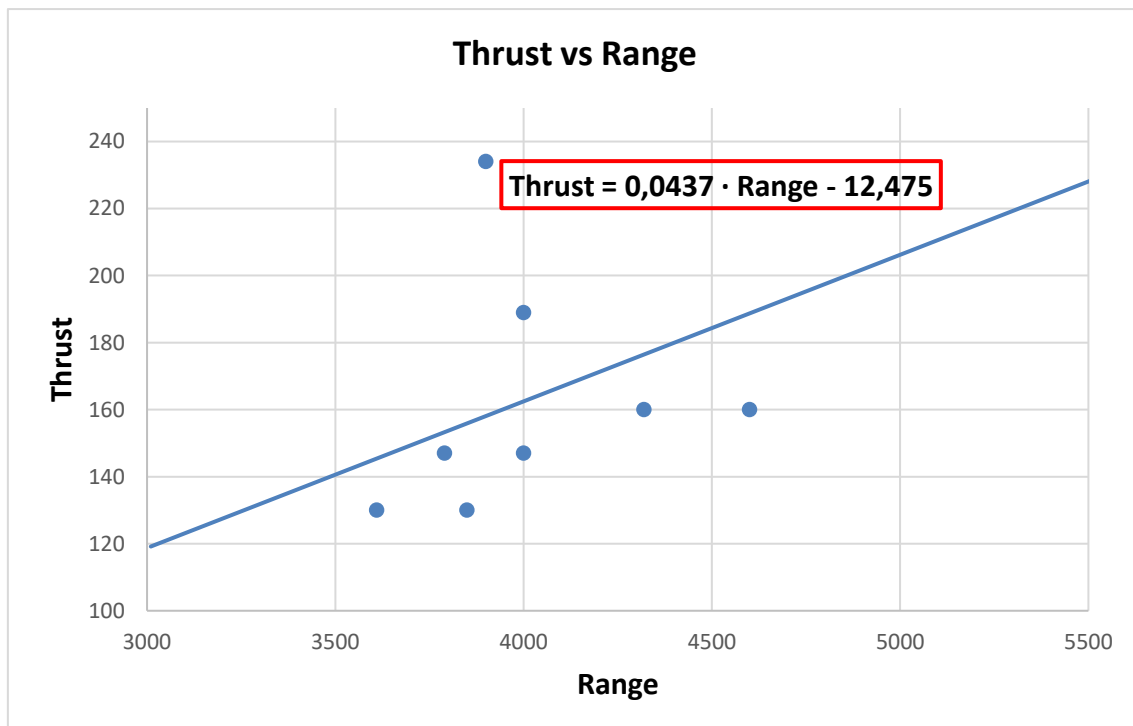


Table 20. Thrust vs Range linear regression

From the linear regression, the following equation is obtained and can be solved for our desired range of 4500 nmi:

Thrust = 0,0437 · Range - 12,475

Thrust = 184,175 kN (41364 lb)

Searching in the market of aircraft engines, the most suitable option found for the aircraft is Pratt & Whitney PW2043 which offers around 190 kN (43000 lbf) and powers all the models of Boeing 757.

PW2043 is a high bypass ratio turbofan engine and is the latest build standard of the PW2000 series, launched in 1994. This engine has a length of 3,729 m and a diameter of 2 m which is ideal for locating it at the rear part between the vertical tail planes, where there is space enough for placing two PW2043.

The performance characteristics of the engine are the following.

- Dry weight: 7100 lb (3,221 kg)
- Maximum thrust: 170,81 - 194,54 kN (38400 - 43734 lb)
- Overall pressure ratio: 27,6 - 31,2:1
- Bypass ratio: 6:1
- Thrust-to-weight: 5,41 - 6,16



Figure 71. Pratt & Whitney PW2043 engine

The only problem that this engine could have is that is an old engine and may not offer the same efficiency as a modern one, but in terms of operability and costs, this engine is a better option than designing a new one.

3.8.2 Engine location for boundary layer ingestion

One of the main characteristics of this kind of aircraft is the location of the engines, looking for the boundary layer ingestion and enhancing the efficiency. The engines are located inside the drag produced by the fuselage and the total drag of the aircraft is reduced.

The dimensions of the engines fit perfectly between the vertical tail plane, knowing that the diameter of both engines is 2 m and the space between the VTP is 4,66 m at the lower part, enough for placing the engines and their supports to the fuselage and VTP.

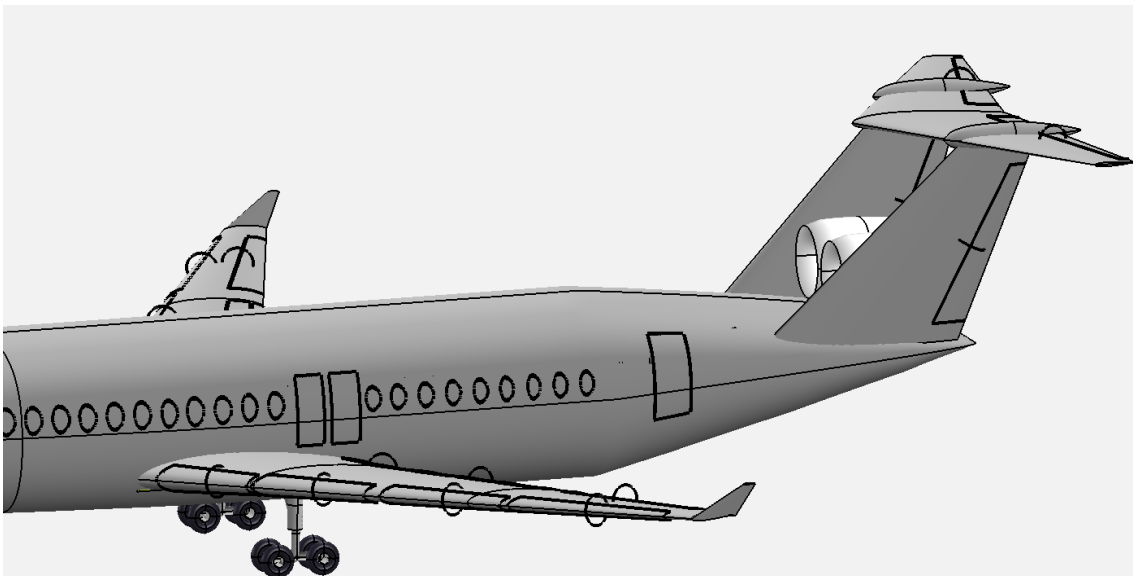


Figure 72. Side view of engines location

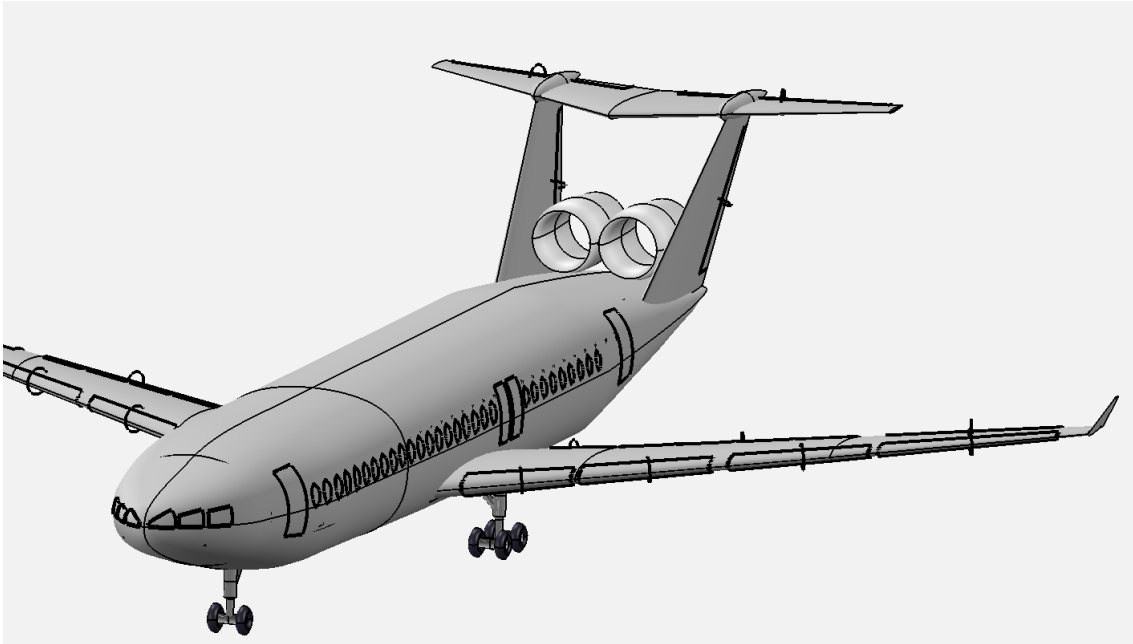


Figure 73. Isometric view of engines location

Chapter 4. Aircraft performance and wing analysis

4.1 Fuel estimations

First of all, we have to do the fuel calculations for the desired range. In order to carry out the calculations some initial parameters like range, specific fuel consumption, thrust and cruise speed are needed.

Specifications	Pratt & Whitney PW2043
SFC	0,582
Maximum thrust	43734 lbs
Bypass ratio	6:1
Overall pressure ratio	27,6 - 31,2:1
Dry weight	7100 lbs
Thrust-to-weight ratio	5,41 – 6,16

Table 21. Pratt & Whitney PW2043 specifications

The cruise thrust must be calculated for obtaining the fuel burn of the aircraft, in commercial aircraft it is estimated that operate at a range between 20 - 30 % of their maximum available thrust while the aircraft is at cruise speeds. The thrust required was calculated before and the value obtained was 41364 lbs

$$Thrust_{cruise} = 0,25 \cdot Thrust_{required}$$

$$Thrust_{cruise} = 0,25 \cdot 41364 \text{ lbf}$$

$$Thrust_{cruise} = 10341 \text{ lbf}$$

Now, the fuel burnt can be calculated by multiplying the cruise thrust times the specific fuel consumption of the selected engine.

$$Fuel_{bunt} = SFC \cdot Thrust_{cruise}$$

$$Fuel_{bunt} = 0,582 \cdot 10341$$

$$Fuel_{bunt} = 6018,42 \frac{lb}{h}$$

Assuming that the aircraft will fly at velocities equal to Mach 0,75 and at altitudes between 30000 and 39000 ft we can estimate a flight velocity of 890 km/h. The maximum range at which the aircraft must fly is 4500 nmi (8334 km). Assuming that the aircraft flies at cruising speed from the departure airport to the arrival airport, the estimated time for the maximum range flight will be 9,36 hours to complete the flight

Now the fuel needed can be obtained by multiplying the flight time times the fuel burn per hour that was calculated before.

$$Fuel_{needed} = T_{flight} \cdot Fuel_{bunt}$$

$$Fuel_{needed} = 9,36 \cdot 6018,42$$

$$Fuel_{needed} = 56332,80 \text{ lb}$$

4.2 Aircraft weight estimation

The total weight of the aircraft is going to be obtained in this chapter and later will be used for obtaining the range calculation. For doing the calculation, some initial parameters are needed and given below in imperial units, as the equations that are going to be used are designed for imperial units.

- $b = 128,21$ ft
- $MTOW = 199820$ lb
- $n = 3,5$
- $\phi = 25,3^\circ$
- $L_f = 131,23$ ft
- $w_f = 17,84$ ft
- $d_f = 11,81$ ft
- $V_H = 480$ knots
- $t_w = 3,5$ ft
- $V_{cabin} = 22249$ ft³
- $L_{cabin} = 110,26$ ft
- $N_{pax} = 216$
- $MZFW = 143487,55$ lb

4.2.1 Fuselage weight estimation

The fuselage weight estimation is going to be calculated by using the formula below, which is proposed by Michael A. Nicolai and is well detailed in the book "Introduction to Aerospace Structural Analysis" written by David H. Allen and Walter E. Hurd.

$$W_{fuselage} = 200 \cdot \left[\left(\frac{n \cdot MTOW}{10^5} \right)^{0,286} \cdot \left(\frac{L_f}{10} \right)^{0,857} \cdot \left(\frac{w_f + d_f}{10} \right) \cdot \left(\frac{V_H}{100} \right)^{0,338} \right]^{1,1}$$

$$W_{fuselage} = 200 \cdot \left[\left(\frac{3,5 \cdot 199820}{10^5} \right)^{0,286} \cdot \left(\frac{131,23}{10} \right)^{0,857} \cdot \left(\frac{17,84 + 11,81}{10} \right) \cdot \left(\frac{480}{100} \right)^{0,338} \right]^{1,1}$$

$$W_{Fuselage} = 24.401,77 \text{ lbs}$$

Where:

- n = ultimate load factor
- L_f = Fuselage length
- w_f = Fuselage width
- d_f = Fuselage height
- V_H = Airspeed

4.2.2 Wings weight estimation

From the Torenbeek method can be obtained the following equation to calculate the wing weight:

$$W_{Wing} = 0,0017 \cdot MZFW \cdot \left(\frac{b}{\cos \phi}\right)^{0,75} \cdot \left(1 + \frac{6,3 \cdot \cos \phi}{b}\right)^{\frac{1}{2}} \cdot n^{0,55} \cdot \left(\frac{b \cdot S}{t_w \cdot MZFW \cdot \cos \phi}\right)^{0,3}$$

$$W_{Wing} = 0,0017 \cdot 143487,55 \cdot \left(\frac{128,21}{\cos 25,3}\right)^{0,75} \cdot \left(1 + \frac{6,3 \cdot \cos 25,3}{128,21}\right)^{\frac{1}{2}} \cdot 3,5^{0,55} \cdot \left(\frac{1595,10 \cdot 128,21}{3,5 \cdot 143487,55 \cdot \cos 25,3}\right)^{0,3}$$

$$W_{Wing} = 15950,38 \text{ lb}$$

4.2.3 Empennage weight estimation

The tail weight estimation is going to be obtained using Torenbeek's method, for the VTP is going to be multiplied times two because the formula is designed for conventional tail configuration and my design has a T-tail configuration with two VTP

- VTP

The following Torenbeek equation applies to aircraft with design dive speeds higher than 250 kt, in our case the result is going to be multiplied times two as explained before

$$W_{VTP} = 2 \cdot \left[k_V \cdot S_V \left(\frac{3,81 \cdot (S_V)^{0,2} \cdot V_D}{1000 \cdot \cos \phi_V} \right) \right]$$
$$W_{VTP} = 2 \cdot \left[1 \cdot 223,67 \left(\frac{3,81 \cdot (223,67)^{0,2} \cdot 480}{1000 \cdot \cos 45^\circ} \right) \right]$$

$$W_{VTP} = 3413,81 \text{ lb}$$

The value of k_V according to Torenbeek is equal to 1 for fuselage mounted vertical tail planes

- HTP

The horizontal tail plane is going to be calculated in the same way as the vertical tail plane.

$$W_{VTP} = k_H \cdot S_H \left(\frac{3,81 \cdot (S_H)^{0,2} \cdot V_D}{1000 \cdot \cos \phi_H} \right)$$
$$W_{VTP} = 1 \cdot 428,18 \left(\frac{3,81 \cdot (428,18)^{0,2} \cdot 480}{1000 \cdot \cos 29,65^\circ} \right)$$

$$W_{VTP} = 3027,37 \text{ lb}$$

4.2.4 Landing gear weight estimation

The landing gear weight, including its structure, according to Torenbeek is around 3,7% of the MTOW and the next equations are going to be used for main and nose landing gear.

- Main landing gear

$$W_{mlg} = 40 + 0,16 \cdot (MTOW)^{0,75} + 0,019 \cdot MTOW + 1,5 \cdot 10^{-5} \cdot MTOW^{1,5}$$

$$W_{mlg} = 40 + 0,16 \cdot (MTOW)^{0,75} + 0,019 \cdot MTOW + 1,5 \cdot 10^{-5} \cdot MTOW^{1,5}$$

$$W_{mlg} = 6688,57 \text{ lb}$$

- Nose landing gear

$$W_{nlg} = 20 + 0,1 \cdot (MTOW)^{0,75} + 2 \cdot 10^{-5} \cdot MTOW^{1,5}$$

$$W_{nlg} = 20 + 0,1 \cdot (MTOW)^{0,75} + 2 \cdot 10^{-5} \cdot MTOW^{1,5}$$

$$\mathbf{W_{nlg} = 2751,54 lb}$$

4.2.5 Engine weight estimation

$$W_{engines} = W_{PW2043} \cdot N_{eng}$$

$$W_{engines} = 7100 \text{ lbs} \cdot 2$$

$$\mathbf{W_{engines} = 14200 lbs}$$

4.2.6 Aircraft systems weight estimation

The weight of the systems of the aircraft is going to be calculated by using the Torenbeek method, which has been used for a long time and dividing the aircraft systems into the following points.

- APU:

The auxiliary power unit implanted in the aircraft is going to be the same one used in A321 neo and the rest of A320 family which is Honeywell's 131-9A. This APU has the advantage that has low maintenance and fuel consumption as well as high performance. This kind of APU is the most used between single-aisle aircraft.

$$\mathbf{W_{APU} = 354,06 lbs}$$

- Instruments and avionics:

The weight is going to be estimated with the MTOW using the formula below:

$$W_{ins} = 0,347 \cdot \left(\frac{MTOW}{2}\right)^{0,555}$$

$$W_{ins} = 0,347 \cdot \left(\frac{MTOW}{2}\right)^{0,555}$$

$$\mathbf{W_{ins} = 206,59 lb}$$

- Hydraulic and pneumatic systems:

The weight of hydraulic and pneumatic systems is calculated with the take-off weight with the following formula:

$$W_{hyd} = 0,0015 \cdot \left(\frac{MTOW}{2}\right) + 272$$

$$W_{hyd} = 0,0015 \cdot \left(\frac{MTOW}{2}\right) + 272$$

$$\mathbf{W_{hyd} = 421,86 lb}$$

- Electrical systems

The electrical system weight estimation with Torenbeek method for commercial jet aircraft is obtained with the cabin area using the next equation:

$$W_{elec} = 10,8 \cdot (V_{cabin})^{0,7} \cdot (1 - 0,018 \cdot (V_{cabin})^{0,35})$$

$$W_{elec} = 10,8 \cdot (73025,43)^{0,7} \cdot (1 - 0,018 \cdot (73025,43)^{0,35})$$

$$\mathbf{W_{elec} = 2555,61 lb}$$

- Air conditioning and anti-icing:

The air conditioning and anti-icing systems weight are related with the cabin length and can be obtained with the following formula:

$$W_{air} = 14 \cdot l_{cabin}^{1,28}$$

$$W_{air} = 14 \cdot 110,26^{1,28}$$

$$\mathbf{W_{air} = 5760 \text{ lb}}$$

- Oxygen system:

The oxygen system weight estimation for aircraft that fly over 25000 ft and have short and medium range flights is calculated with the formula below.

$$W_{oxg} = 30 + 1,2 \cdot N_{pax}$$

$$W_{oxg} = 30 + 1,2 \cdot 216$$

$$\mathbf{W_{oxg} = 289,20 \text{ lb}}$$

- Fuel system

The Torenbeek's method equation for commercial aircraft that are equipped with integral fuel tanks, the estimated weight of the fuel system is obtained with the following formula:

$$W_{Fsys} = 80 \cdot (N_E + N_T - 1) + 15 \cdot (N_T)^{0,5} \cdot \left(\frac{W_f}{K_{fsp}}\right)^{0,333}$$

$$W_{Fsys} = 80 \cdot (2 + 6 - 1) + 15 \cdot (6)^{0,5} \cdot \left(\frac{56332,80}{8,268}\right)^{0,333}$$

$$\mathbf{W_{Fsys} = 1254,50 \text{ lb}}$$

- Furnishing

The total weight estimation of the furnishing of the aircraft is related with the MZFW in the next formula:

$$W_{furn} = 0,196 \cdot MZFW^{0,91}$$

$$W_{furn} = 0,196 \cdot MZFW^{0,91}$$

$$\mathbf{W_{furn} = 9659,55 lb}$$

- Paint and miscellaneous:

The weight of the paint usually represents a 0,006 of the total aircraft weight

$$W_{paint} = 0,006 \cdot MTOW$$

$$W_{paint} = 0,006 \cdot MTOW$$

$$\mathbf{W_{paint} = 1198,92 lb}$$

4.2.7 Final estimated weight

Structure	Weight in lb (kg)
Fuselage	24401,77 lb (11066,56 kg)
Wings	15950,38 lb (7233,73kg)
VTP	3413,81 lb (1548,21 kg)
HTP	3027,37 lb (1372,96kg)
Main landing gear	6688,57 lb (3033,37kg)
Nose landing gear	2751,54 lb (1247,86kg)
Engines	14200 lb (6439,91 kg)
TOTAL	70433,44 lb (31942,60kg)

Table 22. Total estimated weight of the structure

Systems	Weight in lb (kg)
APU	354,06 (160,57 kg)
Instruments and avionics	206,59 lb (93,69 kg)
Hydraulic and pneumatic systems	421,86 lb (191,32 kg)
Electrical system	2555,61 lb (1159,01kg)
Air conditioning and anti-icing systems	5760 lb (2612,24kg)
Oxygen system	289,20 lb (131,16 kg)
Fuel system	1254,50 lb (568,93 kg)
Furnishing	9659,55 lb (4380,75 kg)
Paint	1198,92 lb (543,73 kg)
TOTAL	21700,29 lb (9841,40 kg)

Table 23. Total estimated weight of the systems

Payload weight	Weight in lb (kg)
Payload	51389,75 lb (23306,01 kg)
Fuel	56332,80 lb (25547,76 kg)
TOTAL	107722,55 lb (48853,76 kg)

Table 24. Total estimated weight of the payload

Extra weight	Weight in lb (kg)
Structure	70433,44 lb (31942,60 kg)
Systems	21485,02 lb (9841,40kg)
Extra weight	107722,55 lb (48853,76kg)
TOTAL	199641,01 lb (90540,14 kg)

Table 25. Total estimated weight of the aircraft

The result obtained from the weight estimation of all the components of the aircraft is 90540,14 kg, which is very similar to the result of the linear regression carried out in section 3.5.2, 90637 kg. There is a difference of only 96,86 kg that corresponds approximately to the 0,001% of the MTOW obtained in the linear regression.

4.3 Wing analysis

In this section, a CFD analysis of the wing of the aircraft is going to be performed in Ansys Fluent in order to obtain the contours of pressure, velocity, Mach number, skin friction and the values of the aerodynamic forces, lift and drag, for different angles of attack in order to plot the aerodynamic efficiency of the aircraft. The wing has been imported to the software without the winglets due to geometry errors given by Ansys.

The first step is to create the mesh of the enclosure, which is going to simulate the control volume of the wing. The Ansys Student version allows a maximum of 512000 cells for the mesh, which is very limiting taking into account the wing dimensions and could affect the precision of the results.

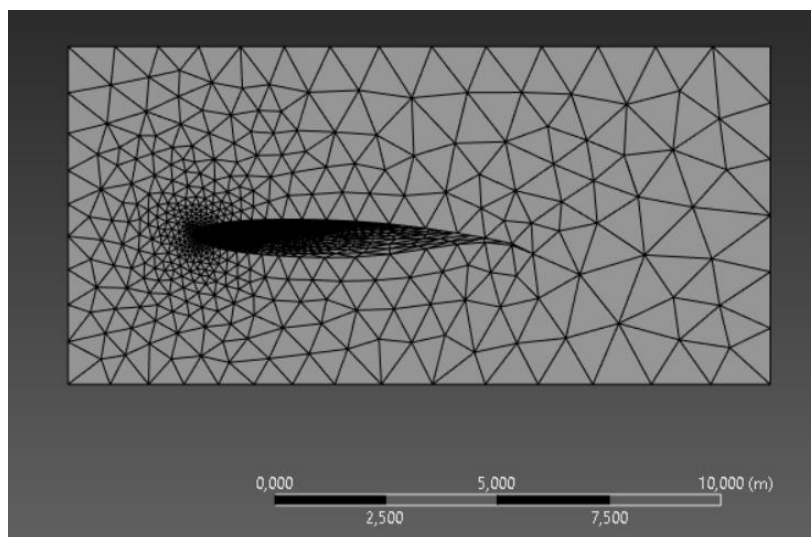


Figure 75. Isometric view of the enclosure mesh

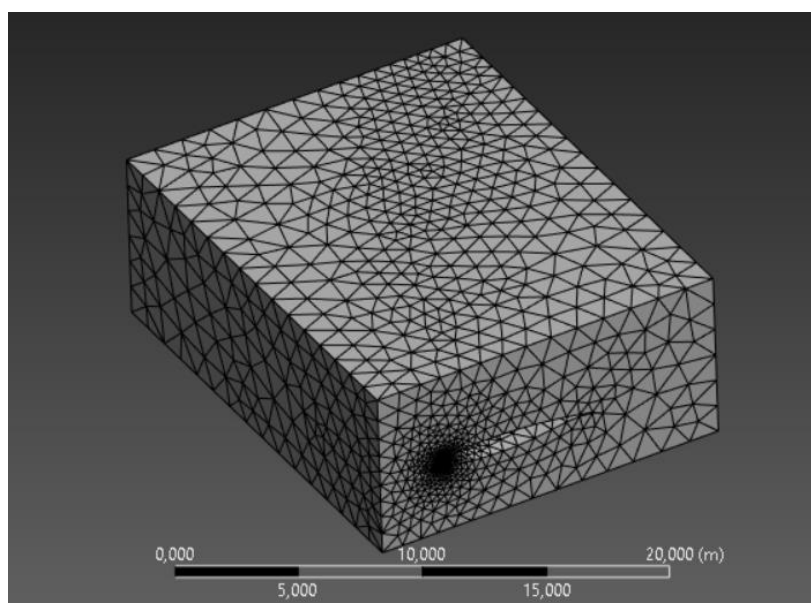


Figure 74. Side view of the enclosure mesh

The viscous model selected for the CFD analysis is k-epsilon turbulence model which is one of the most used methods for turbulent flow and combines two equations that give a description of turbulences by using the two transport equations. For selecting the inlet velocity, the type of inlet is pressure far field, which allows to use a Mach number as a boundary condition for the inlet. The fluid used is air as an ideal gas and the viscosity used is based on the Sutherland law, which is based on the kinetic theory of ideal gases and is commonly used giving low error and accurate results.

For obtaining the velocity, pressure Mach number and skin friction, the analysis is going to be performed at an angle of attack of 0° and at the cruise velocity of Mach 0,75

4.3.1 Velocity

For Mach number 0,75, it can be seen in the figure below that the velocity is going to be higher in the upper surface of the wing, where the pressure is going to reach its lower values. The maximum velocity magnitude that the flow reaches is 367,37 m/s. Besides, at the leading edge can be seen the stagnation point, where the local velocity is zero and the pressure is going to be higher.

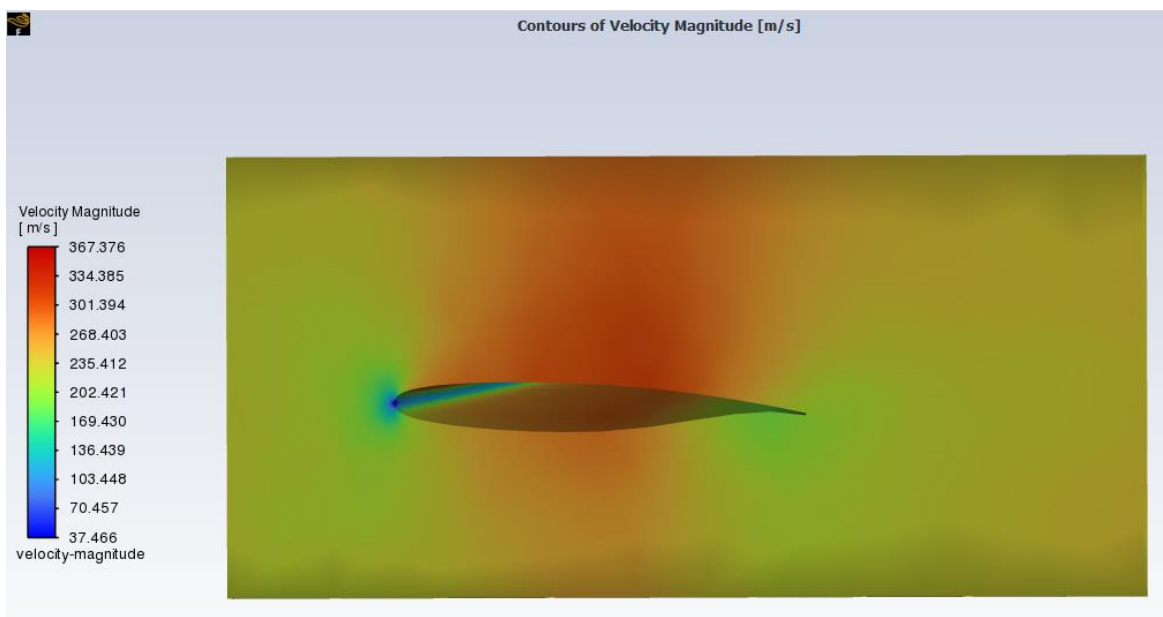


Figure 76. Flow field contours of velocity magnitude

In the figure below, the contour of the velocity magnitude of the flow can be appreciated along the wing, as well as the stagnation point at the leading edge previously mentioned.

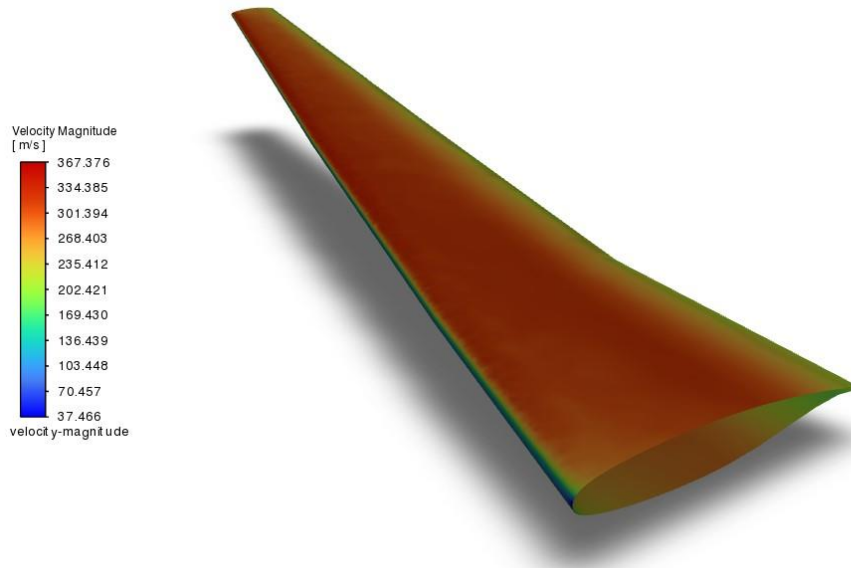


Figure 77. Wing contours of velocity magnitude

4.3.2 Pressure

The pressure distribution varies along the wing and the upper and lower surfaces, in the upper surface the pressure is lower due to the increase in velocity of the air while in the lower surface the pressure is higher as the air velocity is lower. The difference in pressure between the upper and the lower surfaces is going to determine the lift force generated. In Figure 78, can be seen how the pressure of the flow field is different at each part of the wing.

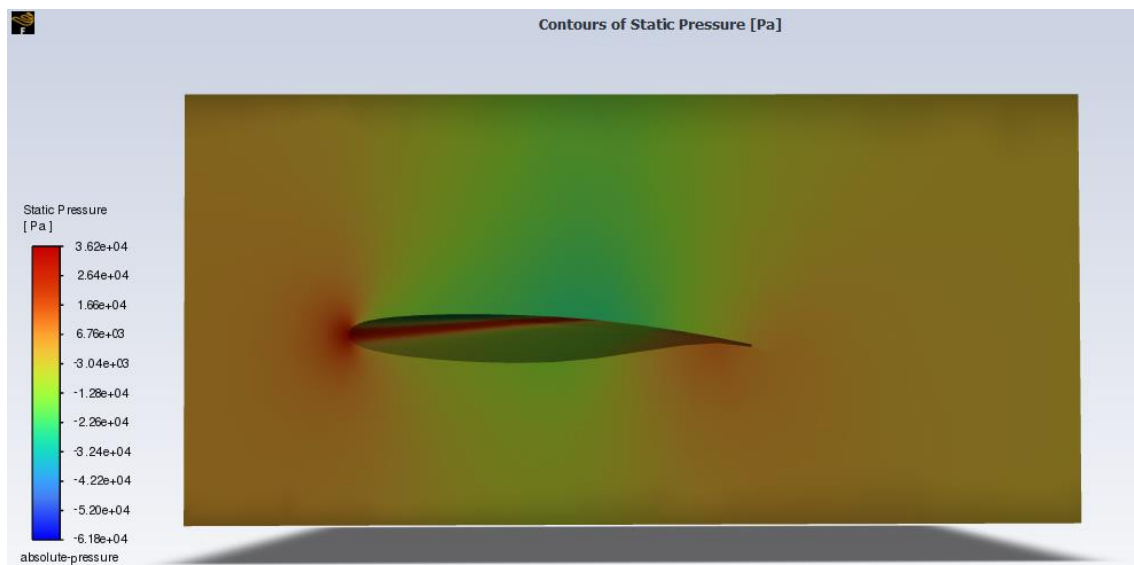


Figure 80. Static pressure contours in the flow field

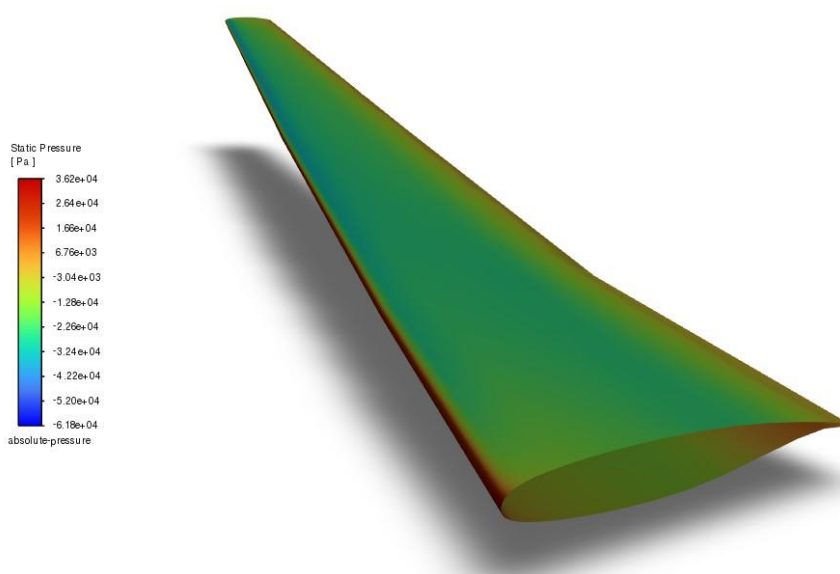


Figure 79. Static pressure contours along the wing

In Figure 79 can be appreciated the stagnation point in the leading edge, this is the point of maximum pressure in the wing and the velocity is zero.

The maximum static pressure reached on the wing is 36,2 kPa and the difference of values can be seen in the colormap at the left-hand side of the contours

4.3.3 Mach number

The Mach number values at each point can be seen also for the flow field and along the wing in the following figures.

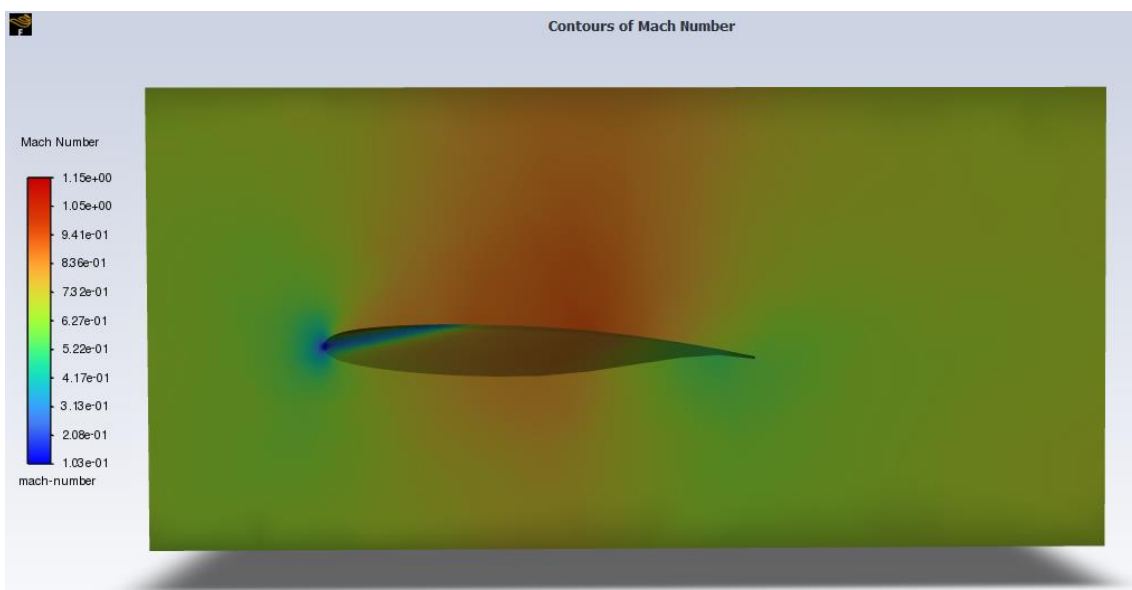


Figure 82. Mach number in the flow field

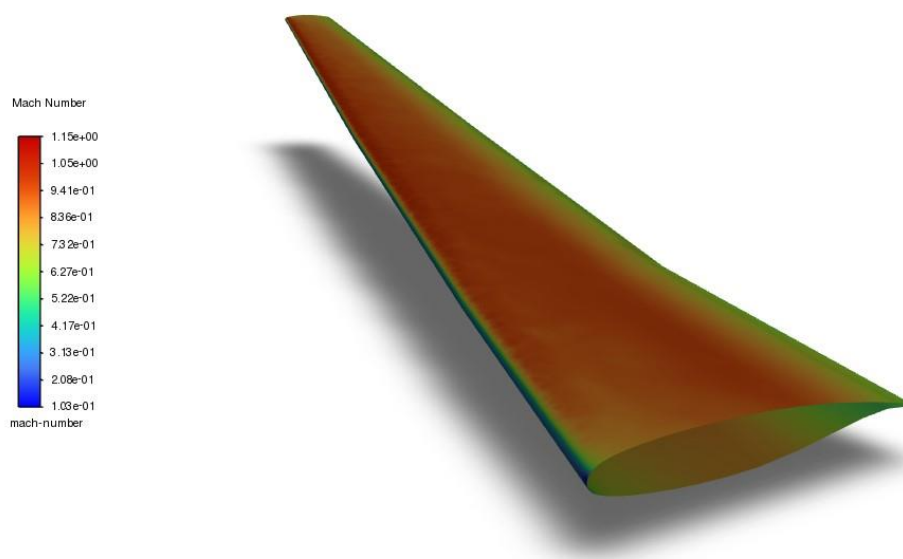


Figure 81. Mach number values along the wing

The Mach number along the wing is a very important factor when designing aircraft, reducing the compressibility effects at high flow velocities is a key aspect of the efficient performance of the wing.

Flying at Mach 0,75, for the analysis parameters selected, the maximum value reached along the wing is 1,15. As the Mach number is higher than one at a local point of the wing, there is not going to be a shock wave but the local aerodynamics could be lightly reduced at that point.

4.3.4 Skin friction coefficient

The skin friction coefficient is a parameter to describe the resistance to the viscous flow of a fluid on a surface, in this case the wing. In the following figures can be observed the distribution of the skin friction along the wing and the maximum value that it reaches, 0,00413 at the leading edge near the root of the wing.

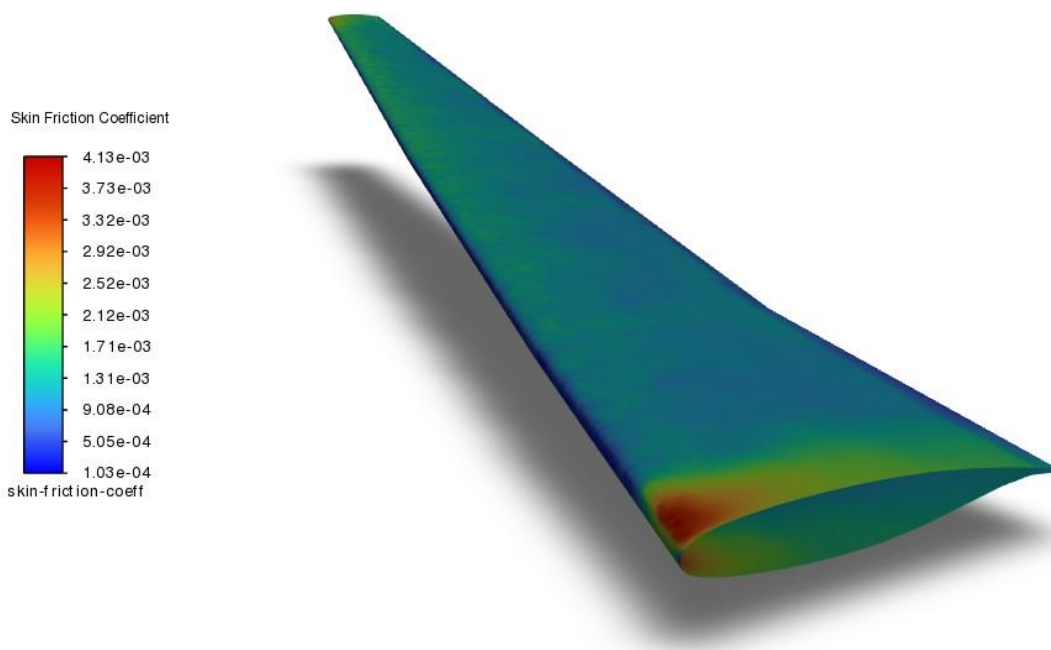


Figure 83. Skin friction coefficient along the wing

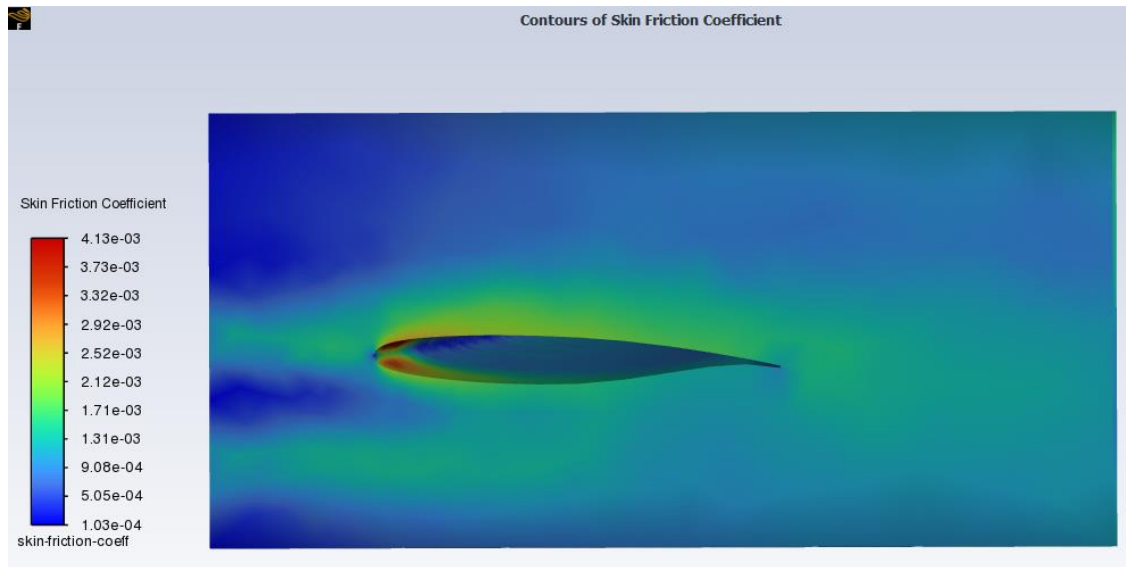


Figure 84. Skin friction coefficient contour of the flow field

4.3.5 Aerodynamic efficiency

The aerodynamic efficiency refers to the ratio between the lift force and the drag force, if the lift-over-drag ratio is higher, the performance and efficiency of the aircraft are going to be higher and the fuel consumption is going to be lower.

In this section, the wing is going to be studied at Mach 0,75 and a range of angles of attack between 0° and 16° with a step of $1,5^\circ$. Then, the reports of lift and drag coefficient created in Fluent are going to give the exact values when the solution of the iterations converge and the Cl/AoA , Cd/AoA and Cl/Cd graphs can be plotted.

The Cl versus the angle of attack is plotted in the table below for Mach 0,75.

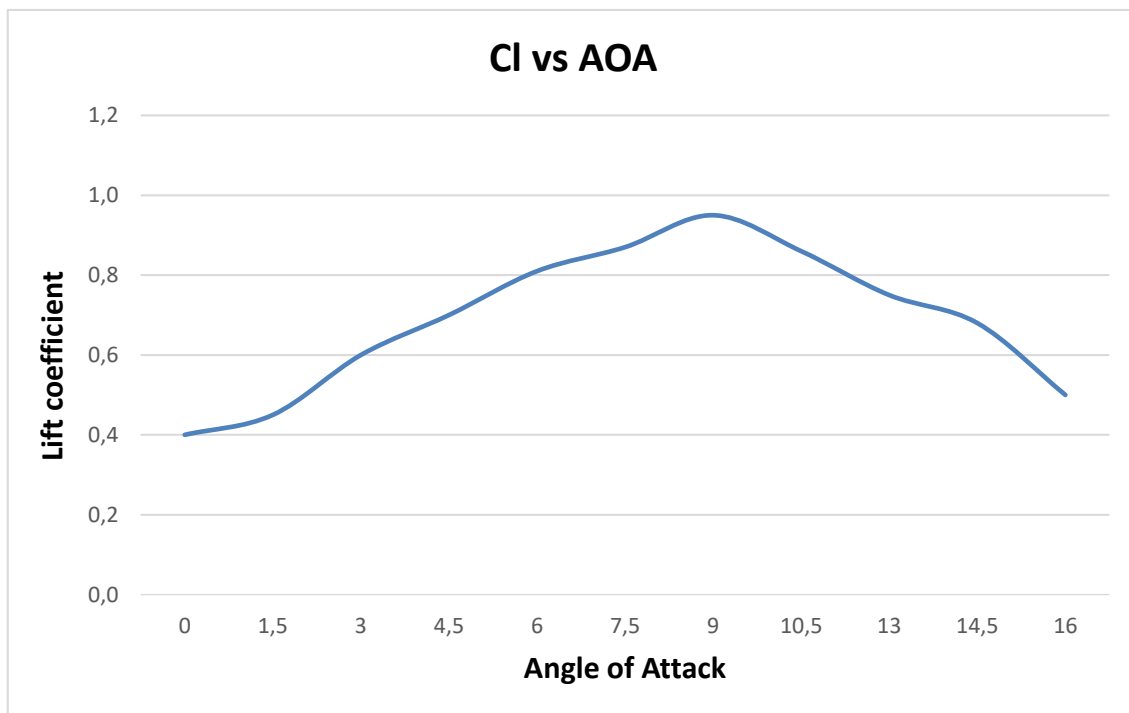


Table 26. Cl vs angle of attack

In the graph can be seen that the maximum lift coefficient of the wing is 0,95 at an angle of attack of 9° and then it starts to decrease as the wing begins to stall. The lift coefficient is not enough high as expected, this value could be increased by adding winglets so as to reduce the induced drag and increase the lift. Also, changing the twist angle along the wing could improve the lift distribution along the wing span.

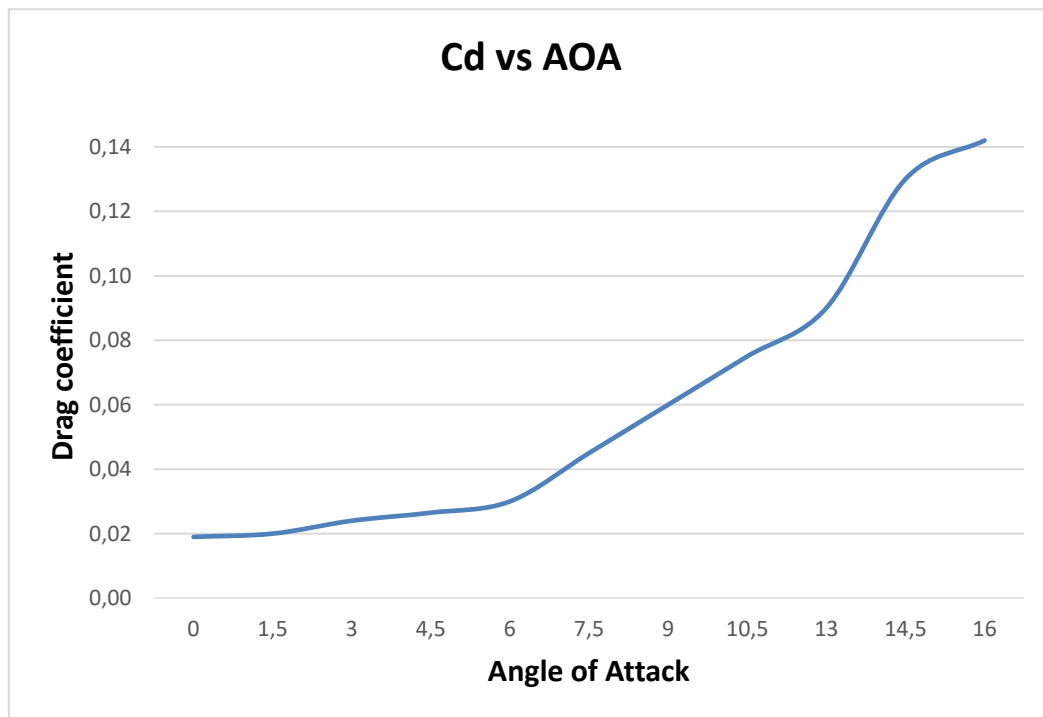


Table 27. Cd vs angle of attack

In the above table, the drag coefficient along the wing is plotted and we can see that the wing maintains the drag values low until 7° when it starts to increase until the highest values.

The drag could be reduced with a higher aspect ratio and furthermore, as previously commented, adding winglets to reduce the induced drag. Adding the winglets could reduce the wing induced drag significantly. Besides, the airfoil selected is very thick and changing the airfoil to a thinner one with less thickness could also reduce the drag of the wing.

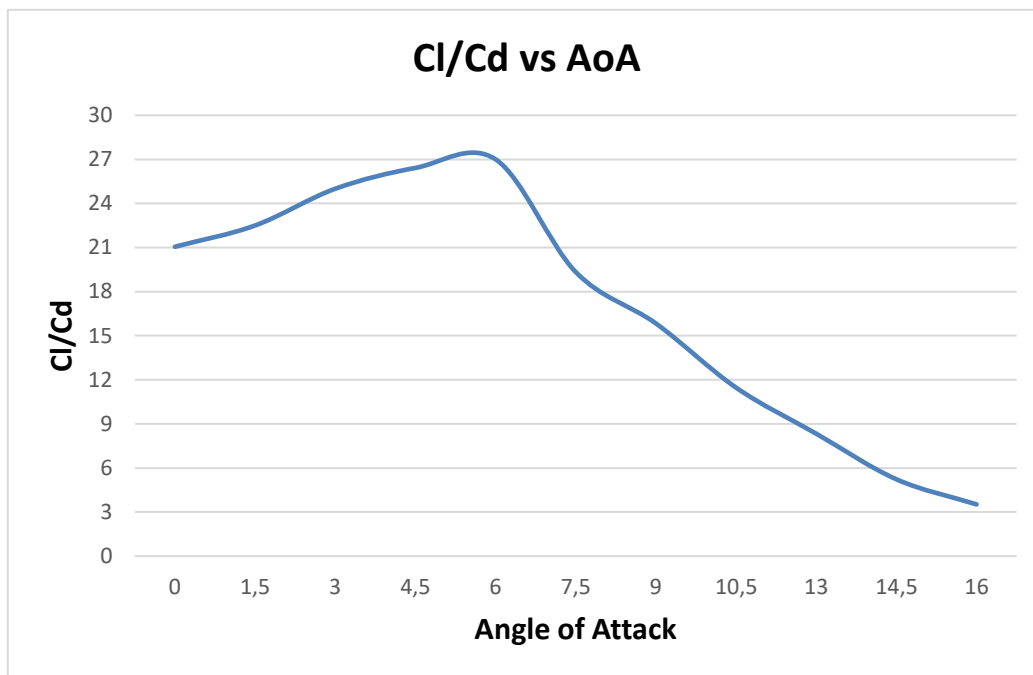


Table 28. Aerodynamic efficiency vs angle of attack

In the above graph is plotted the aerodynamic efficiency of the wing, which is the ratio between the lift and drag coefficients obtained in the analysis and plotted in Tables 26 and 27. The maximum aerodynamic efficiency is reached at an angle of attack of 6° and reaches a value of 27, then the drag starts to increase as can be seen in the Cd vs AoA graph and so the lift-to-drag ratio starts to decrease, been the wing less efficient at those angles of attack.

This data is very important for the calculation of the aircraft range that is going to be performed in the following section. For that calculation, aerodynamic efficiency is required, the maximum value of the wing will be higher than the maximum value of the whole aircraft,

4.4 Range calculation

The maximum range, also called ferry range, of the aircraft refers to the maximum distance that an aircraft can fly between the takeoff and the landing with maximum fuel load. In powered aircraft the range is directly dependent on the maximum fuel that they can store in the tanks, then the maximum distance reachable is going to depend on the specific fuel consumption of the engines, cruise speed and the aerodynamic efficiency.

The range of the aircraft is going to be calculated using the Breguet equation, which assumes that thrust specific fuel consumption is constants during the flight as the aircraft weight is decreased with the fuel burnt. The equation that is going to be used is the following:

$$R = \frac{V}{SFC} \cdot \frac{Cl}{Cd} \cdot \ln\left(\frac{W_0}{W_f}\right)$$

Where:

- V = aircraft velocity
- SFC = Specific Fuel Consumption
- Cl/Cd = aerodynamic efficiency
- W_0 = weight of the aircraft at the start of flight
- W_f = weight of the aircraft at the end of flight

The value of the aerodynamic efficiency of the aircraft for the calculation is going to be assumed constant and the value chosen is the one obtained at 0° , which is 21,01.

The 90 % of the total fuel burnt by aircraft is estimated to be during the cruise stage, so we can assume that the fuel weight at the start of the cruise is a 95 % of the total fuel weight and at the landing is a 10 % of the total fuel weight, reserving that 10% for taxiing and emergency cases. So, the W_0 is going to be the MTOW minus the 0,05% of the fuel weight and the W_f is going to be the MTOW minus the 90 % of the fuel weight.

$$R = \frac{895}{0,582} \cdot 21,01 \cdot \ln\left(\frac{90637,75 - (25547,76 \cdot 0,05)}{90637,75 - (25547,76 \cdot 0,90)}\right)$$

$$\mathbf{R = 8995,11 \text{ km (4856,97 nmi)}}$$

The ideal range of the aircraft estimated for being suitable for the middle of the market was 4500 nmi and the estimated range obtained from the Breguet equation gives us a range up to 4856,97 nmi, which means that the aircraft is suitable for the aimed market.

Chapter 5. Conclusions and future works

5.1 Conclusions

The main objective of the project was to perform a preliminary design of a horizontal double bubble aircraft that could meet the requirements of the middle of the market niche using a nonconventional fuselage cross-section design and perform a CFD analysis of the wing and estimate all the weights of the components and systems of the aircraft for obtaining the range.

The first step of the project has been to do a research on the market, investigating the middle of the market needs and the possible aircraft that can cover this market segment. The analysis resulted in a specific range and number of passengers that were covered by Being 757 and in which Airbus and Boeing have been working during the last years to enter and dominate the market. The aimed range for this market needs is about 4500 nautical miles and between 200 and 250 passenger capacity, which has been successfully achieved during the project.

After designing all the aircraft parts using linear regressions from other aircraft of similar characteristics that are in service nowadays, the dimensions of all the parts of the aircraft have been calculated and the final 3D design model of the aircraft has been carried out using Open VSP software. During the design phase some problems came at the time of designing the cross-section, the integration of the bubbles for creating the final design had to be modified in order to incorporate the desired seats per row, the corners radius of the section had to be increased for the final design for a better integration of the cabin components.

In addition to the design, every part and system of the aircraft has been studied and analyzed to obtain an estimation of its weights by using Torenbeek's method for aircraft weight estimations, obtaining very accurate compared with the ones obtained from the linear regression results. Finally, the weight estimation has been used at the end for the range calculation and the values are ideal for the middle of the market aimed range.

The main problem of the project came at the time of performing the CFD analysis of the wing. The whole aircraft with the fuselage, engines and vertical and horizontal tail planes has been impossible to analyze due to its size and the limited number of elements of the Ansys license and the analysis dimensions reduced to the study of the aerodynamic forces of the wing. The wing geometry was also very big and so as to perform a good analysis of the main aerodynamic force and obtain precise contours, a good and exact mesh was required but the student license has been an important limiting factor.

Despite the limitations for the quality of the mesh, the results obtained look reasonable and the final range calculation successfully meets the objectives set at the beginning of the project for the aimed market.

To conclude, this project has been very enriching from the point of view that I have learned a lot about different topics that are fundamental in today's aviation, such as safety and regulations for the safe evacuation of aircraft, new fuselage concepts that can be fundamental in the future of aviation to improve efficiency and increase the comfort of passengers in the cabin or cover the needs of a market in which there is a niche as can be the middle of the market.

5.2 Future works

In future works, there are many possibilities to improve both the design of the aircraft and the CFD analysis of the wing and the entire structure of the aircraft to obtain more precise results.

The project depth could be improved by implementing the winglets geometry and the whole aircraft into a CFD analysis without license limitations and obtain more realistic data of the aircraft, and thus carry out a more precise analysis to see the real efficiency of this type of cross-section and its viability. The pressure cycles that the fuselage will suffer could be important to study as well as designing a strong internal structure of the fuselage to support the pressure loads assuming an increase of the fuselage thickness that the double bubble section will require.

In terms of security, a study could be carried out to ensure the correct and safe evacuation of the aircraft when changing the fuselage section. Increasing the number of passengers per row increases the risk that the evacuation of the plane will be delayed in addition to the difficulty of the passengers to leave the aircraft.

Another aspect that could be taken into account in future researches is an analysis of the feasibility of placing the engines in the rear part of the fuselage for taking advantage of the boundary layer ingestion. A risk analysis could be performed in order to analyze its feasibility and possible problems that the new location of the engines could generate.

The distance between the engines could also be important to analyze for obtaining better efficiency and allow the nacelles to change the position to reverse thrust taking into account that the distance between both vertical tail planes is very limiting and could influence negatively the reversing thrust of the nacelles.

Using a more precise program for the designing phase of the aircraft could allow to assemble better the wing and tail planes to the fuselage structure as well as the engines location for a better boundary layer ingestion.

APPENDICES

APPENDIX A

Other two possible configurations for the seat arrangement have been studied. The first one offers two different classes for a total of 213 passengers with the following seat dimensions:

- First class:
 - 6 seats per row
 - Seat pitch: 1 m
 - Seat gap: 0,08 m
 - Aisle with: 0,4 m
 - Seat width: 0,6 m
 - Seat length: 0,5 m

- Economy class:
 - 3-3-3 configuration
 - Seat pitch: 0,725 m
 - Seat gap: 0,08 m
 - Aisle with: 0,5 m
 - Seat width: 0,475 m
 - Seat length: 0,5 m

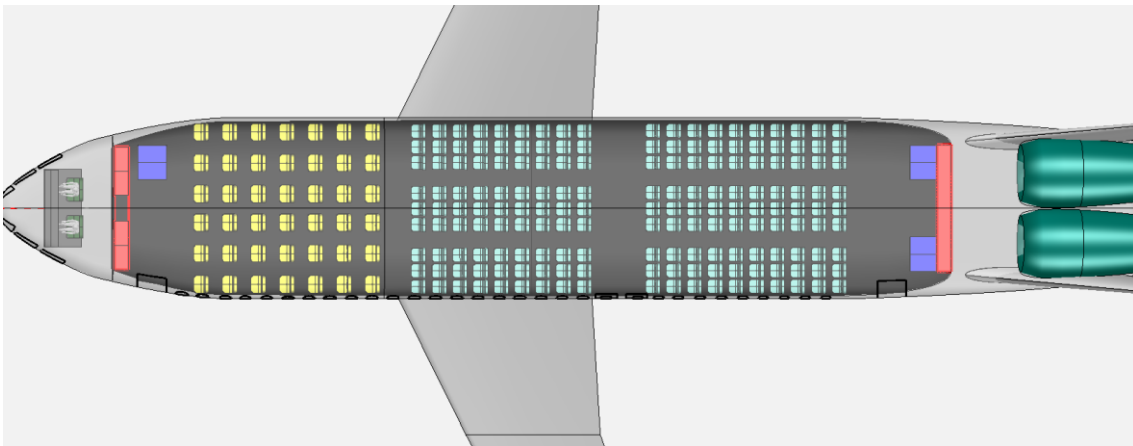


Figure 85. First possible seats configuration

The other possible seat arrangement also studied has a total of 249 maximum passengers and has the following dimensions.

- First class:
 - 8 seats per row
 - Seat pitch: 0,725 m
 - Seat gap: 0,08 m
 - Aisle with: 0,5 m
 - Seat width: 0,5 m
 - Seat length: 0,5 m

- Economy class:
 - 3-3-3 configuration
 - Seat pitch: 0,725 m
 - Seat gap: 0,08 m
 - Aisle with: 0,5 m
 - Seat width: 0,475 m
 - Seat length: 0,5 m

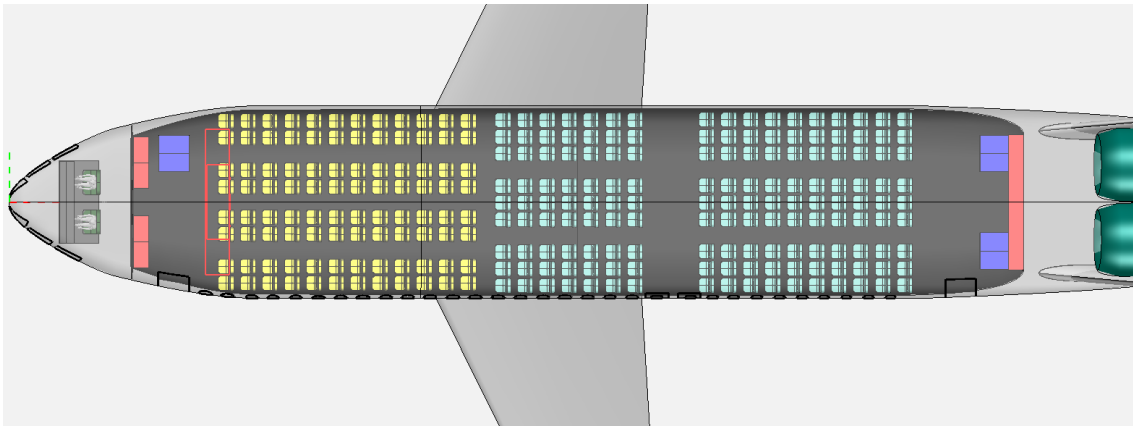


Figure 86. Second possible seats configuration

REFERENCES

- [1] Aérea, Agencia Europea de Seguridad. 2012. *Anexo VI al proyecto de Reglamento de la Comisión sobre «Operaciones aéreas— OPS» Parte-NCC — IR*. 2012.
- [2] 2011. Aerospaceweb. *Airbus A320 Short to Medium-Range Jetliner*. [Online] 2011. <https://aerospaceweb.org/aircraft/jetliner/a320/>.
- [3] 2015. Air charter service. *The MIT Plane of the Future*. [Online] 2015. <https://www.aircharterservice.com/about-us/news-features/blog/the-mit-designed-passenger-plane-of-the-future>.
- [4] Airfoil tools. *NASA SC(2)-0412 AIRFOIL (sc20412-il)*. [Online] <http://airfoiltools.com/airfoil/details?airfoil=sc20412-il#polars>.
- [5] Alejandra Uranga, Mark Drela, Edward M. Greitzer, David K. Hall, Neil A. Titchener, Michael K. Lieu, Nina M. Siu, Cécile Casses, Arthur C. Huang, Gregory M. Gatlin and Judith A. Hannon. 2017. *Boundary Layer Ingestion Benefit of the D8 Transport Aircraft*. 2017.
- [6] Ali, Omran Al-Shamma and Dr. Rashid. *Aircraft weight estimation in interactive design process*. s.l. : University of Hertfordshire.
- [7] Boeing detailed technical data. [Online] <http://www.b737.org.uk/techspecs/detailed.htm>.
- [8] Brian Yutko, Neil Titchener, Christopher Courtin, Michael Lieu, Larry Wirsing, David Hall, John Tytko, Jeffrey Chambers, Thomas Roberts, Clint Church. 2018. *DESIGN AND DEVELOPMENT OF THE D8*. 2018.
- [9] Brian Yutko, Neil Titchener and Christopher Courtin. 2017. *Conceptual desing of a D8 Commercial Aircraft*. 2017.
- [10] cargo, ANA. A320/321. [Online] <https://www.anacargo.jp/en/int/specification/a320.html>.
- [11] Civil jet aircraft. *Boeing aircraft*. [Online] <https://booksite.elsevier.com/9780340741528/appendices/data-a/table-1/table.htm>.
- [12] Civil jet aircraft desing. *Airbus data file*. [Online] <https://booksite.elsevier.com/9780340741528/appendices/data-a/table-1/table.htm>.
- [13] *Double Bubble: the Green Aircraft of the Future*. Hattab, Hanen. 2021. s.l. : Substance. Scientific news and innovation, 2021.

-
- [14] Dowling, Pijush K. Kundu and David R. 2016. *Fluid Mechanics (Sixth Edition)*. 2016.
- [15] Drela, M. 2011. *Development of the D8 Transport configuration*. 2011.
- [16] DSV. *Dimensiones del contenedor aéreo LD3 / AKE / AVE*. [Online] <https://www.dsv.com/es-es/nuestras-soluciones/modos-de-transporte/transporte-aereo/tipos-contenedor-palet-aereo/contenedor-ld3-ake-ave>.
- [17] Electrical and Computer Engineering Department. 2003. Engineering Report Writing. *Univeristy of Connecticut*. [Online] September 2003. [Cited: april 15, 2013.] <http://www.ocf.berkeley.edu/~anandk/math191/Technical%20Writing.pdf>.
- [18] Flight control surfaces. *Wikipedia*. [Online] https://en.wikipedia.org/wiki/Flight_control_surfaces.
- [19] Frigate Ecojet. *Wikipedia*. [Online] https://en.wikipedia.org/wiki/Frigate_Ecojet.
- [20] Galan, Marius Fuentes. 2018. *AIRCRAFT MODELING THROUGH BeX & OpenVSP*. Linköping University : s.n., 2018.
- [21] Global Air. *Airbus A320, Technical Specifications*. [Online] <https://www.globalair.com/aircraft-for-sale/specifications?specid=639>.
- [22] Hardiman, Jake. Flying, Simple. The Airbus P500: The Double Fuselage Plane That Never Was. [Online] <https://simpleflying.com/airbus-p500/>.
- [23] Harris, Charles D. 1990. *A Matrix of Family-Related Airfoils*. Hampton, Virginia : NASA technical paper 2969, 1990.
- [24] *How to write consistently boring scientific literature*. Sand-Jensen, Kaj. 2007. 5, s.l. : Wiley, November 26, 2007, Oikos, Vol. 116, pp. 723-727. <http://onlinelibrary.wiley.com/doi/10.1111/j.0030-1299.2007.15674.x/pdf>.
- [25] ICAO. Future of Aviation . [Online] <https://www.icao.int/Meetings/FutureOfAviation/Pages/default.aspx>.
- [26] Jason R. Welstead, Peter C. Frederic, Jeffrey J. Berton and Michael A. Frederick. 2017. *Cost-Driven Design of a Large Scale X-Plane*. 2017.
- [27] K-epsilon turbulence model. *Wikipedia*. [Online] https://en.wikipedia.org/wiki/K-epsilon_turbulence_model.
- [28] Landing gear. *Wikipedia*. [Online] https://en.wikipedia.org/wiki/Landing_gear.
- [29] Lift-to-Drag ratio. *Wikipedia*. [Online] https://en.wikipedia.org/wiki/Lift-to-drag_ratio.
- [30] Martínez, Isidoro. *AIRCRAFT PROPULSION*.

- [31] Microsoft. Create a bibliography. *Office*. [Online] [Cited: April 25, 2013.]
<http://office.microsoft.com/en-001/word-help/create-a-bibliography-HA010067492.aspx>.
- [32] Middle of the market. *Wikipedia*. [Online]
https://en.wikipedia.org/wiki/Middle_of_the_market.
- [33] Miró Julià, José. 2010. Recursos para aprender a escribir. [Online] 2010.
<http://bioinfo.uib.es/~joemiro/RecEscr/manual.pdf>.
- [34] N. Vinayaka1, C. Akshaya, Avinash Lakshmikanthan, Shiv Pratap Singh Yadav, R. P. Sindhu. 2019. *High Altitude Transonic Aerodynamics of Supercritical Airfoil*. 2019.
- [35] Pandya, Shishir A. 2015. *The D8 Aircraft: An Aerodynamics Study of Boundary Layer and Wake Ingestion Benefit*. s.l. : NASA Ames Research Center, 2015.
- [36] PBWorks. 2013. Citation Management Tools. *DiRT*. [Online] 2013. [Cited: April 25, 2013.]
<https://digitalresearchtools.pbworks.com/w/page/17801648/Citation%20Management%20Tools>.
- [37] Products, Nordisk Aviation. Nordisk AKH (LD3-45). [Online]
<https://www.nordisk-aviation.com/en/ld-containers/akh-ld3-45/nordisk-akh/>.
- [38] Sriram, Tara C. 2018. *Effect of Anthropometric Variability on Middle-Market Aircraft Seating*. Embry-Riddle Aeronautical University : s.n., 2018.
- [39] Sutherland, W. 1893. *The viscosity of gases and molecular force*. 1893.
- [40] T tail. *Wikipedia*. [Online] https://es.wikipedia.org/wiki/Cola_en_T.
- [41] T. Paramasivam, Walter J. Horn,. 1986. *Weight estimation techniques for composite airplanes in general aviation industry*. Wichita, Kansas : Wichita State University, 1986.
- [42] Tipos de Contenedores Aéreos – ESTANDAR. [Online]
<https://abqsa.com/contenedores-aereos-estandar/>.
- [43] Twin tail. *Wikipedia*. [Online]
https://en.wikipedia.org/wiki/Twin_tail#:~:text=A%20twin%20tail%20is%20a,of%20the%20aircraft's%20horizontal%20stabilizer..
- [44] Veeranjanyulu, K., et al. 2022. *Static analysis of conventional aircraft fuselage with different materials*. s.l. : Aip Publishing, 2022.
- [45] Walton, John. 2019. *The 'middle of market' airplane*. s.l. : Aircraft interiors international, 2019.

-
- [46] Wikipedia. 2013. Comparison of reference management software. *Wikipedia*.
[Online] April 15, 2013. [Cited: April 25, 2013.]
http://en.wikipedia.org/wiki/Comparison_of_reference_management_software.
- [47] Wragg, David W. 1973. *A Dictionary of Aviation*. 1973.